MONITORING SETTING AND HARDENING OF CONCRETE USING ACOUSTIC EMISSION AND GUIDED WAVES TECHNIQUES

A Dissertation Submitted

In Partial Fulfillment of the Requirements

For the degree of

MASTERS OF ENGINEERING

IN

STRUCTURAL ENGINEERING

Submitted by:

CHARAT SINGH
(ROLL NO: 801322007)

UNDER THE SUPERVISION OF

DR. SHRUTI SHARMA

Associate Professor

Department of Civil Engineering

Thapar University, Patiala

DEPARTMENT OF CIVIL ENGINEERING

THAPAR UNIVERSITY

PATIALA-147004

JULY 2015

DECLARATION

The author hereby declare that this dissertation entitled ***" MONITORING SETTING AND HARDENING OF CONCRETE USING ACOUSTIC EMISSION AND GUIDED WAVES TECHNIQUES "***, in whole or part has not been used to obtain any degree in this, or any other, institute, except where references have been given in text, it is entirely the author own work. The author conform that the library may lend or copy this upon request for academic purposes.

Charat

(CHARAT SINGH)

REGD.NO. 801322007

CERTIFICATE

This is to certify that the work presented in dissertation entitled ***"MONITORING SETTING AND HARDENING OF CONCRETE USING ACOUSTIC EMISSION AND GUIDED WAVES TECHNIQUES"*** submitted by **Mr. Charat Singh** in partial fulfillment of the requirements for the award of degree of **Master of Engineering** in Structural Engineering at **Thapar University, Patiala,** is a bonafide work carried out by the student under our supervision and guidance. The matter embodied in this report has not been submitted anywhere for award of any other degree.

Shruti Sharma 29/7/2014

Dr. SHRUTI SHARMA
Associate Professor
Department of Civil Engineering
Thapar University, Patiala

COUNTERSIGNED

Dr. NAVEEN KWATRA
Professor and Head
Department of Civil Engineering
Thapar University, Patiala

Dr. S.S. BHATIA
Dean, Academic Affairs
Thapar University, Patiala

ACKNOWLEDGEMENT

With my aesthetic attitude of learning management to the best, I am in a state to submit this precipitous report and would like to express my gratitude to all persons and organizations who contributed directly or indirectly to this report with their support, encouragement and advice.

Acknowledgement is due first and foremost to my supervisor, Dr. Shruti Sharma, Associate Professor, Department of Civil Engineering. I am truly indebted for her advice and guidance. Her abundant knowledge in civil and construction field is a benefit for me.

This report required hard work, sincerity and devotion which I tried my best to put in this project and in turn gained a lot of knowledge and confidence from this report. The cheerful support of my friends Ashutosh Sharma, Karambir Singh, Manmeet Kaur, Harneet Singh, Manpreet Singh Nagi, Mandeep Walia , Gaurav Goel and Amandeep Mahay and Shalini Rajput are sincerely appreciated for helping me in casting, curing and testing of specimens in the laboratory.

I am also thankful to all the staff members of Civil Engineering Department for their full cooperation and help.

Above all, I thank my parents and sister whose love and affectionate blessings have been a constant source of inspiration in making this manuscript a reality. I would like to end by saying that the people mentioned above will hold dear in my heart and will never be forgotten. Thank you all.

(Charat Singh)

ABSTRACT

At early ages of concrete structures, strength monitoring is important to determine the structure's readiness for service. Concrete setting and hardening process are the most critical phases during construction works, influencing to properties of concrete structure, so the application of efficiency non-destructive test methods for early age concrete properties determination is crucial.

In this study, apart from standardized methods like Ultrasonic Pulse Velocity, integrated approaches consisting of Ultrasonic Guided Waves and Acoustic Emission Techniques for young concrete characterization are explored. In ultrasonic method, guided wave is transmitted and received through a waveguide that is embedded in early age concrete. Whereas in Acoustic Emission arising out of the solidifying of the concrete are recorded using sensors mounted at different locations. Both the techniques are different in their nature of application, i.e., Ultrasonic Guided Wave is active in nature and Acoustic Emission Technique is passive in nature. Ultrasonic Guided Wave depends on the transmitted signal whereas the Acoustic Emission Techniques depends on the stress changes occurring inside the system.

Experiments were performed on concrete mixtures with varying water cement ratios i.e. 0.3 and 0.5. For ultrasonic guided waves, cube specimens of size (150mmx150mmx150mm) with embedded mild steel rod of 25 mm diameter and 300 mm length were used to monitor early setting and hardening (i.e. 48 hrs of hydration). And for AET, plain steel bars of diameter 12 mm were placed vertically in the same cube used for UGW. The AET system was paused while UGW reading was taken to in order to prevent the recording of noise. Also, Ultrasonic pulse velocity tests were also performed on the cubes of size 150mmx150mmx150 mm.

The focus of the study is be track every aspect of the setting and hardening process of concrete immediately after pouring of fresh concrete.

CONTENTS

LIST OF FIGURES

LIST OF TABLES

CHAPTER 1
INTRODUCTION

1.1 General

Setting and hardening of fresh concrete are the most critical phases during the construction works, on which depend properties of concrete structure during its service life. During setting process, concrete mixture transforms from fluid state whose properties is important for placing into formworks into solid whose properties are important for the proper behavior of material in the service. Control of hardening phenomena can be used for determination of right moment for formwork removal, or load the structure. So, knowledge of fresh and young concrete is important from both, technical and economical aspects. It follows that accurate and useful testing methods for properties of young concrete properties determination are of great interest.

Conventional testing methods for fresh concrete and mortar properties determination are slump cone test, flow table test, penetration needle test, Vicat apparatus test, hydration temperature measurement, and for young concrete pull-out test. Main drawback of these methods is missing of continuous measurement data. Rheological testing methods which use different types of viscometers mainly isn't successful because apparatus acts to fresh concrete with shear forces which destroy microstructure in the early ages of hydration process.

For this very purpose, various NDT methods like UPV monitoring, UGW monitoring, Fiber optics, Acoustic Emission monitoring etc. are being researched and developed. The main advantage of NDT methods over conventional techniques is that they are able to gives us the continuous in-situ data about the various changes that are taking place inside the concrete. And also, they have an advantage over the fact that the specimens need not to be destroyed for the monitoring purposes.

1.2 Setting and hardening of concrete

Setting time is defined as the transition from a fluid state to a plastic state. The stiffening of the concrete after it has been placed. A concrete can be 'set' in that it is no longer fluid, but it may still be very weak; for example, you may not be able to walk on it. Setting is due to early-stage calcium silicate hydrate formation. The terms 'initial set' and 'final set' are arbitrary definitions of early and later set; there are laboratory procedures for determining these using weighted needles penetrating into cement paste.

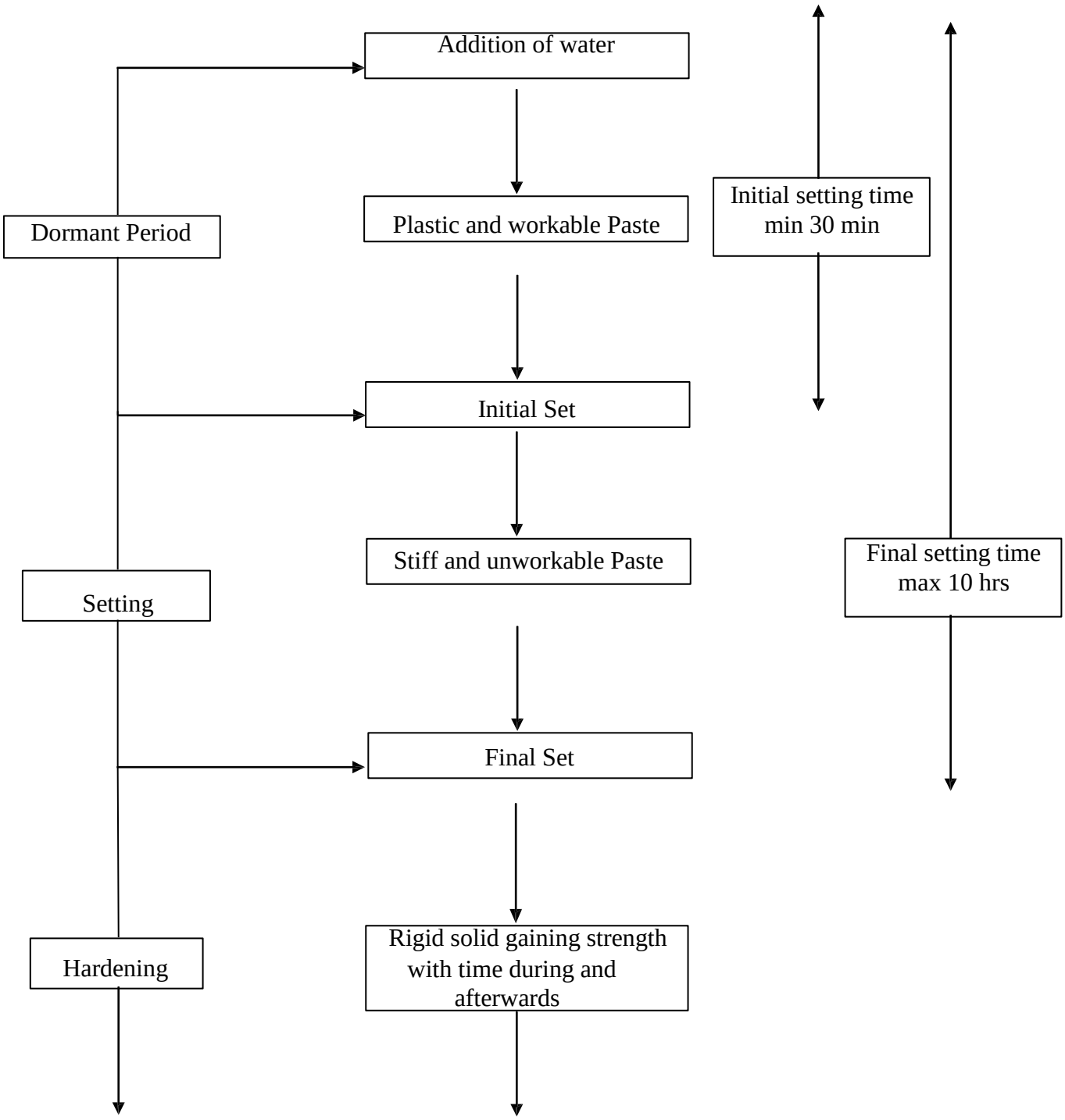

Fig 1.1 Schematic description of setting and hardening of a cement paste

This transition can occur in less than one hour or could take up to 24 hours. Initial set of cement paste is defined as the time when the paste has gained enough rigidity to no longer be in a fluid state. The final setting time is when rigidity has increased to a point that the paste becomes a solid of very low strength. In general, cement exhibit initial set in 2 to 4 hours and final set in 5 to 8 hours. Final set is then followed by substantial increases in strength, referred to as the hardening stage.

Hardening is the process of strength growth and may continue for weeks or months after the concrete has been mixed and placed. Hardening is due largely to the formation of calcium silicate hydrate as the cement hydrates. Hardening time is when concrete has a sufficient bearing capacity to support construction loads. This hardening of concrete may occur in a few hours, or could take up to 2-3 weeks.

Factors that affect the setting and hardening time include, but are not limited to

- Type and amount of cementitious material (cement and fly ash).
- Water content.
- Presence of admixtures (accelerators, air entrainers, and water reducers)
- Volume of fill.
- Properties of surrounding soil (permeability and degree of saturation).
- Ambient temperature and
- Curing conditions.

The complete process of how concrete early setting and hardening takes place has been shown in **Fig 1.1.**

1.3 Motivation and Physical Background

Modern concrete technology faces several challenges:

- There is a great demand by the design engineer for high-strength concrete, high-performance concrete, fiber concrete.
- Contractors are demanding for highly workable concrete, self-levelling concrete, slip formed concrete, retarded mixes.
- There is less workmanship on the construction site available.

- there is increasing quality required for durable concrete structures in an aggressive environment.

The materials producers have a basket full of admixtures and additions which are deemed to affect the fresh or the hardened state of concrete. The user is sometimes inclined to combine various products in order to achieve the maximum success. However, not all mixtures lead to the expected result.

An advanced process technology needs proper control by reliable and - as much as possible - objective measurements. A possible solution is the ultrasonic technique, where amplitude-, velocity- and frequency-variations depending on the age of the mortar can be observed during the hardening process. The properties of cementitious materials are changing from a suspension to a solid during the stiffening process caused by the hydration of the cement-matrix. Biot‟s theory (Biot,1956) describes the physical properties of this class of materials in an adequate way. Based on this approach, using wave propagation theory, it became obvious that ultrasound experiments measuring elastic waves in Pulse-transmission are able to characterize the material during the stiffening process.

Although the whole waveform is representing the material properties, for quantitative analysis techniques some parameters have to be extracted out of the signals recorded by a measuring device. Parameters that are easy to determine are the velocity (extracted by measuring the onset time of the signals knowing the travel path of the wave), the energy (calculating the integral sum of the wave amplitudes) and the frequency content (using Fast-Fourier-Transform techniques). One has to keep in mind that there are, of cause, also several other parameters that can be used. Even though one single wave parameter could be sufficient to characterize the material, the reliability of the method in increased by evaluating more than one.

Till now various NDT techniques like UPV, Penetration Test, Rebound hammer, piezoelectric transducers etc have been used but very less work is done in monitoring early age strength and hardening of concrete using NDT of Ultrasonic guided wave(UGW) techniques and Acoustic emission technique(AET). The objective of this research effort is the comparison of these two NDT for effectively monitoring the setting of concrete and compare the two techniques.

1.4 Various NDT Methods for Concrete

The following methods, with some typical applications, have been used for the NDT of concrete:

Visual inspection, which is an essential precursor to any intended non-destructive test. An experienced civil or structural engineer may be able to establish the possible cause(s) of damage to a concrete structure and hence identify which of the various NDT methods available could be most useful for any further investigation of the problem.

Half-cell electrical potential method, normally involves measuring the potential of an embedded reinforcing bar relative to a reference half-cell placed on the concrete surface. The half-cell is usually a copper/copper sulphate or silver/silver chloride cell but other combinations are used. The concrete functions as an electrolyte and the risk of corrosion of the reinforcement in the immediate region of the test location may be related empirically to the measured potential difference. In some circumstances, useful measurements can be obtained between two half-cells on the concrete surface.

Schmidt/rebound hammer test, is principally a surface hardness tester. It works on the principle that the rebound of an elastic mass depends on the hardness of the surface against which the mass impinges. There is little apparent theoretical relationship between the strength of concrete and the rebound number of the hammer.

Carbonation depth measurement test, used to determine whether moisture has reached the depth of the reinforcing bars and hence corrosion may be occurring. Carbonation of concrete occurs when the carbon dioxide, in the atmosphere in the presence of moisture, reacts with hydrated cement minerals to produce carbonates, e.g. calcium carbonate. The carbonation process is also called depassivation. Carbonation penetrates below the exposed surface of concrete extremely slowly.

The significance of carbonation is that the usual protection of the reinforcing steel generally present in concrete due to the alkaline conditions caused by hydrated cement paste is neutralized by carbonation. Thus, if the entire concrete cover over the reinforcing steel is carbonated, corrosion of the steel would occur if moisture and oxygen could reach the steel.

Permeability test, used to measure the flow of water through the concrete. Permeability of concrete is important when dealing with durability of concrete particularly in concrete used for water retaining structures or watertight sub-structures. Structures exposed to harsh

environmental conditions also require low porosity as well as permeability. Such adverse elements can result in degradation of reinforced concrete, for example, corrosion of steel leading to an increase in the volume of the steel, cracking and eventual spalling of the concrete. Permeability tests measure the ease with which liquids, ions and gases can penetrate into the concrete. *In situ* tests are available for assessing the ease with which water, gas and deleterious matter such as chloride ions can penetrate into the concrete.

Penetration resistance or Windsor probe test, like the rebound hammer, is a hardness tester, and its inventor's claim that the penetration of the probe reflects the precise compressive strength in a localized area is not strictly true. However, the probe penetration does relate to some property of the concrete below the surface, and, within limits, it has been possible to develop empirical correlations between strength properties and the penetration of the probe.

Covermeter testing, used to measure the distance of steel reinforcing bars beneath the surface of the concrete and also possibly to measure the diameter of the reinforcing bars.

Radiographic testing, used to detect voids in the concrete and the position of stressing ducts. As we know the intensity of a beam of X rays or gamma rays suffers a loss of intensity while passing through a material. This phenomenon is due to the absorption or scattering of the X or gamma rays by the object being exposed. The amount of radiation lost depends on the quality of radiation, the density of the material and the thickness traversed. The beam of radiation, which emerges from the material, is usually used to expose a radiation sensitive film so that different intensities of radiation are revealed as different densities on the film.

Ultrasonic pulse velocity testing, mainly used to measure the sound velocity of the concrete by passing ultrasonic waves and hence the compressive strength of the concrete.

Ultrasonic methods, using an instrumented hammer or transducers to produce ultrasonic guided waves inside the concrete specimen or a wave guide providing both sonic echo and through transmission methods.

Acoustic emission technique, in which the changes on the atomic levels of the materials are being detected through sound waves using a series of sensors mounted on the material.

1.5 Review of Literature for Monitoring Setting of Mortar and Concrete Using NDT Techniques

Guang et al. (2001) conducted an ultrasonic experimental set-up to monitor the development of the microstructure of fresh concrete at different temperatures (isothermal curing at 10,20,30 and 50^{o} C) and water/cement ratios(0.40,0.45 and 0.55). The Ultrasonic Pulse velocity (UPV) was used as an indication for microstructure development of concrete at early age. The results indicated that the ultrasonic pulse velocity largely depends on the water/cement ratio and state of hydration during first 24 hours. The numerical cement hydration simulation model HYMOSTRUC was also used for investigating the relation between the change of microstructure and evolution of ultrasonic pulse velocity. The result indicated the relation between ultrasonic pulse velocity and compressive strength is almost linear at early stage. Thus it was concluded that ultrasonic pulse velocity method is proved to be applicable in the recording and monitoring the microstructure development and strength at early stage.

Reinhardt & Grosse (2003) studied the two main properties of cementitious mortar and concrete, i.e. rheology and setting and hardening. A testing device was developed which utilizes the velocity of ultrasound (US)-waves in order to continuously monitor the setting and hardening of cementitious materials. Two development steps were emphasised, i.e. the design of the container and the exact determination of the transmitted Ultrasonic-pulse. It was shown that the method leads to very reproducible results. The results showed that the beginning of setting can be determined from the velocity vs. age of mortar curve by a mathematical procedure, the final setting is still due to empirical experience. It was concluded the method is adjustable to concrete and can also be used for other materials like gypsum, lime, starch and other stiffening materials. The paper also suggested, it can be used for quality control in production of admixtures and new binders and for control of constancy of concrete production.

Lee et al. (2004) observed that the present standard test available for the setting times of concrete is the penetration resistance test specified by ASTM C403. This test, while good for standard concrete mixtures, may not be appropriate for high-performance concrete (HPC)

because of the high viscosity of the mortar. To address this issue, the ultrasonic pulse velocities (UPV) were measured using an ultrasonic monitoring system during the first 24 hrs of age for mortar and concrete specimens having various water-to-cementitious materials (w/cm) ratios and with and without fly ash (FA). Various characteristics observed from the measured UPV agreed with the previous theory of cement hydration, which describes the mixture as viscous suspension transforming into saturated porous solid phase. It was also found that the development of UPV in concretes, particularly without FA, was faster than that of mortars with the same w/cm. The values of concrete UPV corresponding to the initial and final setting (ASTM C403) didn‟t showed a trend consistent with those of mortar UPV. Two alternative criteria were applied to determine the setting characteristics from the UPV evolution curves. They were found to better represent the microstructural changes than the penetration method, as suggested by the consistent trend with decreasing w/cm among various mortars and concretes. Thus, the potential use of these alternative methods was suggested by specifying, at each w/cm, general target UPVs that are valid for both mortar and concrete with or without FA. It was finally concluded that the methods and monitoring device used in this research were useful for the in-situ monitoring of the setting of concrete, particularly in HPC.

Mikulić et al. (2005) studied the importance of non-destructive test methods like ultrasound methods for monitoring young concrete setting and hardening process which are the most critical phases during construction works .This paper shows how Ultrasonic waves can propagate through media as transversal, longitudinal and Rayleigh waves. With ultrasonic methods, it is possible to determine the kinetics and degree of hydratation, setting time, compressive strength and dynamic modulus of elasticity (Sekulić D. et al., 2004). In this paper measurements of longitudinal compressive wave velocity through concrete and mortar during hardening process were performed. For mixtures preparation different additives were used. Obtained results indicate possibility for hardening process monitoring and time of cementitous materials setting determination.

Dhonde et al. (2006) studied Piezoelectric-based strength monitoring methods which provided an innovative experimental approach to conduct concrete strength monitoring at early ages. In this paper piezoelectric transducers in the form of „smart aggregates‟ were embedded into the concrete specimen during casting. Piezoceramic materials were used as actuators to generate

high frequency vibrating waves, which propagated within concrete structures; meanwhile, they were also used as sensors to detect the waves. The strength development of concrete structures was monitored by observing the development of harmonic response amplitude from the embedded piezoelectric sensor at early ages. From experimental results, it was found out that the amplitude of the harmonic response decreases with increasing concrete strength, as concrete strength increases at a fast rate during the first few days and at a decreasing rate after the first week. Concordantly, the amplitude of the harmonic response from the piezoelectric sensor drops rapidly for the first week and continues to drop slowly as hydration proceeds, matching the development of the concrete strength at early ages. In this paper, a fuzzy logic system is trained to correlate the harmonic amplitude with the concrete strength based on the experimental data. The experimental results showed that the concrete strength estimated by the trained fuzzy correlation system matches the experimental strength data. The proposed piezoelectric-based monitoring method had the potential to be applied to strength monitoring of concrete structures at early ages.

Robeyst et al. (2007) studied the setting of fresh mortar and concrete samples, made with Portland cement and four types of blast-furnace slag cement. The early age properties of mortar and concrete samples were continuously monitored with the ultrasonic wave transmission method. A revised measurement setup with new sensors and a preamplifier improved the quality of the acquired signal at very early age. The evolution of the velocity and frequency spectrum of the ultrasonic wave was investigated and compared with the results of traditional methods, such as penetrometer tests.

The results lead to the conclusion that characteristic points in the graphs of penetration resistance and the ultrasonic velocity curves are correlated.

Chang and Lien (2008) utilized the impact pulse velocity nondestructive method to estimate the compressive strength of the concrete at early age. The results concerning the correlation between the compressive strength at early ages of concrete and that hardened under standard conditions. The relationship of pulse velocity and strength were established for concrete but they were controlled under various water-cement ratio. The result highlighted that Pulse velocity correlates well with strength at early ages but was insensitive to increases in compressive strength after concrete curing. This paper also discusses the influence of the curing time in concrete and

water-cement ratio on the coefficients of variation of the compressive strength deduced both in a destructive and nondestructive methods. Lastly, it was concluded that accuracy of compressive strength estimation can be predicted by the impact method.

Darquennes et al. (2009) conducted three different techniques to study the evolution of the setting and the hardening of concrete which were later compared: (1) ultrasonic monitoring using the FreshCon system, (2) a resistivity method and (3) the mechanical Kelly-Bryant method. The experimental tests were carried out on two slag cement concretes in order to compare these methods and to evaluate their ability to monitor continuously the setting and hardening process of concretes with different slag content in the cement. Globally, the initial setting age values given by the three methods was in good agreement, but only the two non-destructive methods (ultrasonic and electric) allow determining the final setting. However, it was concluded that the three methods were complementary and the nondestructive methods give additional information (like chemical reactions, stiffness evolution) about the hydration process of cementitious materials. They were also able to tackle the differences in the setting behaviour due to the slag content in the cement.

Muhammad et al. (2009) studied the setting and hardening properties for understanding the green concretes behaviour at early age. The setting and hardening behaviour since casting time of six green concrete mixtures containing high percentage of mineral additions were monitored by applying non-destructive ultrasonic waves. During the test, the ultrasonic velocity, the energy and the frequency spectrum (FFT algorithm) evolution as function of concrete age were computed. The point corresponding to the first inflexion point on the velocity vs. age plot was related to the initial setting time. Tests were carried out at two temperatures (20°C and 10°C) for six mixtures proportions : a reference concrete with Portland cement and the others containing various proportions of blast furnace slag (30%, 50% and 75% of the binder mass content) and fly ash (30% and 50%). In order to check the results obtained with the ultrasonic method, the initial setting time was compared with the Kelly Bryant method. It was concluded that the initial setting measured by the ultrasonic velocity coincides rather well with the time of increase of the pulling force by Kelly Bryant method & increase in mineral addition content delays the setting phenomenon, in case of slag due to its latent hydraulic property and due to slow pozzolanic reaction in fly ash. Result also showed that initial temperature has an inverse effect on the setting of concrete, lower temperature delays the setting notably.

Nicolas & Nele (2009) noted that research on ultrasonic methods to monitor the setting of concrete has mainly focused on the wave velocity as a useful quantity. So in order to investigated the application of wave energy as a parameter, the ultrasonic wave transmission technique was performed on several concrete and mortar samples in which increasing amounts of the Portland cement was replaced by blast-furnace slag or fly ash. The transmitted ultrasonic wave energy was calculated as the sum of the squared amplitudes of the received signal, divided by the reference energy (E/Eref). The increase of the energy during setting was retarded if ordinary Portland cement was replaced by blast-furnace slag or fly ash. The final setting determined by the standard penetration resistance test occurred shortly after the peak in the derivative curve of the ultrasonic energy. In addition, the values E/Eref = 0.02 and 0.15 were proposed to easily calculate respectively initial and final setting based on the ultrasonic energy measurements. Due to the sensitivity of the energy measurement to the quality of the sensor contact, it was suggested that care should be taken to limit drying shrinkage of the cementitious samples.

Zhu & Kee (2010) noted that conventional ultrasonic setups typically measure longitudinal (P) waves in fresh cement pastes and need access two sides of the specimen. This type of setup was not suitable for in-situ field testing. In this study, embedded piezoelectric bender elements were used to generate and measure both P and shear (S) waves in fresh cement pastes. The shear waves were observed at very early age of the cement hydration. The velocities of P and S waves are obtained from B-scan images of a collection of recorded signals over time. Experimental results indicate that the shear wave velocity was closely related to the setting time of cement pastes and less affected by air contents than the P wave velocity. Shear modulus and Poisson‟s ratios of the cement pates were derived from the measured P and S wave velocities.

Lee & Tawie (2010) studied the advances in piezoelectric materials to develop new nondestructive evaluation and monitoring techniques. In this study, piezoceramic (PZT) sensors were embedded in concrete by bonding the sensors on steel reinforcing bars to perform non-destructive monitoring. To evaluate the performance of the PZT sensors and electromechanical impedance (EMI) sensing technique, a series of experiments were carried out to monitor the bond development between steel rebar and concrete by measuring the electrical response of the

PZT bonded to the steel rebar using an impedance analyzer. From the EMI measurements, the gradual adhesion between the steel rebar and fresh concrete was detected via the measured changes in the conductance spectra of the PZT sensor bonded to the steel rebar. The bond development could be attributed to the transformation of concrete from liquid to solid state controlled by the hydration of cement and by monitoring the hydration of concrete with respect to time, the status of bonding was estimated. The results showed that the early-age development of bonding between steel rebar and concrete is affected by various factors such as varying water–cement ratio, low curing temperature and poor compaction.

Pazdera et al. (2010) studied concrete properties during early age process. It was made clear that fissuring is mainly during early age. Some nondestructive testing methods such as Acoustic Emission Method and Nonlinear Spectroscopy were applied which indicate interesting results. The results concluded that Acoustic emission, Non-linear (ultrasonic) spectroscopy or Impedance spectroscopy are suitable tools for monitoring concrete structure over its lifetime. Using these methods simultaneously brought better evaluation of micro changes into concrete structure from its making.

Sharma & Mukherjee (2014) demonstrated an ultrasonic, in-situ guided wave monitoring technique for studying the setting characteristics of freshly poured concrete with varying workabilities. The solidification and curing of freshly poured concrete is monitored through the propagation of ultra-sonic waves in embedded steel reinforcing bars. As concrete solidifies and cures, more wave energy escapes into the surrounding solidifying concrete resulting in signal attenuation. Two types of concrete specimens are prepared – one with moderate slump (80 mm) named as Conventional Concrete (CC) and other with high slump (675 mm) referred as Self-Compacting Concrete (SCC) and are monitored with carefully selected ultrasonic signal patterns. Destructive tests such as compressive strength and reinforcement pullout strength are also performed at different stages of setting of the two concrete types. Relationships for estimating the strengths from ultrasonic tests are developed. The ultrasonic guided waves are very promising for discerning the early age characteristics of concrete with varying workabilities.

Sharma & Mukherjee (2015) studied that concrete can be judged a great deal from its properties when it is freshly poured. This paper demonstrates an ultrasonic in-situ monitoring technique for

freshly poured concrete. The solidification and curing of freshly poured concrete is monitored through the propagation of ultrasonic waves in waveguides such as steel reinforcing bars. As concrete solidifies and cures, more wave energy escapes into the surrounding concrete resulting in signal attenuation. RC beam specimens are monitored with carefully selected ultrasonic signal patterns during the first 24 h of setting of concrete. Destructive tests such as bar pull out and compressive strength are also performed at different stages of setting of concrete. The ultrasonic signals have been calibrated for determination of early age concrete properties.

1.6 Objective of the Research

The purpose of this research is to investigate the feasibility of using ultrasonic guided waves and Acoustic emission technique for characterizing the setting of early age cementitious materials. The research is the first step forward in monitoring the setting and hardening of in-place concrete. The objective of using new methods of Ultrasonic Guided Wave and Acoustic Emission Technique the work can be summarized as follows:

- Provide an integrated ultrasonic guided wave technique and Acoustic emission technique to monitor early age setting & strength of concrete.
- To relate the ultrasonic guided wave and acoustic emission technique measurements with established techniques of ultrasonic pulse velocity and destructive test of strength.
- Provide information that can be used to estimate and evaluate the setting with strength development process of concrete for safe and efficient construction practices.

1.7 Closing Remarks

This chapter gives a general aspect and introduction about the early age strength and hardening of concrete. The motivation behind this report and physical background of monitoring young concrete has been emphasized. Various NDT techniques for monitoring concrete & main objective of thesis have also been highlighted.

The next chapter will throw light on the various details particularly to the use ultrasonic guided waves as a tool for NDT.

CHAPTER 2
ULTRASONICS AS NDT TOOL

2.1 Fundamentals of Ultrasonic Waves in Media

It is known that frequency range of sound audible to humans is approximately 20 to 20,000 Hz (cycles per second). Ultrasound is simply sound that are above the frequency range of human hearing. When a disturbance occurs at a portion in an elastic medium, it propagates through the medium in a finite time as a mechanical sound wave by the vibrations of molecules, atoms or any particles present. Such mechanical waves are also called elastic waves. Ultrasound waves or ultrasonic waves are the terms used to describe elastic waves with frequency greater than 20,000 Hz and normally exist in solids, liquids, and gases. A simple illustration of the ultrasonic waves produced in a solid is shown in **Fig. 2.1**, where distortion caused depending on whether a force is applied normal or parallel to the surface at one end of the solid can result in producing compression or shear vibrations, respectively, so that two types of ultrasonic waves, i.e. longitudinal waves or transverse waves, propagate through the solid. The energy of the wave is also carried with it.

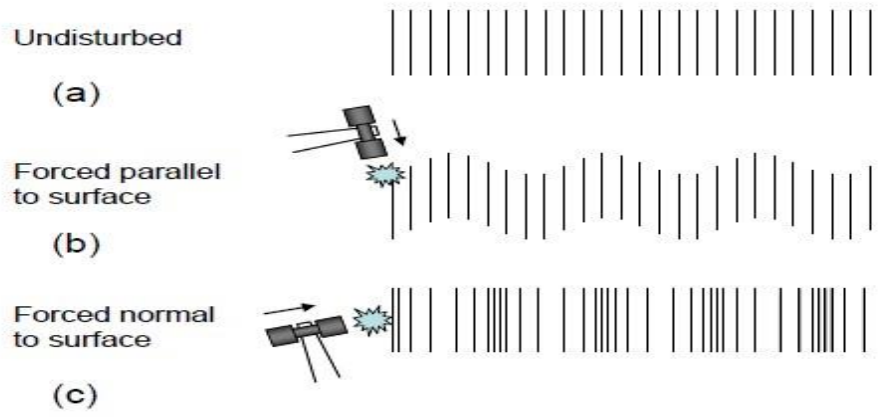

Fig. 2.1 Schematics of ultrasonic waves in a bulk specimen: (a) equilibrium state with no disturbance, (b) waves relating to shear (transverse) vibrations (c) waves Relating to longitudinal vibrations. (http://www.googleimages.com)

In a continuous medium, the behavior of ultrasonic waves is closely related to a balance between the forces of inertia and of elastic deformation. An ultrasonic wave moves at a velocity (the wave velocity) that is determined by the material properties and shape of the medium, and occasionally the frequency. The ultrasonic wave imparts motion to the material when it propagates. This is referred to as particle motion, to distinguish it from the wave motion. This particle motion is usually specified as a particle velocity *v*. It is noted in ultrasonic measurements that the particle velocity is much smaller than wave velocity. Also, one can understand that no ultrasonic wave propagates in vacuum because there are no particles that can vibrate in vacuum.

2.2 Basic Concepts of Wave Propagation

2.2.1 Some Common Terms Used:

• **Sound Waves:** Sound waves are simply organized mechanical vibrations traveling through a medium, which may be a solid, a liquid, or a gas. These waves will travel through a given medium at a specific speed or velocity, in a predictable direction, and when they encounter a boundary with a different medium they will be reflected or transmitted according to simple rules. This is the principle of physics that underlies ultrasonic flaw detection.

• **Frequency:** All sound waves oscillate at a specific frequency, or number of vibrations or cycles per second, which we experience as pitch in the familiar range of audible sound. Human hearing extends to a maximum frequency of about 20,000 cycles per second (20 KHz), while the majority of ultrasonic flaw detection applications utilize frequencies between 500 KHz to 10 MHz. At frequencies in the Megahertz range, sound energy does not travel efficiently through air or other gasses, but it travels freely through most liquids and common engineering materials.

• **Wave Speed:** The speed of a sound wave varies depending on the medium through which it is travelling, affected by the medium‟s density and elastic properties. Different types of sound waves will travel at different velocities.

• **Wavelength (λ)**: It is the distance between any two corresponding points in the wave cycle as it travels through a medium. Wavelength is related to frequency and velocity by the simple equation

$$\lambda = c/\upsilon \qquad \textbf{(2.1)}$$

Where, λ = wavelength, c = sound velocity, υ = frequency

In ultrasonic flaw detection, the generally accepted lower limit of detection for a small flaw is one-half wavelength, and anything smaller than that will be invisible. In ultrasonic thickness gauging, the theoretical minimum measurable thickness is one wavelength.

• Attenuation

When an ultrasonic wave propagates through a medium, ultrasonic attenuation is caused by a loss of energy in the ultrasonic wave and other reasons. The attenuation can be seen as a reduction of amplitude of the wave. There are some factors affecting the amplitude and waveform of the ultrasonic wave, such as ultrasonic beam spreading, energy absorption, dispersion, nonlinearity, transmission at interfaces, scattering by inclusions and defects, Doppler effect and so on. To characterize the ultrasonic attenuation quantitatively, attenuation coefficient α is defined as follows;

$$A = A_0 \cdot e^{-\alpha x} \qquad \textbf{(2.2)}$$

where A is the peak amplitude of the wave at propagation distance x, A_0 is the initial peak amplitude.

The attenuation coefficient α is experimentally determined from the variation of the peak amplitude with the propagation distance, and it can be given in decibel per meter (dB/m) or in neper per meter (Np/m). In general, the attenuation coefficient highly depends on frequency. Since this frequency dependence reflects microstructures of materials, it can be used for characterizing microscopic material properties relating to chemical reactions and mechanical processes.

• Acoustic impedance (Z)

Sound travels through materials under the influence of sound pressure. Because molecules or atoms of a solid are bound elastically to one another, the excess pressure results in a wave propagating through the solid. The Acoustic impedance (Z) of a material is defined as the product of its density (ρ) and acoustic speed in medium

$$Z = \rho V \qquad \textbf{(2.3)}$$

Acoustic impedance is important in determining acoustic transmission and reflection at the boundary of two materials having different acoustic impedances.

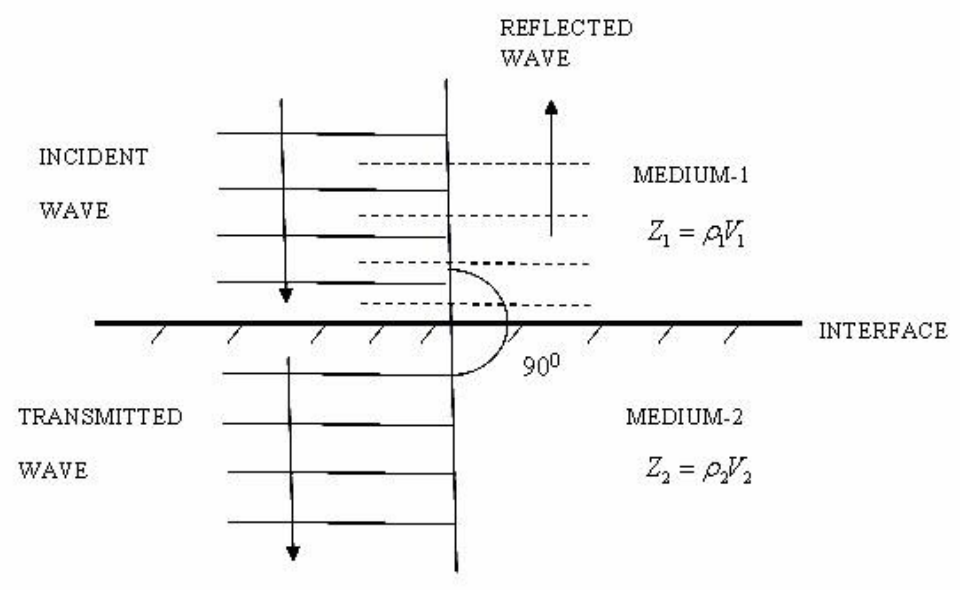

Fig 2.2 Reflection and Transmission of sound wave at normal incidence (Bindal, 1999)

• Reflection and Transmission Coefficients

Ultrasonic waves are reflected at boundaries where there is a difference in acoustic impedances (Z) of the materials on each side of the boundary as shown in the **Fig. 2.2**. This difference in Z is commonly referred to as the impedance mismatch. The greater the impedance mismatch, the greater the percentage of energy that will be reflected at the interface or boundary between one medium and another. The fraction of the incident wave intensity that is refracted can be derived because particle velocity and local particle pressures must be continuous across the boundary. When the acoustic impedances of the materials on both sides of the boundary are known, the fraction of the incident wave intensity that is reflected can be calculated with the equation below. The value produced is known as the reflection coefficient.

$$\text{Reflection coefficient, } R = \frac{Z_2 - Z_1}{Z_2 + Z_1} = \frac{\rho_2 V_2 - \rho_1 V_1}{\rho_2 V_2 + \rho_1 V_1} \quad \textbf{(2.4)}$$

$$\text{Transmission coefficient, } T = \frac{2Z_2}{Z_2 + Z_1} = \frac{2\rho_2 V_2}{\rho_2 V_2 + \rho_1 V} \quad \textbf{(2.5)}$$

2.2.2 Reflection, Refraction and Mode Conversion of Waves

When sound travels in a solid material, one form of wave energy can be transformed into another form. For example, when a longitudinal wave hits an interface at an angle, some of the energy can cause particle movement in the transverse direction to start a shear (transverse) wave. Mode conversion occurs when a wave encounters an interface between materials of different acoustic impedances and the incident angle is not normal to the interface.

When sound waves pass through an interface between materials having different acoustic velocities, refraction takes place at the interface. The larger the difference in acoustic velocities between the two materials, the more the sound is refracted. Notice that the shear wave is not refracted as much as the longitudinal wave. This occurs because shear waves travel slower than longitudinal waves. Therefore, the velocity difference between the incident longitudinal wave and the shear wave is not as great as longitudinal waves but it is between the incident and refracted longitudinal waves. Also note that when a longitudinal wave is reflected inside the material, the reflected shear wave is reflected at a smaller angle than the reflected longitudinal wave. This is also due to the fact that the shear velocity is less than the longitudinal velocity within a given material. Snell's Law holds true for shear waves as well as longitudinal waves and can be written as

$$\frac{\sin\theta_1}{VL_1} = \frac{\sin\theta_2}{VL_2} = \frac{\sin\theta_3}{VS_3} = \frac{\sin\theta_4}{VS_4} \qquad \text{.....(2.6)}$$

2.2.3 Modes of Wave Propagation:

The ultrasonic waves propagate in a number of ways in a medium. On the basis of the mode of particle displacement, these waves can be classified as given in **Table 2.1**

a) Longitudinal or Compressional waves (L-waves)

b) Transverse or Shear waves (S-waves)

c) Surface or Rayleigh waves

d) Lamb or Plate waves

e) Creeping or Head waves

Out of these longitudinal and transverse wave propagations are most important and are extensively used in ultrasonic NDT applications for Civil structures. Surface waves and Lamb waves are used for monitoring of thin plate geometries to locate surface defects.

Table 2.1 Types of Waves Propagation (http://www.ndt-ed.org)

Sr. no	Type of wave	Direction of motion of particles
1	Longitudinal or Compression waves (L-waves)	Parallel to wave direction
2	Transverse or Shear waves (S-waves)	Perpendicular to wave direction
3	Surface or Rayleigh waves	Elliptical orbit – symmetrical mode
4	Plate waves- Lamb	Component perpendicular to surface (extensional wave)
5	Plate waves- Love	Parallel to plane layer, perpendicular to wave direction
6	Stoneley (Leaky Rayleigh Waves)	Wave guided along interface
7	Sezawa	Anti symmetric mode

Longitudinal or Compressional waves:

In longitudinal waves, the oscillations occur in the longitudinal direction or the direction of wave propagation. Since compressional and dilatational forces are active in these waves, they are also called pressure or compressional waves. Compression waves can be generated in liquids, as well as solids because the energy travels through the atomic structure by a series of comparison and expansion (rarefaction) movements.

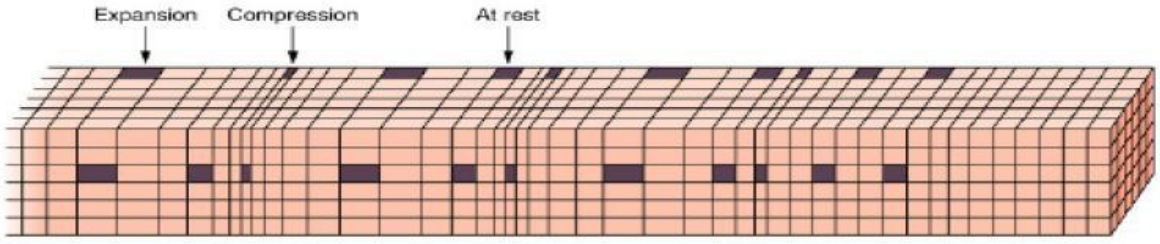

Fig 2.3 Propagation of Longitudinal waves

(http://www.googleimages.com)

Transverse or Shear waves:

In the transverse or shear wave, the particles oscillate at a right angle or transverse to the direction of propagation.

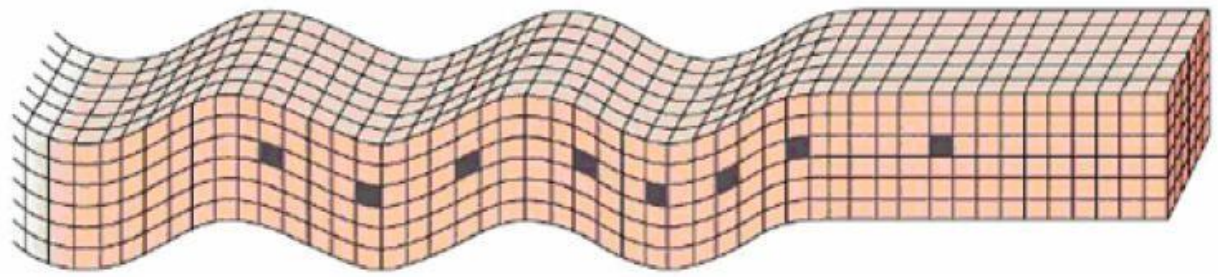

Fig 2.4 Propagation of Transverse or Shear waves
(http://www.googleimages.com)

Shear waves require an acoustically solid material for effective propagation, and therefore, are not effectively propagated in materials such as liquids or gasses. Shear waves are relatively weak when compared to longitudinal waves.

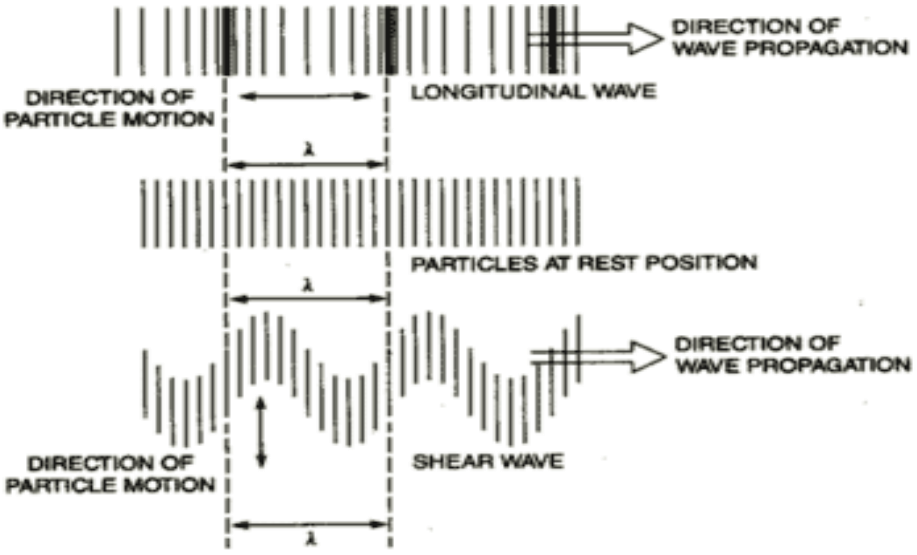

Fig 2.5 Particle Movement Showing the Propagation of Longitudinal and Shear Waves (http://www.ndt-ed.org)

Surface (or Rayleigh) waves:

Surface (or Rayleigh) waves travel the surface of a relatively thick solid material penetrating to a depth of one wavelength. The particle movement has an elliptical orbit as shown in the image below. Rayleigh waves are useful because they are very sensitive to surface defects and they follow the surface around curves. Because of this, Rayleigh waves can be used to inspect areas that other waves might have difficulty reaching.

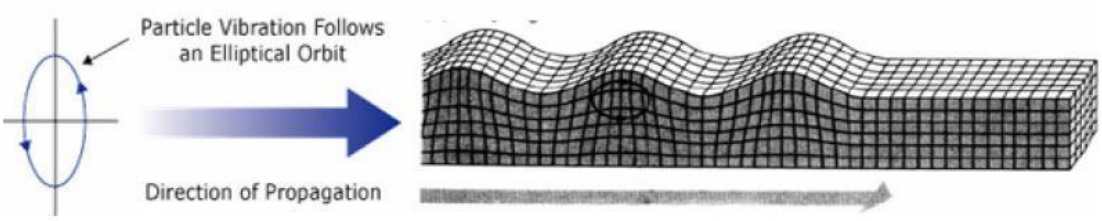

Fig 2.6 Propagation of Surface or Rayleigh Waves

(http://www.googleimages.com)

Lamb waves or Plate waves:

Plate waves can be propagated only in very thin metals. Lamb waves are the most commonly used plate waves in NDT. Lamb waves are complex vibrational waves that travel through the entire thickness of a material. Propagation of lamb waves depends on the density and the elastic material properties of a component. They are also influenced a great deal by the test frequency and material thickness.

With lamb waves, a number of modes of particle vibration are possible, but the two most common are symmetrical and asymmetrical. The complex motion of the particles is similar to the elliptical orbits for surface waves. Symmetrical lamb waves move in a symmetrical fashion about the median plane of the plate. This is sometimes called the extensional mode because the wave is "stretching and compressing" the plate in the wave motion direction. Wave motion in the symmetrical mode is most efficiently produced when the exciting force is parallel to the plate. The asymmetrical lamb wave mode is often called the "flexural mode" because a large portion of the motion moves in a normal direction to the plate, and a little motion occurs in the direction parallel to the plate. In this mode, the body of the plate bends as the two surfaces move in the same direction.

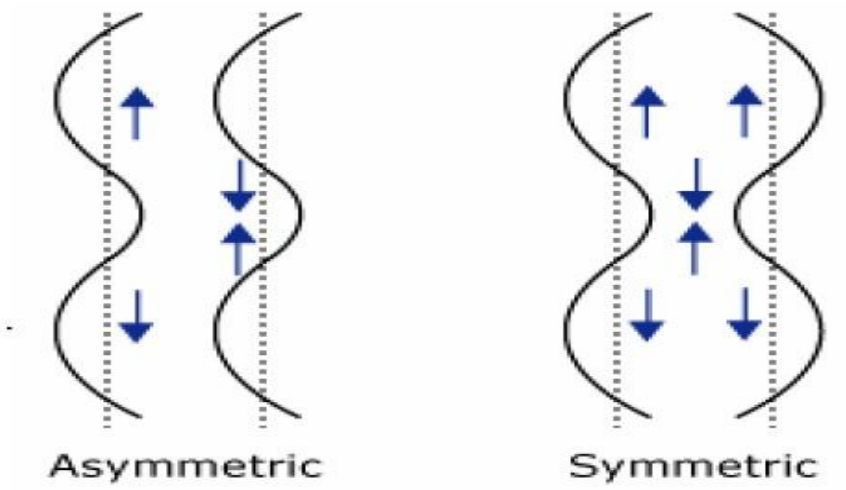

Fig 2.7 Lamb Waves Propagation (a) Symmetrical (Dilatational) and (b) Asymmetrical (Bending) waves (http://www.googleimages.com)

Creeping or Head waves:

These waves are also called head waves. The behavior of creeping waves is similar to that of longitudinal waves. They travel as fast as longitudinal waves and the creeping waves should not be misunderstood as moving slowly. These are generated parallel to scanning surface, enabling detection of surface breaking defects. These have limited range and as these travel just below the surface and not on the surface, so the couplant has no influence.

2.3 Ultrasonic Testing

2.3.1 Basic Principles of Ultrasonic Testing

Ultrasonic Testing (UT) uses high frequency sound energy to conduct examinations and make measurements. Ultrasonic inspection can be used for flaw detection/evaluation, dimensional measurements, material characterization, and more. To illustrate the general inspection principle, a typical pulse/echo inspection configuration as illustrated below in **Fig 2.8** will be used.

A typical UT inspection system consists of several functional units, such as the pulser/receiver, transducer, and display devices. A pulser/receiver is an electronic device that can produce high voltage electrical pulses. Driven by the pulser, the transducer generates high frequency ultrasonic energy. The sound energy is introduced and propagates through the

materials in the form of waves. When there is a discontinuity (such as a crack) in the wave path, part of the energy will be reflected back from the flaw surface. The reflected wave signal is transformed into an electrical signal by the transducer and is displayed on a screen. In the applet below, the reflected signal strength is displayed versus the time from signal generation to when echo was received. Signal travel time can be directly related to the distance that the signal traveled. From the signal, information about the reflector location, size, orientation and other features can sometimes be gained.

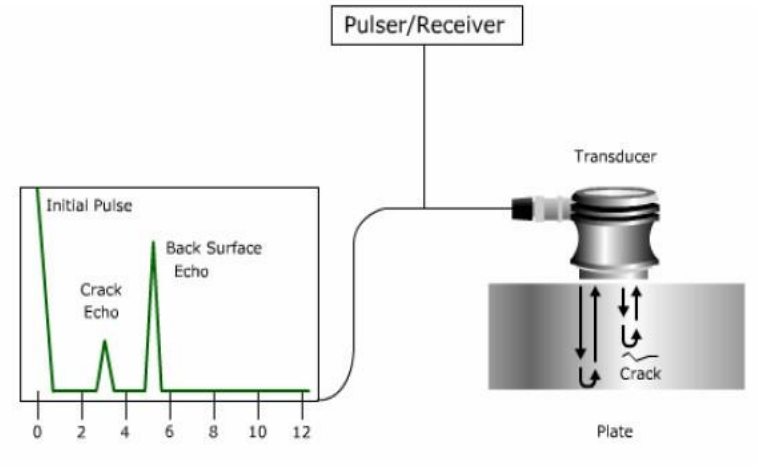

Fig 2.8 General (pulse echo method) ultrasonic Inspection Principle.

(http://www.ndt- ed.org)

2.3.2 Methods of Ultrasonic Testing

1. Pulse echo method

2. Pulse transmission method

3. Two Transducer Method

Pulse echo method

In the pulse-echo method, a piezoelectric transducer with its longitudinal axis located perpendicular to and mounted on or near the surface of the test material is used to transmit and receive ultrasonic energy as shown in **Fig 2.9**. The ultrasonic waves are reflected by the opposite face of the material or by discontinuities, layers, voids, or inclusions in the material, and received by the same transducer where the reflected energy is converted into an electrical signal. The electrical signal is computer processed for display on a video monitor or TV screen. The

display can show the relative thickness of the material, depth into the material where flaws are located, and (with proper scanning hardware and software), where the flaws are located in the X-Y plane.

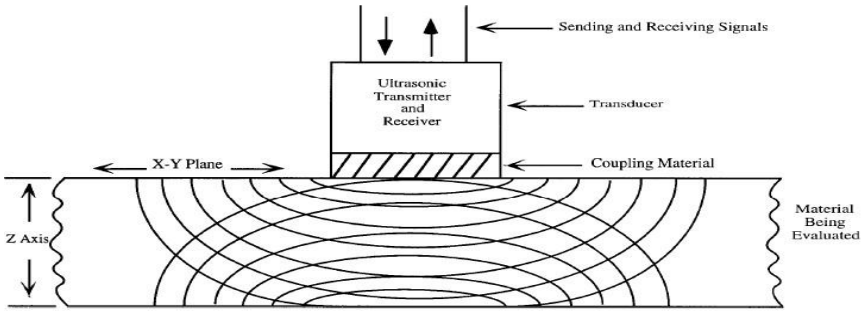

Fig 2.9 Principle of pulse echo method of inspection

(www.google.com)

Pulse-Transmission Method

In the pulse-transmission method, an ultrasonic transmitter is used on one side of the material while a detector is placed on the opposite side. One unit acts as transmitter and the other unit as receiver. The beam from the transmitter T travels through the material to its opposite surface where the receiving transducer R is placed as shown in **Fig 2.10**. Scanning of the material using this method will result in the location of defects, flaws, and inclusions in the X-Y plane.

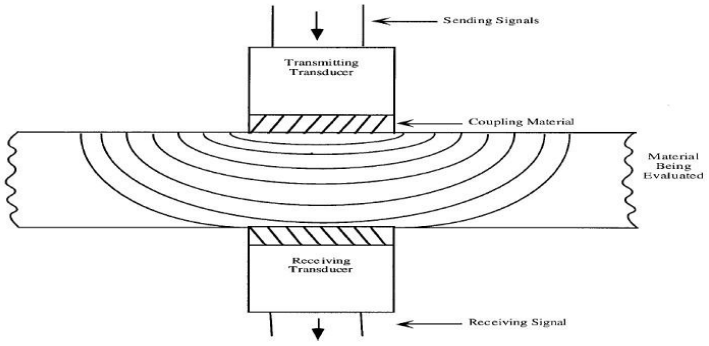

Fig 2.10 Principle of through transmission of ultrasonic testing

(www.google.com)

Two Transducer Method

The pulse echo method can be used with either single or double crystal unit in single transducer unit the probe acts as both transmitter and receiver .In two transducer arrangement, one transmits

and other receives the ultrasonic waves .These are placed on same side of specimen and pulse wave is send in to the specimen by the transducer T (Transmitter) and the echoes reflected from the back surface or any defect are received by the transducer R (Receiver) and displayed on the flaw detector screen. For specific applications like wall thickness measurement special type of transducers in which the transmitting and the receiving crystals are housed in a single unit are also used .These transducers are popularly known as „twin" or T-R probes. For example, **Fig 2.11** in which two transducers are placed on the same side of the plate at certain angle to detect the damage.

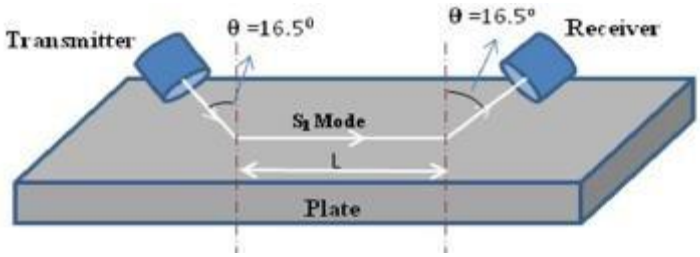

Fig 2.11 Transducers arranged at an angle to the Plate
(http://www.googleimages.com)

2.4 Classification of Ultrasonic Waves for NDT Applications

Ultrasonic waves can be classified in two types depending upon the NDT applications;

- Body waves or bulk waves
- Surface waves or guided waves.

Body waves propagate through a bulk material, hence attenuate, while the surface waves propagate along the surface of a body as shown in **Fig 2.12**. The inspection of large structures using conventional ultrasonic bulk wave (*longitudinal and shear waves)* techniques is slow because scanning is required if the whole structure is to be tested.

Surface waves are often called guided waves because the geometry of the body guides them. Ultrasonic guided waves (*Rayleigh and Lamb waves, bar, plate and cylindrical guided waves)* potentially provide an attractive solution to this problem because they can be excited at one location on the structure and will propagate many meters (Cawley.2002).Guided waves refer

to mechanical (or elastic) waves in ultrasonic and sonic frequencies that propagate in a bounded medium (such as pipe, plate, rod, etc.) parallel to the plane of its boundary.

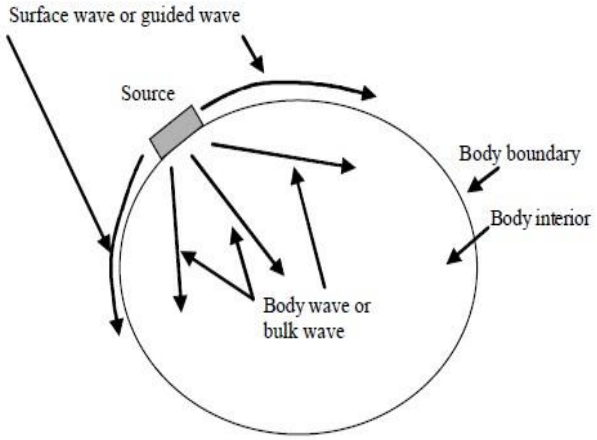

Fig 2.12 Body waves and surface waves generated by an ultrasonic source (Kundu, 2007)

Guided waves can further be classified into following types, as shown in **Fig 2.13**:

- Bar waves
- Cylindrical wave
- Rayleigh waves
- Lamb waves
- Rayleigh-Lamb waves

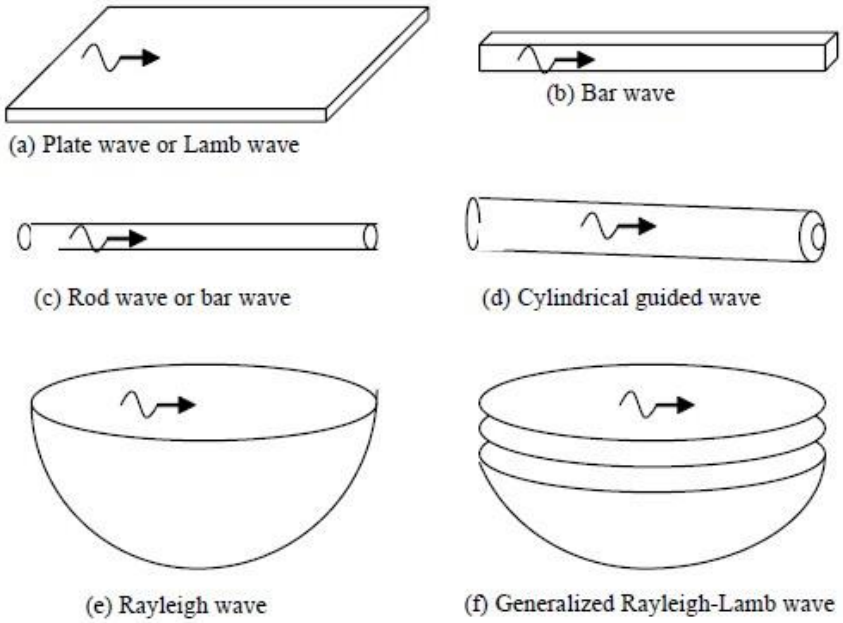

Fig 2.13 Different types of guided waves in various problem geometries (Kundu, 2007)

Cylindrical Guided Waves: Elastic waves propagating through a hollow cylinder or pipe are called cylindrical guided waves (**Fig 2.13(d))**. Since for a cylinder the two stress-free surfaces-inner and outer surfaces – are parallel to each other as in a plate, sometimes the cylindrical guided waves are also called Lamb waves.

Bar waves: When guided waves propagate through a rod or bar they are known as bar waves (**Fig 2.13(c))**.

Rayleigh wave: If the structure is a homogenous half-space then the guided wave propagating along the surface of the half-space is called Rayleigh wave (**Fig 2.13(e))**.

Lamb waves: Waves propagating through a plate type structure with two parallel stress-free boundaries are known as Lamb waves, again named after its inventor. Lamb waves are also known as plate waves because they propagate through plates (**Fig 2.13(a))**.

Rayleigh-Lamb waves: Waves propagating parallel to the free surface of a multilayered solid half-space are known as generalized Rayleigh-Lamb waves or simply Rayleigh waves (**Fig2.13(f))**.

2.5 Ultrasonic Guided Waves

In an infinite isotropic solid medium only two types of independent wave propagation exist, i.e., compressional and shear waves. Both waves propagate with constant velocities and are non-dispersive. When geometry constraints are introduced and the dimensions are close to the wavelength, the wave becomes dispersive and is called a guided wave (Reis et al,2005).

In an infinite bulk of a perfectly elastic material, ultrasonic waves travel as bulk waves, decaying in amplitude because of the spread of the wave front. However, in a finite perfectly elastic medium, the sound wave is reflected from the structure boundaries, and the energy is contained within the elastic medium as a guided wave, which propagates with constant amplitude.

To think of the utilization of ultrasonic guided waves we can consider a variety of different natural wave guides as outlined in **Table 2.2**. Guided wave inspection is a natural for any of these structures so when you really think about it guided waves can be applied to many, many structures very quickly and efficiently.

Table 2.2: Natural Waveguides (Rose,2004)

Plates (aircraft skin)
Rods (cylindrical, square, rail, etc.)
Hollow cylinder (pipes, tubing)
Multi-layer structures
Curved or flat surfaces on a half-space
Layer or multiple layers on a half-space
An interface

Table 2.3: Benefits of Guided Waves over Bulk waves (Rose, 2004)

Inspection over long distances from a single probe position
By mode and frequency tuning, to establish wave resonances and excellent overall defect detection and sizing potential.
Often greater sensitivity than that obtained in standard normal beam ultrasonic inspection or other NDT techniques. (Beam focusing is on the horizon for even improved sensitivity.)
Ability to inspect hidden structures and structures under water, coatings, insulations, and concrete with excellent sensitivity.
Cost effectiveness because of inspection simplicity and speed.

An understanding of the basic wave mechanics and wave propagation principles for various sensors and mode types is essential, though, if one is to carry out some reliable tests. The benefits of guided waves are illustrated in **Table 2.3**. The most interesting one of course is to be able to inspect over long distances from a single probe position.

The wave is termed "guided" because it travels along the medium guided by the geometric boundaries of the medium. Since the wave is guided by the geometric boundaries of the medium, the geometry has a strong influence on the behavior of the wave (Redwood et al.,

1960 and Achenbach, 1975). In contrast to ultrasonic waves used in conventional ultrasonic inspections that propagate with a constant velocity, the velocity of the guided waves varies significantly with the wave frequency and the geometry of the medium. In addition, at a given wave frequency, the guided waves can propagate in different wave modes and orders (Sang-Young Kim et al., 2001). Guided waves travel either at boundaries (Surface Waves) or between the boundaries (Lamb Waves) as shown in **Fig 2.14**. Guided waves are the result of the intersection occurring at the interface between the two different materials. This interaction produces reflection, refraction and mode conversion between longitudinal and shear waves which can be predicted using appropriate boundary conditions. Guided waves are highly dependent on wavelength and frequency, and propagating guided waves can only exist at specific combinations of frequency, wave number and attenuation.

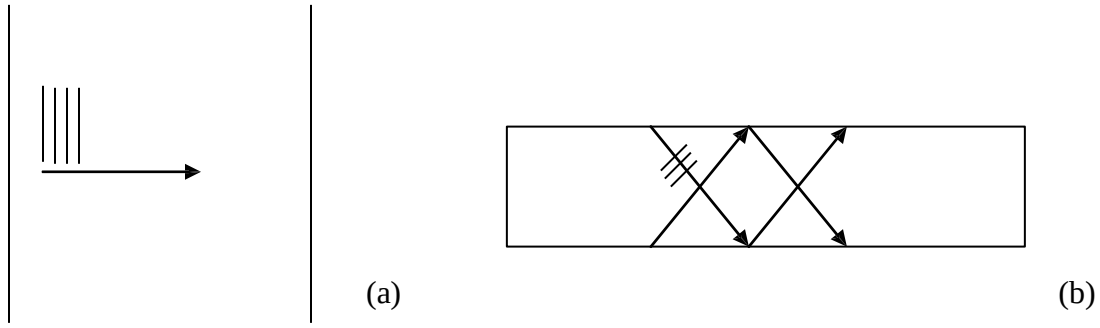

Fig 2.14 Schematic of (a) bulk wave and (b) Guided wave propagation

When the waveguide is imbedded in a solid, leakage by both longitudinal and shear waves can occur which leads to very high attenuation rates, especially when the acoustic impedances of the waveguide and the surrounding solid are similar. **Fig 2.15** shows two layers, layer one (bar) represent a finite layer and layer two (concrete) represents an infinite medium surrounding the cylinder. The partial waves (L±, SV±, SH±) combine to form a guided wave in the axisymmetric cylindrical structure.

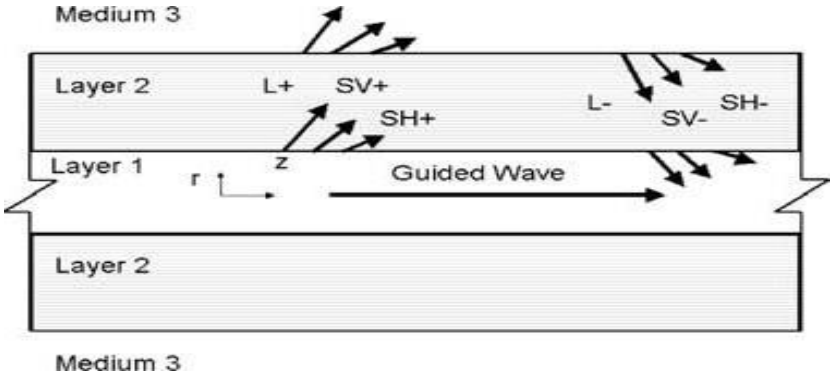

Fig 2.15 Schematic of a bar embedded in concrete (Kundu et al. 2002)

For a layered system, the solution includes phase velocity, frequency and attenuation. Attenuation is due to material absorption and energy leakage into the surrounding concrete. The waves propagate in longitudinal, flexural and torsional modes due to complex effect of boundaries and they have frequency dependant properties. In such cases specific modes can be excited selectively by choosing a frequency bound. Longitudinal waveforms have axial and radial displacements, torsional waveforms have angular displacements and flexural waveforms have all three displacements.

2.6 Literature review of ultrasonic guided waves

Lobkis et al. (1997) examined the behavior of guided elastic waves in the presence of rough surfaces. These investigations lead to a broader understanding of the phenomenon of rough-surface interactions with elastic guided waves. Extensive measurements in immersion, contact mode, and with a knife-edge coupler demonstrated the wide range of physical behaviour of elastic guided waves and their dependence on the condition of the guiding surfaces. Author configured experimental conditions to maximize the rough-surface damping contrast, by measuring below and above the Compressional critical angle.

Pavlakovic et al. (2001) studied the dispersion relationships of a system comprising a circular bar imbedded in a solid medium having a lower acoustic impedance than the bar had been predicted. A generic study of such systems have been undertaken, motivated by a particular interest in the case of a circular steel bar imbedded in cement grout which had application to the inspection of tendons in post-tensioned concrete bridges; measurements to confirm the predictions had been carried out for this case. The attenuation dispersion curves show a series of attenuation minima at roughly

equal frequency spacing. The attenuation minima occurred at the same frequencies as energy velocity maxima and they correspond to points at which the particle displacements and energy of the particular mode are concentrated towards the center of the bar so leakage of energy into the imbedding medium is minimized. The attenuation at the minima decreased with increasing frequency as the energy becomes more concentrated at the middle of the bar, until the material attenuation in the bar becomes a significant factor and the attenuation at the minima rises again. For the particular case of a steel bar in cement grout, the minimum attenuation is reached at a frequency-radius product of about 23 MHz-mm. The frequency-radius product at which the minimum attenuation is reached and the value of the minimum attenuation both increase as the acoustic impedance of the imbedding medium increases.

Kim et al. (2001) studied that long-range guided wave inspection is a new emerging technology for rapidly and globally inspecting a large area of a structure from a single test location. Also, a general overview of the guided wave properties and its application for long-range inspection of structures, the principle and instrument system for a guided wave inspection technology called "magnetostrictive sensor (MsS)" that generates and detects guided waves electromagnetically in the material under testing, and examples of long-range guided wave inspection of structures that can be accomplished using the MsS.

Kundu et al. (2001) investigated the feasibility of detecting and quantifying delamination at the interface between steel bar and concrete using ultrasonic guided waves. These waves can propagate a long distance along the reinforcing steel bar or concrete beam as guided waves are sensitive to interface bonding condition between the steel bar and concrete. The traditional ultrasonic methods are good for detecting large voids in concrete but are not efficient for detecting delamination at the interface between concrete and steel bar since they used reflection, transmission and scattering of longitudinal waves by internal discontinuities. He studied, special solid couplers between the steel bars (or concrete beam) and ultrasonic transducers had been used to launch flexural cylindrical guided waves (or lamb waves) in steel bar (or concrete). That investigation showed that the guided wave testing technique was an efficient and effective tool for health monitoring of reinforced concrete structures.

Kundu et al. (2002 a) studied the feasibility of detecting and quantifying delamination at the interface between steel bar and concrete using ultrasonic guided waves was investigated in this paper. These waves can propagate a long distance along the reinforcing steel bar or concrete beam as guided waves are sensitive to interface bonding condition between the steel bar and concrete. The traditional ultrasonic methods are good for detecting large voids in concrete but are not efficient for detecting delamination at the interface between concrete and steel bar since they use reflection, transmission and scattering of longitudinal waves by internal discontinuities. In this study, special solid couplers between the steel bars (or concrete beam) and ultrasonic transducers have been used to launch flexural cylindrical guided waves (or lamb waves) in steel bar (or concrete). This investigation showed that the guided wave testing technique was an efficient and effective tool for health monitoring of reinforced concrete structures.

Kundu et al. (2003) investigated the feasibility of detecting interface degradation and separation of steel bars in concrete beams using Lamb waves. The Lamb wave can propagate a long distance along the reinforcing steel bars embedded in concrete as the guided wave and is sensitive to the interface bonding condition between the steel bar and the concrete. The traditional ultrasonic methods for inspecting defects in concrete use reflection, transmission, and scattering of longitudinal waves by internal defects. These methods are good for detecting large voids in concrete, but they are not very efficient for detecting delamination at the interface between concrete and steel bars. He studied a special coupler between the steel bar and ultrasonic transducers had been used to launch non-axisymmetric guided waves in the steel bar. This investigation showed that the Lamb wave inspection technique is an efficient and effective tool for health monitoring of reinforced concrete structures.

Reis et al. (2005) studied the development of a wireless embedded sensor system to monitor and assess corrosion damage in reinforced concrete, reinforced mortar specimens were manufactured with seeded defects to simulate corrosion damage. Taking advantage of waveguide effects of the reinforcing bars, these specimens were then tested using an ultrasonic approach. Using the same ultrasonic approach, specimens without seeded defects were also monitored during accelerated corrosion tests. Both the ultrasonic sending and the receiving transducers were mounted on the steel rebar. Advantage was taken of the lower frequency (<250 kHz) fundamental flexural propagation mode because of its relatively large displacements at the interface between the

reinforcing steel and the surrounding mortar. Waveform energy (indicative of attenuation) was presented and discussed in terms of corrosion damage. Current results indicated that the loss of bond strength between the reinforcing steel and the surrounding concrete can be detected and evaluated.

Rokhlin et al. (2007) discussed about the sizing and locating of internal defects in fatigue samples. For the monitoring of crack initiation and evolution ultrasonic Lamb waves were excited and acquired in the sample continuously during fatigue tests at different levels of fatigue load using a high-speed data acquisition system. The cracks were localized and sized using the vertical C-scanning technique (VC-scan). The scanned ultrasonic images were compared with micro radiographic images and were found to be in good agreement. Data fusion from three NDE techniques enables one to determine the initiation times, shapes, orientations and sizes of fatigue cracks.

Reis et al. (2008) studied the guided longitudinal modes in both low (<200 kHz) and high (2– MHz) frequency ranges were invoked to monitor damage in reinforced mortar specimens undergoing accelerated uniform corrosion. The fundamental longitudinal mode, i.e. L(0, 1), and the L(0, 9) mode were invoked for low- and high-frequency testing, respectively. Because of the significant amount of axial displacement at the steel/mortar interface, the L(0, 1) mode was so appreciably attenuated for the particular specimen size used that it was not detected until after corrosion had initiated and corrosion product accumulation caused mortar cracking. Once detected, the L(0, 1) mode was sensitive to the combined effects of bond deterioration and mortar stiffness reduction. The L(0, 9) mode had negligible radial and axial displacement at the steel/mortar interface. As a result, the L(0, 9) mode was relatively insensitive to the surrounding interface conditions at high frequencies. This allows for changes in the steel cross-sectional area and bar topography to be isolated and monitored from the onset of corrosion up to severe pitting.

Ervin et al. (2009) studied the creation of an embeddable ultrasonic sensing network for assessment of reinforcement deterioration. Towards this effort, guided ultrasonic waves were used to monitor reinforced mortar specimens undergoing accelerated uniform and localized corrosion. Longitudinal waves were invoked at higher frequencies (2- 9MHz), where the attenuation is a local minimum. Using a through transmission configuration, waveforms were sensitive to both forms of

corrosion damage. Scattering, mode conversions and reflections from irregularities at the bar surface from uniform corrosion and the severely tapered cross-section from localized corrosion were thought to cause the increase in attenuation. Because localized corrosion did not yield a discontinuity that was nearly perpendicular to the bar axis, incident waves were severely scattered, mode converted and rapidly attenuated. As evidence, this was the inability of pulse-echo testing to detect reflected waveforms for the localized corrosion.

Sharma and Mukherjee (2010) discussed the use of longitudinal guided ultrasonic waves to monitor notch and debond defects in steel bars in concrete simulating pitting and de lamination phenomenon caused by corrosion. The low and high frequency ultrasonic pulse echo and pulse transmission technique was used for early detection of damages in steel in RC beams. The exact location and magnitude of damage was indicated by efficient combination of the two ultrasonic monitoring techniques. Ultrasonic guided wave monitoring utilizing specific core and surface seeking modes was applied to identify corrosion mechanism in a bar embedded in concrete. In general, huge pitting and non-uniform area loss was highlighted by severe signal attenuation marks chloride corrosion, which was well unravelled by core seeking mode. It began with de lamination shown by signal rise with surface seeking mode. It was concluded that through judicious selection of ultrasonic modes, the complete corrosion mechanism in RC structures can be successfully identified.

Sharma and Mukherjee (2011) investigated the type of corrosion mechanism in chloride and oxide environments in RC beams. Ultrasonic guided waves with specific core and surface seeking modes were used for monitoring rebar corrosion in beams. It was observed that in case of Chloride corrosion in beams, when core-seeking mode was propagated, the signal was highly attenuated, thus indicating pitting and non-uniform area loss. When surface seeking mode was propagated, there was an initial rise in the signal strength and then a fall, thus indicating delamination followed by local loss of material. In case of Oxide corrosion in beams, it was observed that when core-seeking mode was propagated, there was a slow fall in signal strength, indicating the absence of pitting. When the surface-seeking mode was propagated, there was an initial drop in the signal due to the pressure build up by the formation of corrosion products, indicating a slow corrosion rate and localized corrosion and eventually, a gradual rise in signal strength was observed, indicating slow bond deterioration. The ultrasonic voltage trends of the received signal in both chloride and oxide

corrosion specimens using surface-seeking and core-seeking mode are shown in **Fig. 2.16 (a) and 2.16 (b)** respectively.

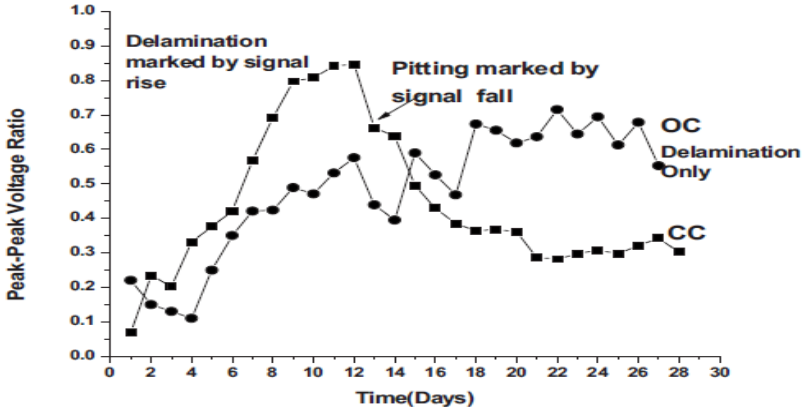

Fig.2.16 (a) Peak-peak voltage ratio with surface-seeking mode

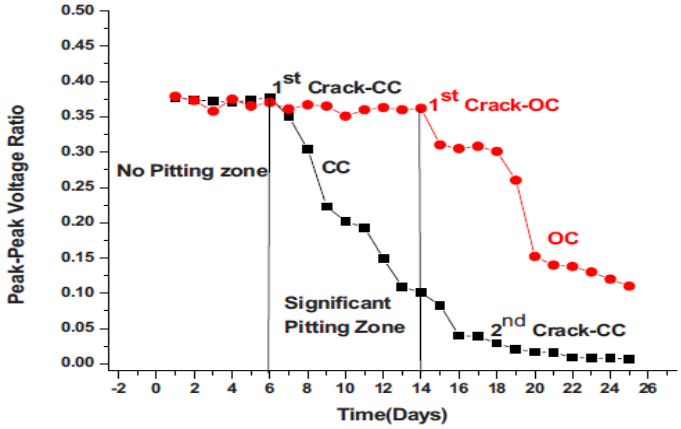

Fig.2.16 (b) Peak-peak voltage ratio with core-seeking mode.

Thus, the mechanism and rate of rebar corrosion was successfully monitored in chloride and oxide environments through appropriate selection of modes. Simultaneous destructive tests were also carried out on RC beams, and it was found, that non-destructive Ultrasonic technique correlate well with the destructive technique.

Sharma and Mukherjee (2013) reported non-destructive evaluation of reinforcing bars that are corroding in the presence and absence of chlorides utilizing ultrasonic guided waves. Ultrasonic guided wave monitoring utilizing specific core and surface seeking modes to identify the type, rate, and mechanism of corrosion in a reinforcing bar in concrete subjected to different exposure conditions was discussed. The experimental investigation involved monitoring of RC beams undergoing accelerated impressed current corrosion. In general, huge pitting and non-uniform area loss was highlighted by severe signal attenuation marks chloride corrosion, which was well picked

up by core seeking mode. It began with de lamination shown by signal rise with surface seeking mode. In oxide corrosion, the rate of corrosion was slow, localized, and marked by slow bond deterioration as depicted by signal strength rise in surface seeking mode. Pitting was insignificant in core seeking mode in OC. Thus, it was observed that through a judicious selection of ultrasonic modes, different types of corrosion in RC structures can be successfully identified. Bars at different stages of corrosion were ultrasonically monitored in both oxide and chloride environments to explore the ability of ultrasonics to predict the level of deterioration of the bars. It was done successfully by correlating ultrasonic voltage ratio with destructive parameters of mass loss, tensile strength and bond strength in the two common corrosion environments. It was concluded that, although the use of guided waves is effective in identifying the presence of corrosion in rebars in widely varying environments, the method needs access to the ends of rebars. At site, bars that are most susceptible to corrosion need to be exposed at the ends to perform the test. Also the signal-to-noise ratio should be above the ground noise level.

2.7 Closing Remarks

This chapter highlights the various details of ultrasonic waves and discusses in detail the classifications of ultrasonic waves into Bulk and Surface Waves.

The principal advantage of guided or surface waves over bulk wave is that inspection over long distances with excellent sensitivity from a single probe position can be achieved and also enable one to inspect hidden structures and structures under water, coatings, insulations, and concrete. The next chapter highlights the various details of using ultrasonic guided waves in early strength and hardening of concrete and emphasize on the work done on the same till date.

CHAPTER 3
ACOUSTIC EMISSION AS NDT TOOL

3.1 Introduction

Acoustic emission (AE) is defined as the elastic energy liberated from materials which are undergoing deformation (Miller and Hill, 2005). Also it can be defined as "the transient elastic waves which are generated by the rapid release of energy from localized sources within a material" (Moore et. al, 2005).

The rapid release of elastic energy, the AE event, propagates through the structure to arrive at the structure surface where a piezoelectric transducer is mounted. These transducers detect the displacement of the surface at different locations and convert it into a usable electric signal.

By analysis of the resultant waveform in terms of feature data such as amplitude, energy and time of arrival, the severity and location of the AE source can be assessed. **Fig. 3.1** and **Fig. 3.2** show a summary of the AE detection process.

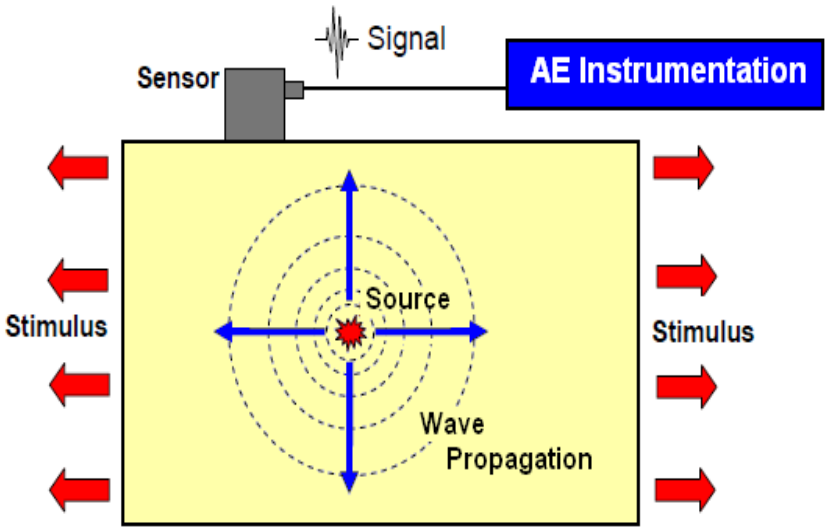

Fig. 3.1: Acoustic emission method (ASTM 1982)

The phenomenon is also sometimes called stress wave emission, stress waves, micro seismic activity, microseism and rock noise. AE testing is often considered the most sensitive method of non-destructive testing because it is the only technique which can detect the defect process as it is occurring.

Test object and application of load produce mechanical tensions
Source mechanisms release elastic energy
Wave propagation from source to sensor
Sensors converting a mechanical wave into electrical AE signal
Acquisition of measurement Data converting an AE signal into an electronic data set
Display of measurement data Plotting the recorded data into diagrams
Evaluation of the display from diagrams to safety-relevant interpretation

Fig. 3.2 The AE chain (Baxter 2007)

AE techniques can be used to monitor a wide range of structures and materials such as metals, non-metals and combinations of these when load is applied. There are two main differences between AE testing and other non-destructive techniques which are:

1. The energy which is detected is generated from the test object itself in AE testing.
2. The dynamic processes associated with the degradation of structures can be detected by only AE testing. **(Miller and Hill, 2005; Bunnori, 2008).**

The advantages of AE testing compared with other non-destructive methods include **(Miller et. al., 2005; Hellier, 2001):**

1. AE testing is a dynamic test technique.

2. The significance of discontinuities in the entire structure during a single test can be detected and evaluated by AE testing (real-time evaluation).

3. AE testing can be applied to vessels and other pressure systems during service which requires no downtime.

4. Catastrophic failure of systems with unknown discontinuities can be prevented by AE monitoring.

5. AE testing requires only limited access to detect discontinuities.

6. AE testing can be used in all stages of testing such as pre-service testing, in-service testing, leak detection and location, in-process weld monitoring and mechanical property testing.

The limitations of AE testing include (Moore et. al., 2005, Hellier 2001):

1. Repeatability: AE is stress unique and each loading is different.

2. Attenuation: The AE wave in the component will be attenuated during testing.

3. History: Testing is highly effective when the loading history of a component is known.

4. Noise: Extraneous noise may affect AE testing.

There are several mechanisms which give rise to acoustic emission in materials. In metals source mechanisms include moving dislocations, slip, crack growth, grain boundary sliding, twinning and fracture and decohesion of inclusions. In composite materials matrix cracking and the debonding and fracture of fibres are AE sources.

3.2 Fundamentals of Acoustic Emission

The principal idea of acoustic emission is that elastic waves or acoustic emission is released from solid materials or components due to deformation or fracture which occurs during applied mechanical or thermal stress.

The purpose of the AE test is to detect and locate sources of the emission and to gain sufficient information about them. The detected waveform contains qualitative and quantitative information for characterization of a source. The main factors which influence the AE signals are the source's characteristics, a path between the source and transducer, transducer's characteristics and the measuring system.

The main parameters of waveform are AE hit, AE count, AE hit energy, signal amplitude, signal duration and signal rise time. **Fig.3.3** shows the definitions for a simple waveform (Moore et al., 2005).

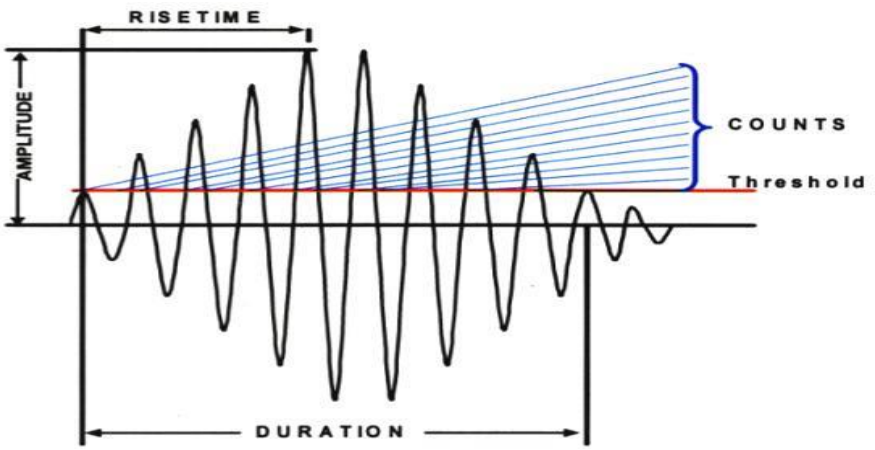

Fig. 3.3 Characteristics of a burst type of AE signal (Eaton, 2007)

(1) Emission Hits and Count

Separate signal bursts, which are generated by local material changes, are called AE hits. However, the number of times a signal crosses a preset threshold is called hit count which depends on the transducer frequency, the transducer damping characteristics, the damping characteristics of structure and the threshold level (Miller et al., 2005).

(2) Acoustic Emission Event Energy

The acoustic emission event energy is the rapid release of energy in the material which can be expressed by the true energy which is proportional to the area under the AE waveform (Moore et al., 2005). The electrical energy, U, present in a transient hit can be defined as:

$$U = \frac{1}{R}\int_0^\infty V^2(t) \qquad \textbf{(3.1)}$$

where, R is the electrical resistance (ohm) of measuring circuit, V is the output potential (volt) and t is time (second). Direct energy analysis can be achieved by digitizing and integrating the waveform signal or by special devices performing the integration electronically (Miller et al., 2005).

(3) Acoustic emission signal amplitude

AE signal amplitude is the peak voltage of the signal waveform which depends on the intensity of the AE source in the material. Peak amplitude measurements are generally achieved using a log amplifier (logarithmic scale) to cope with a wide range of signal amplitudes (large and small signals) (Miller et al., 2005).

A usual unit for measuring the amplitude of an acoustic signal is the decibel (dB). The decibel is not a fixed measurement unit but rather expresses a logarithmic ratio between two conditions of the same dimension. In acoustic emission, the reference level 0 dB AE is defined as a signal of 1 μV at the transducer before any amplification.

The fundamental decibel is

$$N_{dB} = 10\log_{10}\frac{P}{P_o} \quad \textbf{(3.2)}$$

where,Pis the measured power and $P_o$is the reference power in watts.

In a sense, the power is a square function of voltage

$$N_{dB} = 10\log_{10}(V/V_o)^2$$
$$N_{dB} = 20\log_{10} V/V_o \quad \textbf{(3.3)}$$

where,V is the measured potential and Vo is the reference potential in volts.

(4) Acoustic Emission Source Location

AE source location is very important to assess the areas of active damage. The most commonly used source location technique is the time of arrival (TOA) approaches, which is an integral part of all commercially available AE software. There are other source location methods such as Single Sensor Modal Analysis Location (SSMAL), the recently developed DeltaT mapping method and energy based spatial location.

Time of arrival (TOA) technique is based on the source being located by several sensors in an array and measuring the time delay between pairs of sensors within the array. Several source location applications are appropriate for linear source location, i.e., where a single position along a measurement axis is adequate to define the location of a source. Most applications of AE source location are interested with locating a source in a fundamentally two- dimensional shell type component. Three-dimensional source location is required if the thickness of the object under test is significant relative to the other two dimensions or if the area of interest is internal to the specimen. For linear location, the minimum number of transducers is two; however three are required for two-dimensional location and four are required for three- dimensional location (Baron and Ying, 1987). Pullin (2007) describes a technique that determines the location of an event in one dimension between two sensors where the propagating velocities of different wave modes of a signal and the time of arrival at a signal sensor is known.

(5) Linear (1D) Location

Fig. 3.4 (a, b, c and d) shows a situation where three sensors are placed on a linear structure such as a beam. An AE event occurring at any point in this beam will emit stress waves propagating in both directions.The simplest technique of locating this source is zonal location which examines the order in which the event reaches the sensors in the array, i.e. the "hit" sequence. With reference to **Fig 3.4a**, if the first sensor hit is sensor 2 then the region for possible location is the mid point between sensor 1 and 2 then the region for possible location is the mid point between sensor 1 and 2 to the mid point between sensor 2 and 3. Further location accuracy can be gained by examining the second sensor that is 'hit' in the array. In Fig. 3.4b, sensor 1 is the second sensor to receive the hit and therefore the source can be located between the midpoint between sensors 1 and 2 and sensor

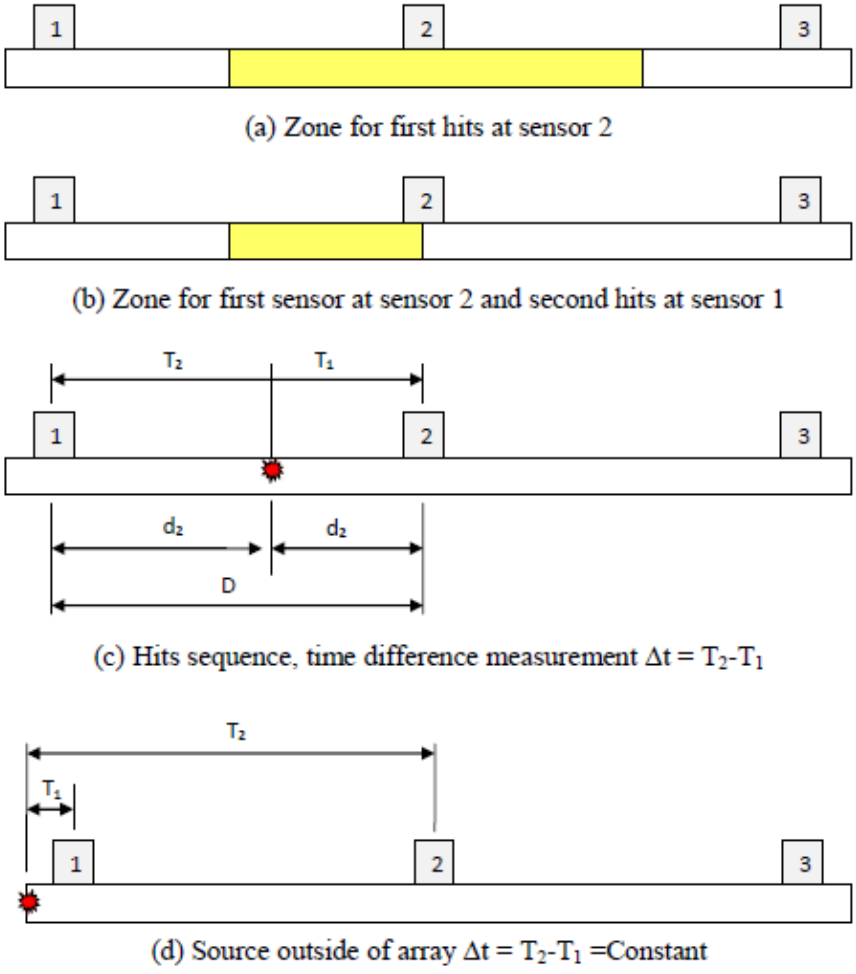

Fig. 3.4 Linear location using time of arrival (TOA) theory (Miller and Mclntire, 1987)

This method can be made more accurate by examining not only the hit order, but the difference in time arrival of the hit at the sensors. For instance, **Fig 33.4c** represents a hit arriving at sensor 2 first followed by sensor 1. The timedifference between these hits can be calculated as:

$$\Delta t = \frac{d_2 - d_1}{C_{AE}} \quad \textbf{(3.4)}$$

where,

C_{AE}= calculated wave velocity

Δt =time difference between sensor

d_1= distance from source to first hit sensor

d_2= distance from source to second hit sensor

This is however, commonly expressed in terms of d_1

$$d_1 = \frac{D - C_{AE}\Delta t}{2} \quad \textbf{(3.5)}$$

where, D is the total distance between sensors. If the source originates from outside the array, Fig. 3.4d, then the time difference measurement always corresponds to the time of flight between the outer sensor pair. The source will be located at the sensor at the edge of the array; in the case of the example, at sensor 1.

Two dimensions (2D) Location:

The same method can be used for 2D location. **Fig 3.5** considers two sensors placed a distance of D apart on an infinite plane. If the stress wave from a source is assumed to propagate at a constant velocity in all directions, then it can be shown that:

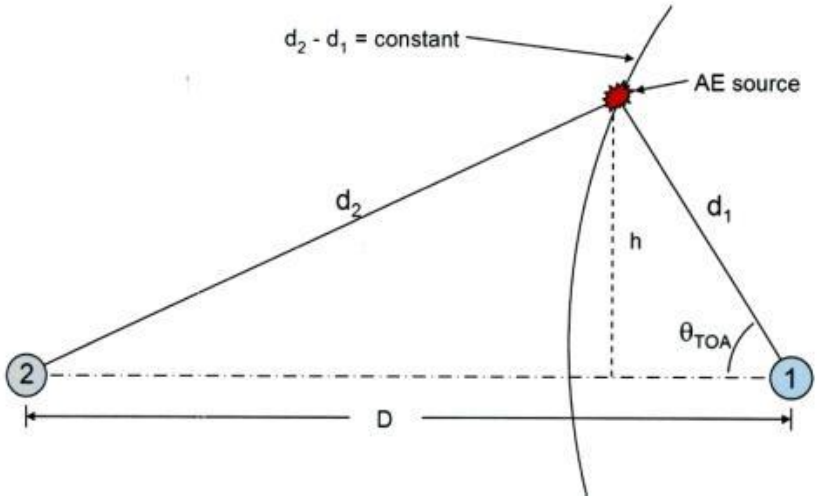

Fig. 3.5 2D location on an infinite plate (Miller et. al., 2005)

$$\Delta t\, C_{AE} = d_2 - d_1$$

and,

$$h = d_1 \sin \Theta_{TOA}$$

$$h^2 = {d_2}^2 - (D - d_1 \cos \Theta_{TOA})^2$$

then,

$${d_1}^2 (\sin \Theta_{TOA})^2 = {d_2}^2 - (D - d_1 \cos \Theta_{TOA})^2$$

$${d_1}^2 = {d_2}^2 - D^2 + 2D d_1 \cos \Theta_{TOA}$$

Substituting $d_2 = d_1 + \Delta t\, C_{AE}$ gives

$$d_1 = \frac{1}{2} \frac{(D^2 - (\Delta t\, C_{AE})^2)}{(\Delta t\, C_{AE} + D \cos \Theta_{TOA})} \qquad \textbf{(3.6)}$$

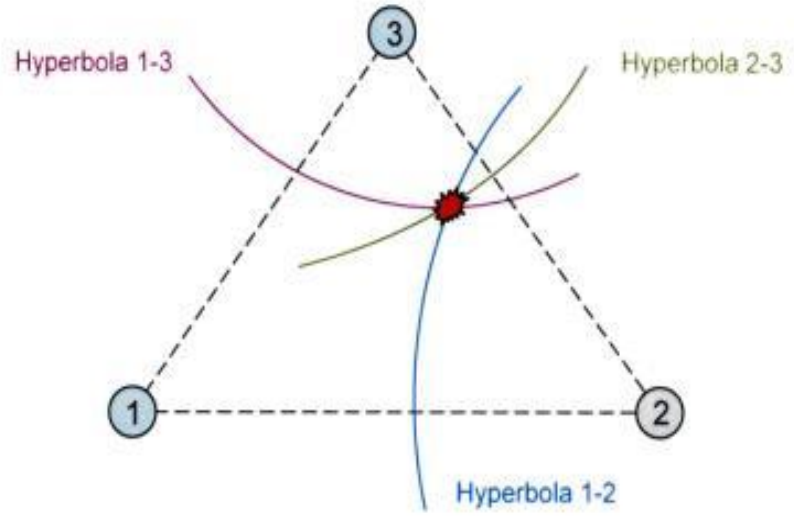

Fig. 3.6 2D location with three sensors (Miller et. al., 2005)

This provides insufficient information to locate the source. However, by adding a third sensor to the array as shown by Figure 3.6, it is possible to repeat this process for the three pairs of sensors 1-2, 2-3 and 1-3. The intersection point of three resulting hyperbola provides a more accurate 2D location. The adding of further sensors increases the number of hyperbola and consequently the accuracy and confidence of location.

3.3 AE Parameter analysis

AE parameter analysis is the fundamental method for identifying types of damage in a structure. It utilizes features that describe the detected waveform. Typical parameters investigated include amplitude, energy, counts (number of threshold crossings), frequency, duration and rise time.

According to many researchers (Aggelis 2011, Ohno and Ohtsu 2010, Ohtsu and Tomoda 2007, Soulioti et. al., 2009, JCMS-III 2003), the relationship between RA values (rise time/ amplitude) and AF value (average frequencies = counts/duration) can be used for classification of crack type in concrete structures. They reported that when an AE signal has low AF value and high RA value it is classified as shear type crack/movement. However when it has a high AF and low RA value is classified as tensile type crack as shown **Fig 3.7 and 3.8**. It should be noted that some researchers describe the shear movement as a shear "crack" but that this is not strictly correct; concrete will only crack under tensile forces and then move due to shear forces.

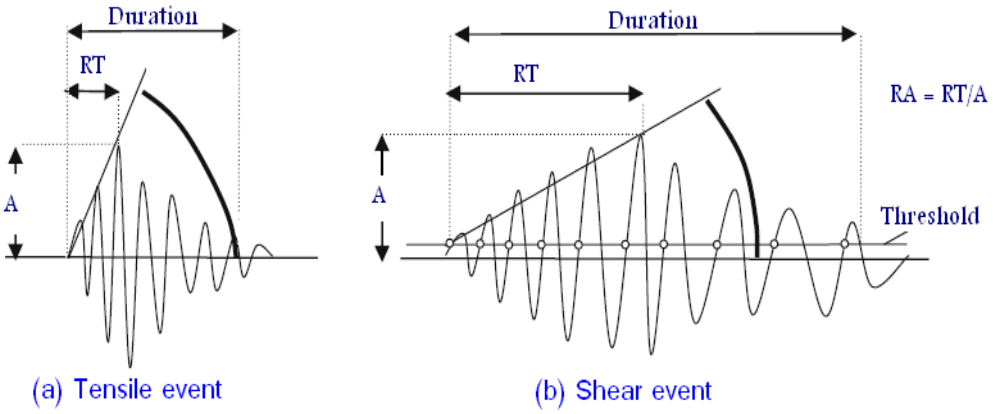

Fig 3.7 Typical waveforms (Soulioti et. al.,2009)

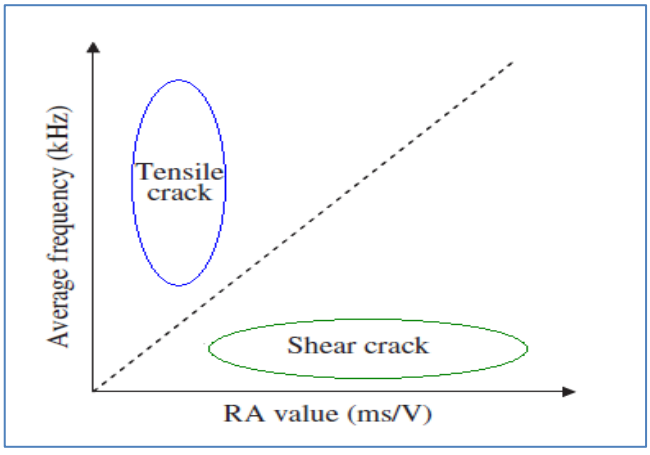

Fig. 3.8 Crack classifications (Ohno and Ohtsu, 2010)

Furthermore, several works and studies on concrete fracture have shown that a single synthetic parameter, namely the b-value can be used to characterize fracture and damage growth (Carpinteri et al. 2009).

The b-value is defined as the relationship between the number of AE events, N, and amplitudes, A, as

$\log_{10} N = a - b \log_{10} A$

where, a and b are empirical constants (Ohtsu and Tomoda, 2007).

In the case that large scales of fracture are dominant then the b-value becomes small. Conversely, b-value is large when small scales of fracture are dominant (Aggelis 2011, Kawasaki *et. al.,* 2010, Watanabe *et. al.,* 2007). A size distribution of AE sources can be estimated by using the b-value. (Ohtsu and Tomoda, 2007).

Moreover, crack kinematics on locations, types and orientations can be quantitatively determined by using moment tensor analysis (Uddinet. al., 2004, Ohtsu 1989).

3.4 Application of Acoustic Emission on RC Structures

Yoon et al. (2000) studied damage in corroded Reinforced concrete using the Acoustic emission. He conducted a series of normal strength concrete beams tests using four-point flexural loading. The beams were 100 mm wide, 150 mm deep and 1150 mm long. Several different types of beams were tested to simulate different sources of damage and the list of beams tested is shown in **Fig 3.9**.

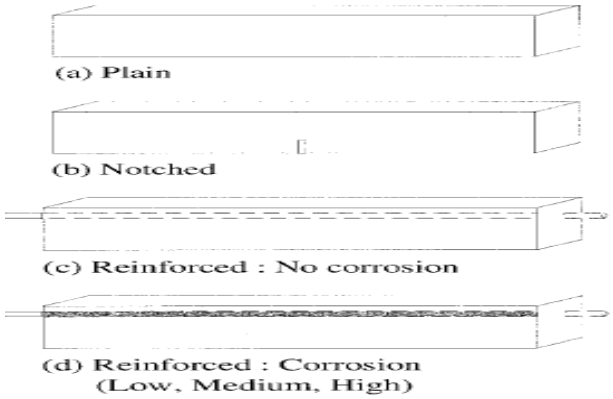

Fig 3.9 Types of concrete beam specimens (Yoon et al., 2000)

Three plain unreinforced beams and three notched plain unreinforced beams were used to obtain the initial response of distributed micro crack development and localized crack propagation, respectively. The reinforced specimens allow the determination of the characteristic AE response of a reinforced concrete element from several sources such as Micro cracking, Localized crack Propagation, Flexural cracking, Shear cracking and De bonding. In addition, three reinforced beams were corroded to three levels of distress using anodic current that was applied after 28 days of standard moist curing. The typical Load-displacement envelope for the plain and notched beams

is shown in **Fig 3.10 (a).** The response of the non corroded and highly corroded beams is shown in **Fig 3.10 (b)**. The response of the unreinforced beams is divided into two regions to describe the presence of distributed micro cracking throughout the beam in region A and localized crack development in the region B. The response of the reinforced beam was divided into four regions: Region A represents the distributed microcraking; Region B describes the beginning of first crack localization in the constant moment region; Region C describes the continued development of micro cracking; and the Region D appears to correspond to the development of either a shear crack in the beam or bond-spitting cracking along the reinforcing bar.

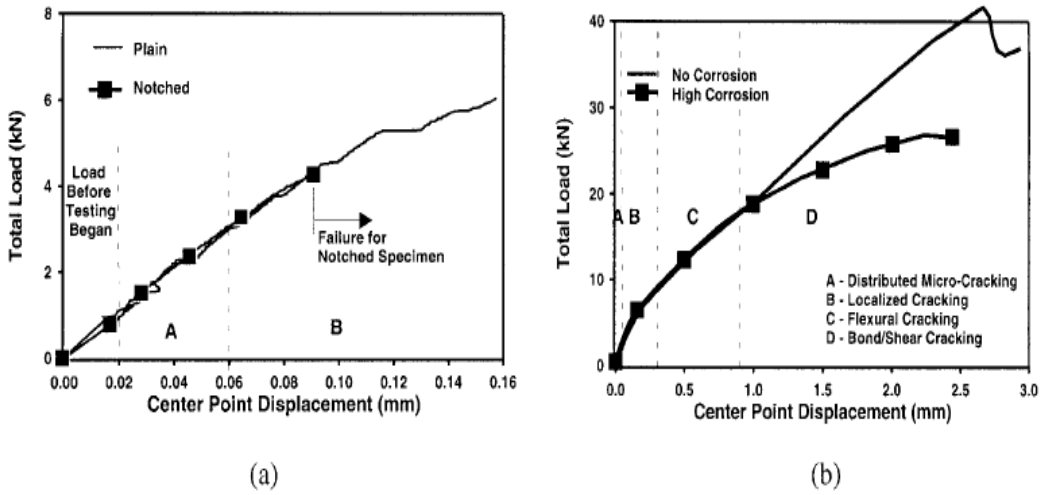

Fig 3.10 Load Displacement envelope for a) Unreinforced beams b) Reinforced beams

Fig 3.11 and 3.12 shows the occurrence of AE events as a result of cyclic loading for different unreinforced and reinforced specimen. The load cycle shown as a fine line is also plotted in each figure. On the whole, in each load cycle the AE activity decreased as the load was held constantly or unloaded.

From **Fig 3.11 and 3.12**, it can be seen that there were fewer AE events during the whole test in the plain and the notched concrete specimens than the reinforced concrete specimens. Also it has been observed that secondary peaks of AE events develop in the unloading response after approximately four cycles (**Fig 3.12a-d**). this phenomenon does not appear in the unreinforced specimen (**Fig 3.11, a-b**).In early stages of loading, there is a large difference between the no. of AE events as shown in (**Fig 3.11, a-b**).a large no. of AE events were generated in the un corroded specimens whereas fewer AE events were observed in the corroded specimen; in the reinforced beams the

higher the degree of corrosion, the lower the AE activity. Thus, the majority of micro cracking and longitudinal cracking along the reinforced beam has already dissipated by damage process due to corrosion.

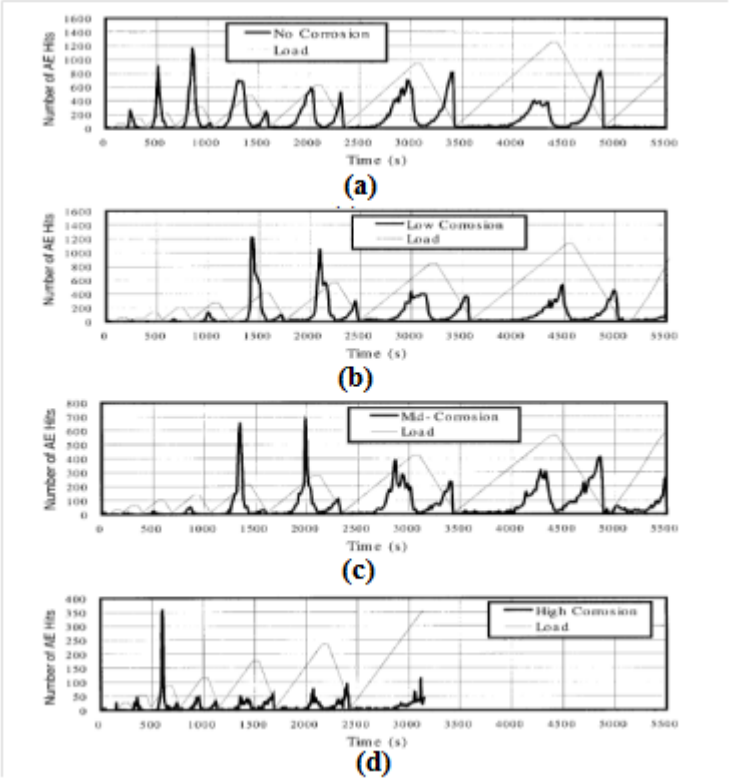

Fig 3.11 AE hits versus cyclic loading for reinforced beams (corroded and uncorroded beams)

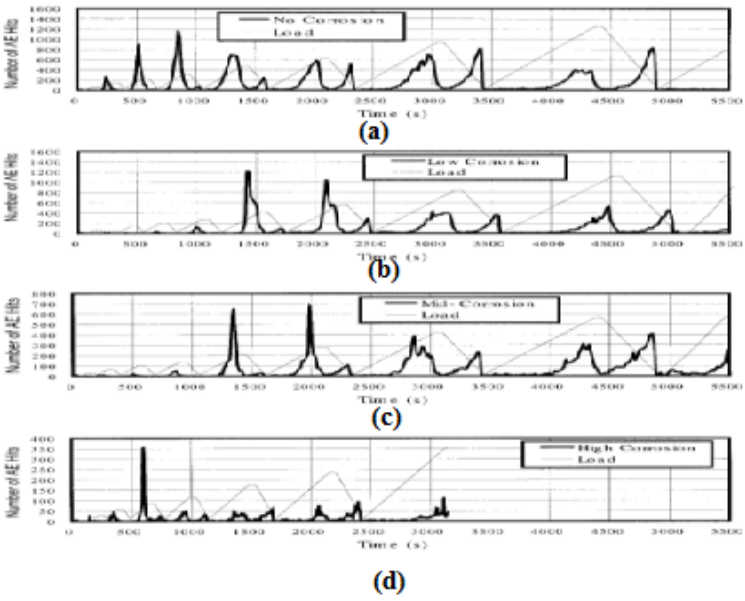

Fig 3.12 AE hits for cyclic loading for unreinforced beams (plain and notched)

The cross-plot is an effective technique to analyze the features of an entire AE signal at a glance for the purpose of distinguishing signal characteristics. **Fig 3.12** shows the results of a cross-plot of amplitude and duration of AE signals for unreinforced beams (plain and notched). The black diamond's indicate AE events from the notched specimen, whereas open circles indicate AE events from the un-notched concrete specimen. Signals correspond to Stage A and part of Stage B. These loading stages are characterized by distributed micro cracking and formation of localized cracks, respectively.

Tomoda et al. (2003) studied corrosion monitoring in reinforced concrete by acoustic emission. In the accelerated corrosion test, two types of mixture were employed. The water-to-cement ratios (w/c) were 0.45 and 0.55. In the crack-expansion test, w/c of concrete was 0.5. In the accelerated corrosion test, reinforced concrete slabs of dimensions 10 cm x 25 cm x 40 cm were made. In the crack-expansion test, a concrete plate of dimensions 10 cm x 25 cm x 25 cm was made. In order to simulate radial pressure due to corrosion product, expansive agent of dolomite paste was poured into a hole of 30 mm diameter. Three specimens were prepared for each W/C ratio, and the chloride contents were measured after accelerated corrosion. For w/c = 0.45, core samples were taken at 4 days, 10 days, and 12 days elapsed, while for w/c = 0.55 at 4 days, 8 days, and 10 days elapsed. These periods are determined from a comparison between AE activities. and half-cell potentials. High AE activities are observed at two stages of 3 days and 7 days elapsed. For non-destructive evaluation of corrosion, the half-cell potential measurement is normally carried out. From the potentials measured at the surface, the probability of corrosion is estimated as more than 90% when the potentials are lower than –350 mV.

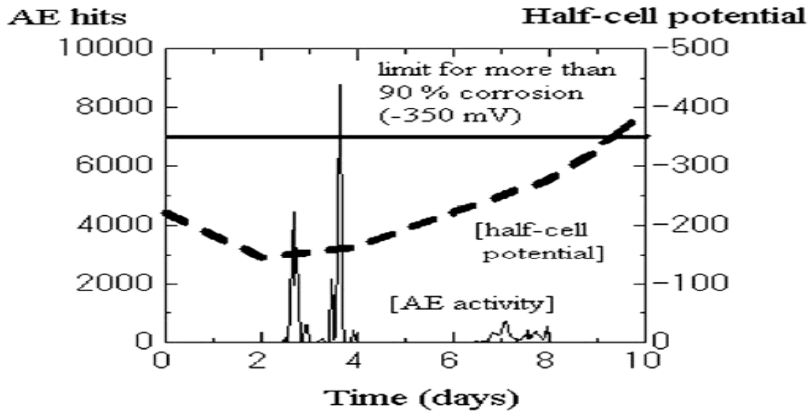

Fig 3.13 AE activity and half-cell potential vs. time during accelerated corrosion (w/c=0.5)

As seen in **Fig 3.13,** the potentials start to decrease, around at the first AE activity (finished at 4 days). Then the potential reaches lower than –350 mV after 10 days, following the second AE activity (finished at 8 days). Consequently, the test of one specimen for w/c=0.5 was finished at 4 days, and the other was completed at 8 days. The third specimen was conducted up to 10 days. Results in **Fig 3.14** reveal that AE activities could provide earlier warning than the half-cell potential measurement. Distribution of chloride contents in depth was determined, and results are given in **Fig 3.14**. At the location of concrete cover, chloride ions per m3 becomes higher than 1.2 kg after 12 days in a sample with w/c=0.45. In contrast, it reaches over 1.2 kg after only 8 days for w/c=0.5. This is because the permeability increases with an increase in w/c ratio in concrete. According to the Standard Specification (JSCE, 2001), the lower and upper bounds for triggering corrosion are prescribed as 0.3 kg/m3 and 1.2 kg/m3, respectively.

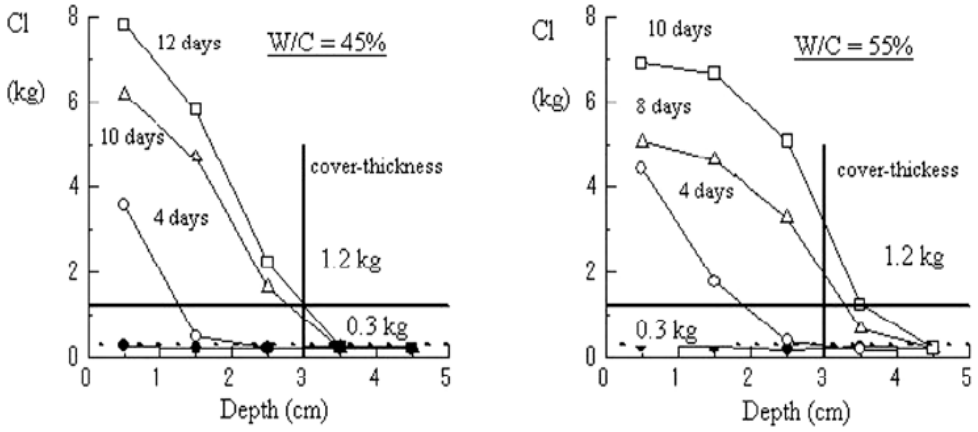

Fig 3.14 Distribution of chloride ions in depth (Tomoda et al.,2003)

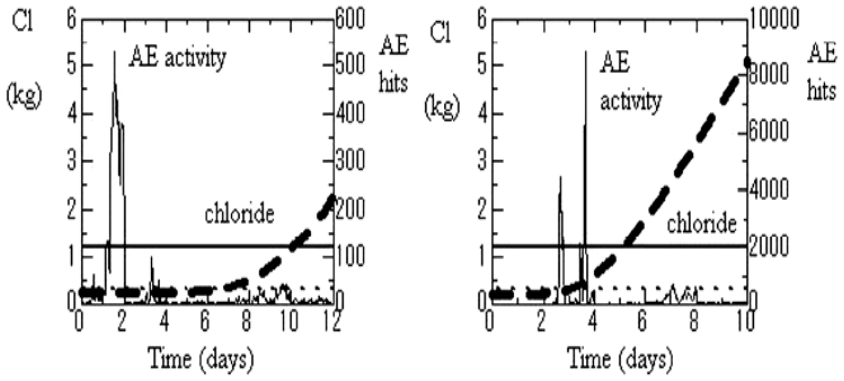

Fig 3.15 Comparison between AE activities and chloride contents (Tomoda et al., 2003)

Consequently, the amount of chloride contents, C(t), was computed at cover-thickness based on

Fick's law

$$C(t) = Co\ (1 - erf\ (x/2[Dt]1/2)) \quad \textbf{(3.7)}$$

where, Co is the surface concentration, D is diffusion coefficient, t is time and erf is Gauss's error function. Results are compared with AE activities in **Fig 3.15**. Here, chloride contents in concrete were determined first from potentiometric titration. The surface concentration and the diffusion coefficient were estimated by the regression analysis, by fitting the distribution using fick's law equation. Obtained values of the surface concentration, Co, and the diffusion coefficient, D, are 10.02 kg/m^3 and 6.05 x 10-8 cm^2/sec, respectively. Right after the chloride contents become higher than the lower bound (0.3 kg), the first high AE activity is observed in both cases of W/C = 45% and 55%. At the stage where the chloride content exceeds the upper bound (1.2 kg), another high AE activity is observed. These results demonstrate that high AE activities of the two stages are observed in the accelerated corrosion test. One is the stage where the chloride content reaches 0.3 kg/m^3, and the other is the stage where the chloride level becomes higher than 1.2 kg/m^3 in concrete. These are in remarkable agreement with the deterioration process due to salt attack, which is prescribed in the Standard Specification. According to the process shown in **Fig 3.16**, there exist the first stage for the initiation of corrosion from the incubation to the development period, and the second for the nucleation of cracking from the development period to the accelerated corrosion.

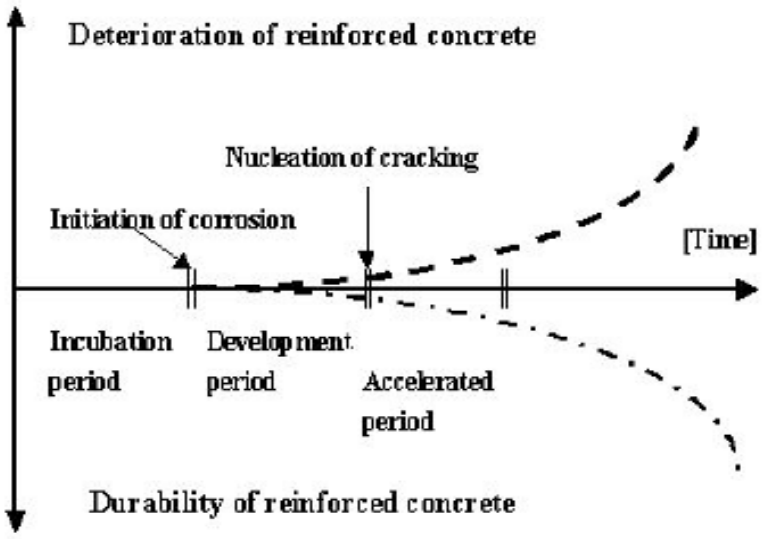

Fig 3.16 Deterioration process due to salt attack. (Tomoda et al., 2003)

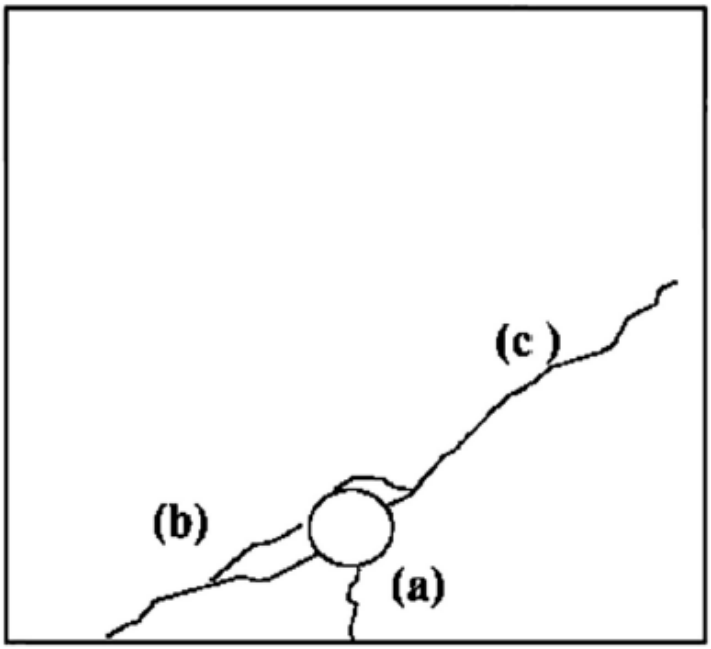

Fig 3.17 Crack pattern observed after the test (Tomoda et al., 2003)

Nucleation of typical corrosion cracks was simulated by employing expansive agent. A hole of 30 mm diameter to represent the rebar location was made at 3 cm depth from the side, corresponding to 3 cm cover-thickness. After casting expansive agent into the hole, surface cracks were observed after two days. During extension of these cracks, AE events were detected by six AE sensors .After the test, SiGMA analysis was conducted. Three main cracks observed are shown in **Fig 3.17**, which are labelled as crack traces (a), (b), and (c). In reference to the cross-section of a reinforced concrete member this model simulates, crack trace (a) corresponds to a surface crack, which is normally observed as corrosion cracking. Crack trace (b) is commonly observed as a spalling crack due to corrosion. An internal crack (crack trace (c)) is generally not taken into account, because this is inaccessible to usual visual inspection. AE events analyzed by SiGMA procedure were first located, and then were classified as three clusters responsible for crack traces (a), (b) and (c) from **Fig 3.18**. All the results of SiGMA analysis are plotted in **Fig 3.19**. AE events analyzed are marked with arrow or cross symbols. The arrow symbol represents a tensile crack, and the arrow direction indicates the crack opening direction. Shear cracks are denoted by cross symbols, and their two orientations correspond to the crack motion vector and the crack normal vector, respectively.

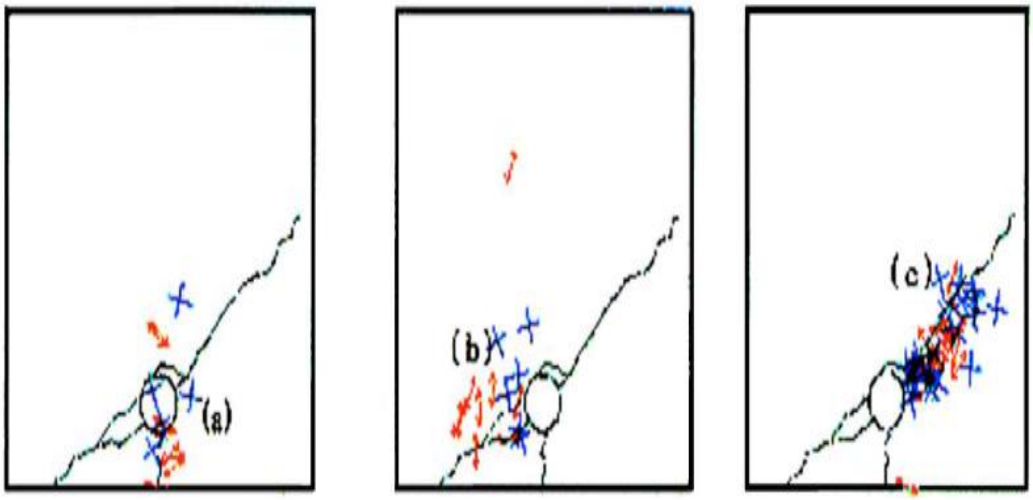

Fig 3.18 Results of SiGMA analysis classified in three clusters (Tomoda et al.,2003)

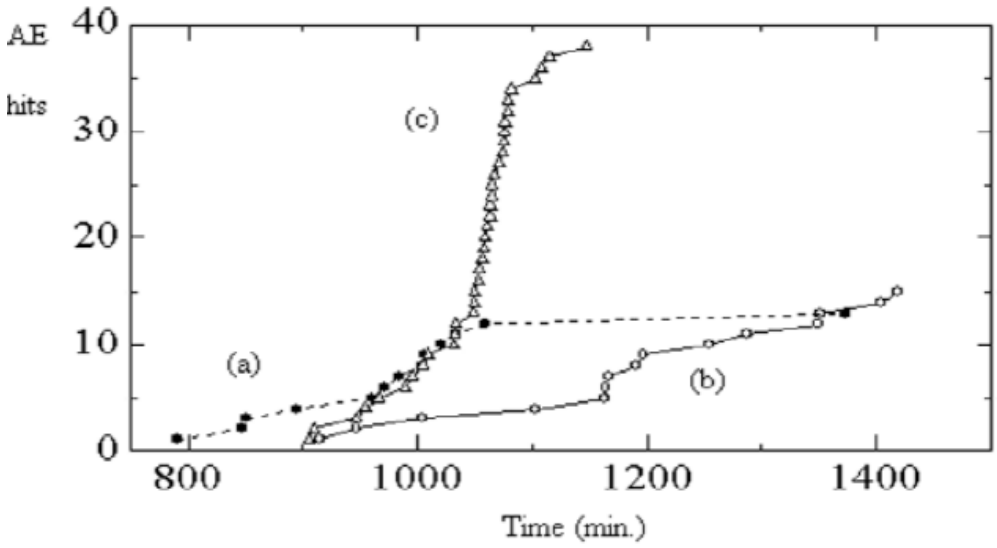

Fig 3.19 AE activities during nucleation (Tomoda et al., 2003)

Concerning crack trace (a), tensile cracks running vertically to the surface are mostly visible from outside. In contrast, shear cracks are not explicitly associated with the extension of surface-breaking cracks. For crack trace (b), tensile cracks are primarily observed at the locations far from the reinforcement or close to the stress-free surface, while shear cracks are mostly observed near the reinforcement. In crack trace (c), tensile and shear cracks are fully mixed up. Results obtained are summarized, as follow:

In the accelerated corrosion tests, AE occurrence is monitored continuously. Investigating ingress of chloride ions, a relationship with chloride concentration and AE activity is obtained. Right after the chloride contents become higher than 0.3 kg/m^3, a high AE activity period is observed. Subsequently, at the stage where the chloride contents become higher than 1.2 kg/m^3, another high AE activity period is observed. Two stages of high AE activities are observed in the accelerated corrosion test, which remarkably correspond to the two stages in the deterioration process due to salt attack. These are the initiation of corrosion from the incubation period to the development and the nucleation of cracking from the development period to the accelerated. This suggests that these two stages are possibly identified by in situ AE monitoring. The corrosion probability by the half-cell potential reaches over 90% after the appearance of these two stages. It confirms that AE monitoring could provide earlier warning of corrosion than the half-cell potential measurement. Applying SiGMA procedure, nucleation mechanisms of a surface crack, a spalling crack, and an internal crack due to the expansion of corrosion product are identified. The surface breaking crack is nucleated dominantly by tensile cracks. For the spalling crack, both the tensile and the shear cracks are generated. Tensile cracking is dominant near a stress-free surface, but the main mechanism of the internal crack is of shear-crack motion.

In the case of visual inspection, the detection of the surface and spalling cracks is the main target. Monitoring the nucleation of tensile cracks by applying SiGMA procedure, it is possible to estimate and predict the extension of these two type s of cracking. It is noted that the internal crack could be generated following the surface crack, and the main mechanism of the internal crack is of shear.

Ohtsu et al., (2007) studied the corrosion process in Reinforced concrete identified by Acoustic emission. RC slabs tested were of dimensions 300mm × 300mm ×100mm. Reinforcing steel bars of 13 mm diameter are embedded with 15 mm cover thickness for longitudinal arrangement. An accelerated corrosion test and cyclic wet -dry test were conducted. Half cell potentials at the surface of the specimen were measured by portable corrosion-meter. In the accelerated corrosion test, the measurement was conducted twice a day, right after discontinuing the current. Chloride concentrations were measured at several stages .At first; the initial concentration was measured by using a standard cylinder sample after 28-day moisture curing. A relationship between the AE activity and the half-cell potentials measured are shown in the **Fig 3.20**

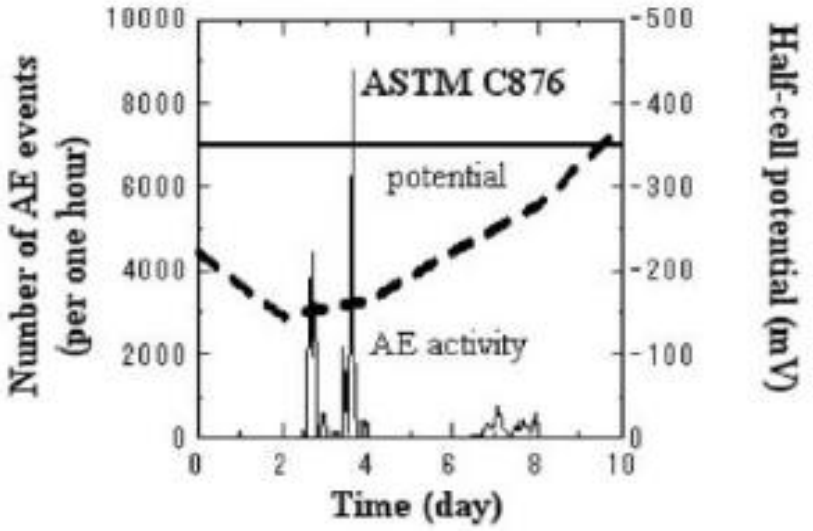

Fig 3.20 AE activities and Half-cell potential in accelerated corrosion (Ohtsu et al., 2007)

The no. of AE events is plotted as a total of two channels counted for one hour. Two periods of high AE activities are clearly observed at around 3 days elapsed and 7 days elapsed. It is noted that half cell potentials start to decrease after the first activity, but are still higher than -350mV around the second activity. Because the half cell potential lower than -350mV is prescribed as more than 90% probability of corrosion. Results suggest that the corrosion in the rebar is detected by AE activity more confidently than the half cell potential.

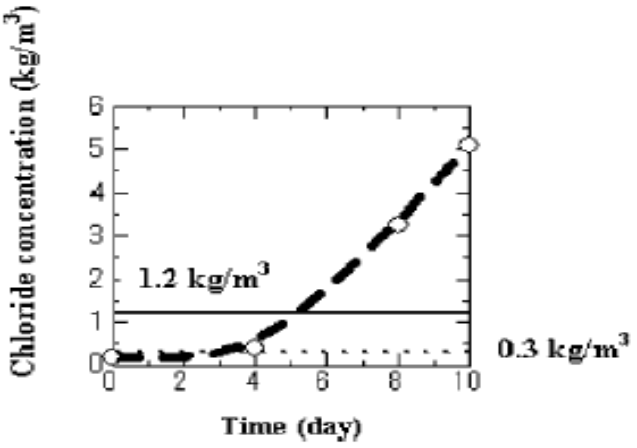

Fig 3.21 Ingress of chloride ions during accelerated corrosion test (Ohtsu et al., 2007)

Total chloride concentrations were determined in depths, and the chloride concentrations at cover thickness were analytically estimated. **Fig 3.21** shows the ingress of chloride ions during the accelerated corrosion test. A broken curve shows the estimated values analytically and open circles indicate the measured values in the test agreement between the estimated and the measured values are reasonable. Two threshold values are denoted, one is the lower-bound threshold for the onset of

corrosion (0.3 kg/m^3 in concrete volume) and the other is the threshold value for performance based design. Acc. to the code [standard specifications for concrete structures- version of construction [(JSCE 2002)], concrete with chloride content over 1.2 kg/m^3 in concrete volume is not accepted for construction to prevent the corrosion. Comparing with the **Fig 3.20**, it is observed that chloride concentration becomes higher than 0.3 kg/m^3 after the first AE activity , and it reaches over 1.2 kg/m^3 following the second AE activity. For AE activities in cyclic Test, the no. of AE events and the half cell potentials during the cyclic test are shown in the **Fig 3.22**. The no. of AE events for one hour is again plotted. AE events are periodically observed along with the cycles of wet and dry. The first high AE activity is observed at 40 days elapsed, while the second activity is not obvious. According to half cell potentials, the values start to decrease at around 100 days elapsed.

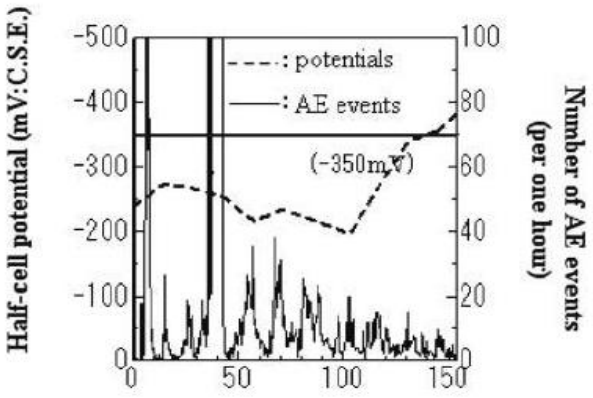

Fig 3.22 AE Activities and Half cell potentials in cyclic wet-dry test (Ohtsu et al., 2007)

In order to identify the second AE activity, the RA values and the average frequency were determined analytically. Corresponding to first period as denoted by an arrow symbol, the RA values becomes large and the average frequency is low.

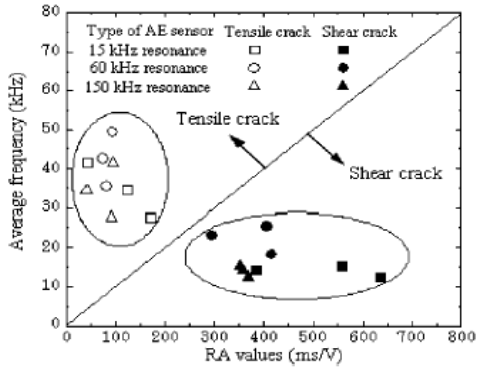

Fig 3.23 Classification of cracks by AE indices (Ohtsu et al., 2007)

Acc. to **Fig 3.23**, AE sources are classified as shear cracks. Toward 100 days elapsed, the increase in the RA value is observed. Thus, the second period is reasonably identified around at 100 days elapsed, where the RA values are low and the average frequencies are high. From **Fig 3.23**, tensile cracks are to be nucleated at the period. The b-value was determined for each wet-dry cycle as the average value. The b-value becomes large at the 1st period and then the b-values keep fairly low. This result implies generation of small shear cracks at the first period. He concluded, That during the 1st period of high AE activities, the RA values become high, the average frequencies are low and the b-value is large. This implies that small shear cracks are actively generated as AE sources. Approaching to the 2nd period, the RA values become low, the average frequencies are getting higher and the b-values are small. The fact reasonably suggests that fairly large tensile cracks are generated due to expansion of corrosive product. Compared with AE results, it is found that the onset of corrosion starts, when the chloride concentration exceeds the lower -bound threshold. Removing rebars from the specimen, it is confirmed that rebars could corrode after chloride concentration reaches over the specified threshold, and AE activities after 100 days result from concrete cracking due to expansion of corrosive products in rebars.

Ohtsu et. al. (2010) studied the Acoustic emission Techniques for rebar corrosion in Reinforced corrosion. A reinforced concrete specimen tested was of dimensions 1000 mm × 570 mm ×100 mm. Two deformed steel-bars (rebars) of 13 mm nominal diameter were embedded with 20 mm cover -thickness. Configuration of the specimen is illustrated in **Fig 3.24**.

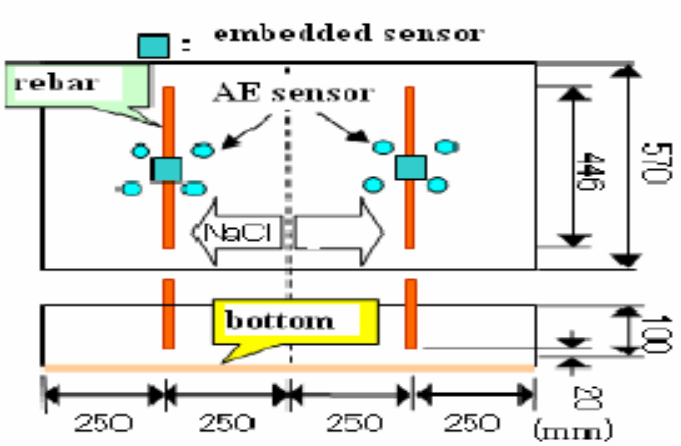

Fig 3.24 Sketch of reinforced concrete slab tested (Ohtsu et al., 2010)

A cyclically dry-wet test was conducted. Half cell potential at the surface of the specimen was measured by a portable corrosion meter. Chloride concentrations were measured at several periods.

Total number of AE hits and the half -cell potentials during the test are shown in **Fig 3.25**. In the figures, the total number of AE hits observed during the test is plotted by a solid curve. The 1st AE activity around at 14 days elapsed is clearly observed, while the 2nd activity is found at 60 day around in the NaCl portion.

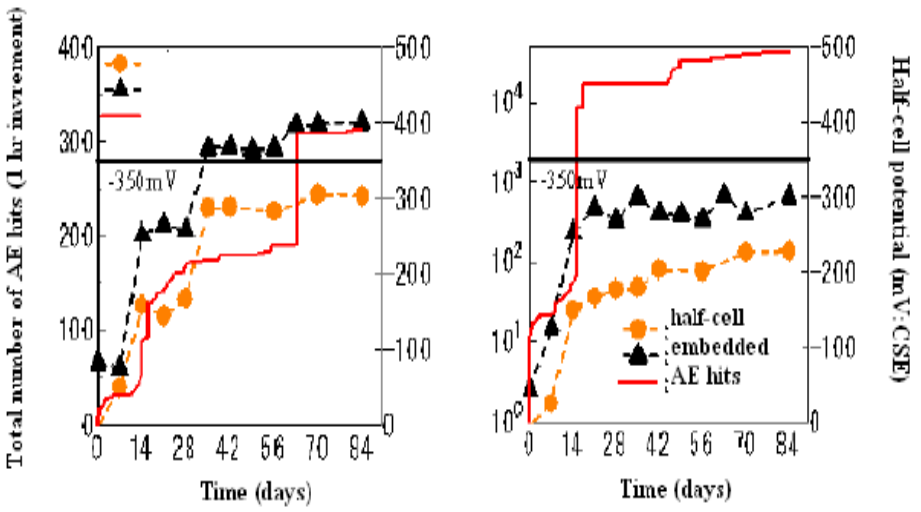

Fig 3.25 Total AE hits and half cell potentials in the NaCl portion (left) and water portion (right)

The curve of AE activity in the NaCl portion is in remarkable agreement with the typical corrosion loss of the phenomenological model. The AE activity could be generated by concrete cracking due to expansion of corrosion products (Zongjin et. al, 1998). It suggests that AE activity can be observed in concrete specimen. Comparing AE activity with half-cell potentials, it is found that with the increase in the number of AE hits, the potentials shift to more negative values. Here, two kinds of potentials are plotted. One is the potentials measured at the surface and the other is those by the embedded sensor. The embedded sensor shows more negative potentials. Still, the decreasing trends are similar. In the NaCl portion, at the 2nd period of high AE activity around 60 days elapsed, the potentials reach to more negative than -350 mV. In the water portion, the decreasing manner of the potentials is in reasonable agreement with that of AE activity. In this case, the 1st high AE activity is only observed, and the potentials did not reach more negative than -350 mV. Relations between chloride concentrations at the cover thickness and AE activities are shown in **Fig 3.26**.

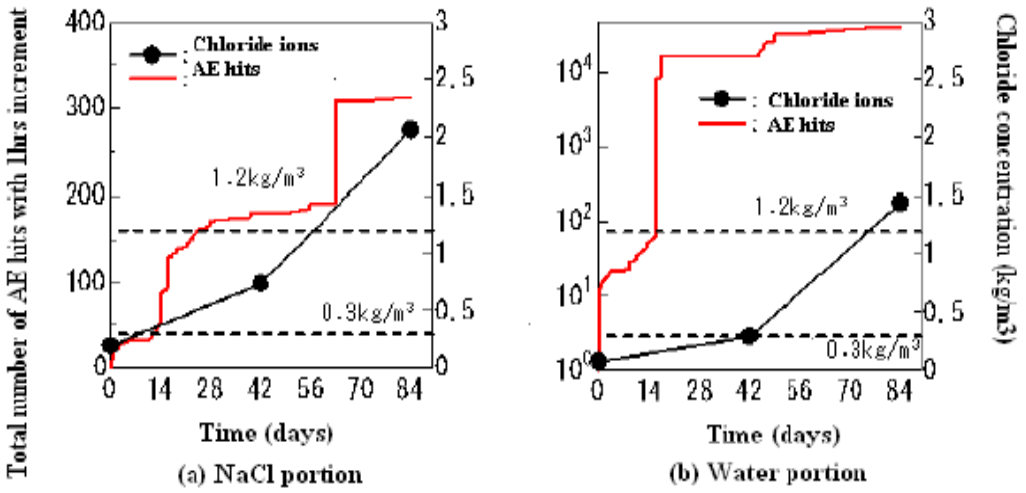

Fig 3.26 Total number of AE hits and chloride concentration (Ohtsu et al., 2010)

It is found that chloride concentration becomes higher than 0.3 kg/m^3 around at the 1st high AE activity, and it reaches higher than 1.2 kg/m^3, resulting in the 2nd high AE activity in the NaCl portion. In the water portion, the 1st high AE activity is observed prior to the stage, where chloride concentration becomes over 0.3 kg/m^3. Comparing AE activities in **Fig 3.25 and 3.26** with the typical curve of corrosion loss for steel in sea water immersion (**Mlchers and Li, 2006**), it could be summarized that two high AE activities reasonably correspond to two periods of the onset of corrosion and the nucleation of cracking. Corresponding to high AE activities twice, two active periods of AE events are observed in the NaCl portion. In contrast, only activity at the 2nd period is emphasized in the water portion. By employing the flaw location procedure, AE events were located. Then, it was found AE events located at the 1st period in the NaCl portion were only found around locations of AE sensors. So, AE wave-forms were examined. AE events detected at the 1st period were of so small amplitudes that AE sources could be mistakenly located at the location of the nearest sensor, where AE waveform was detected of the biggest amplitude. Consequently, AE source locations at the 2nd period of high AE activity are shown in **Fig 3.27**. It is realized that AE sources are reasonably located around rebar locations. This implies that corrosion activity due to concrete cracking, which is generated by expansion of corrosion products in rebar, is readily detected and located by AE technique.

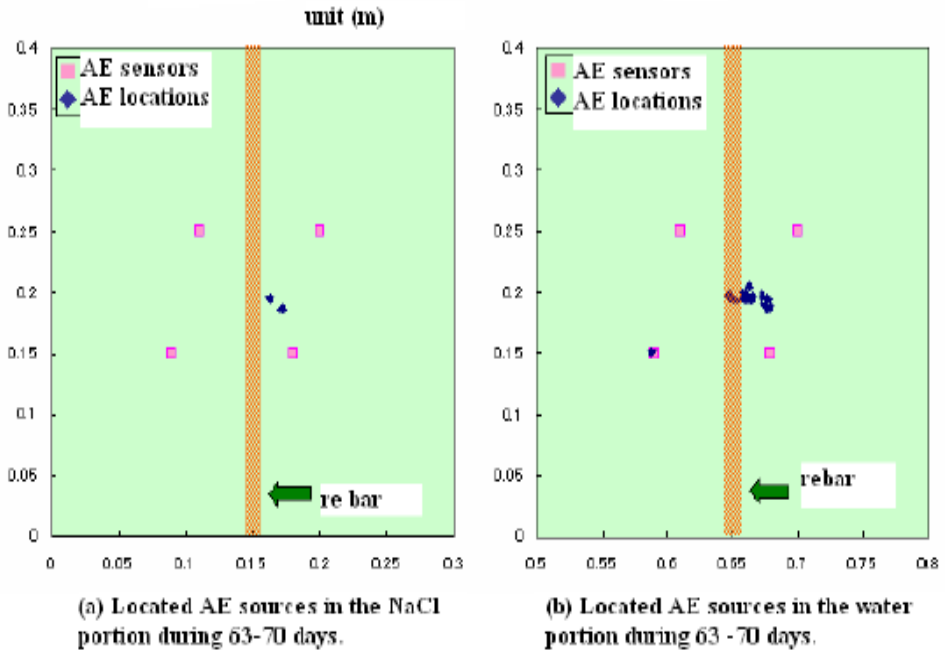

(a) Located AE sources in the NaCl portion during 63-70 days.

(b) Located AE sources in the water portion during 63 - 70 days.

Fig 3.27 AE sources located at the 2nd high AE activities in the test (Ohtsu et al., 2010)

Kawasaki et al. (2013) studied the corrosion mechanisms in Reinforced concrete by acoustic emission. In the paper, AE activities under a cyclic wet and dry test are investigated and these results are investigated by an electron probe microscope (EPMA). In order to investigate the Kinematical information of AE sources and nucleation of micro-cracks inside concrete, AE sources due to rebar corrosion in reinforced concrete are identified by SiGMA analysis (Simplified Green's functions for Moment tensor Analysis). In addition, characteristics of AE signals are investigated by using AE parameter analysis and Ib-value analysis. Three beams of dimensions 100mm X 75mm X 400 mm were made. A deformed rebar of 13 mm diameter is embedded with 20 mm cover -thickness. The process of corrosion due to salt attack was simulated by a cyclic dry and wet test. AE measurement was continuously conducted using an AE measuring system. Six sensors of 150 kHz were attached to the surface of the beam. The frequency range of the measurement was 10 kHz to 2MHz every week; the AE measurements were temporarily stopped to conduct a half cell potential measurement. After AE measurement, the other two beams were cut and SEM (scanning Electron Micrograph) observation was conducted to investigate the microstructures around the rebar.

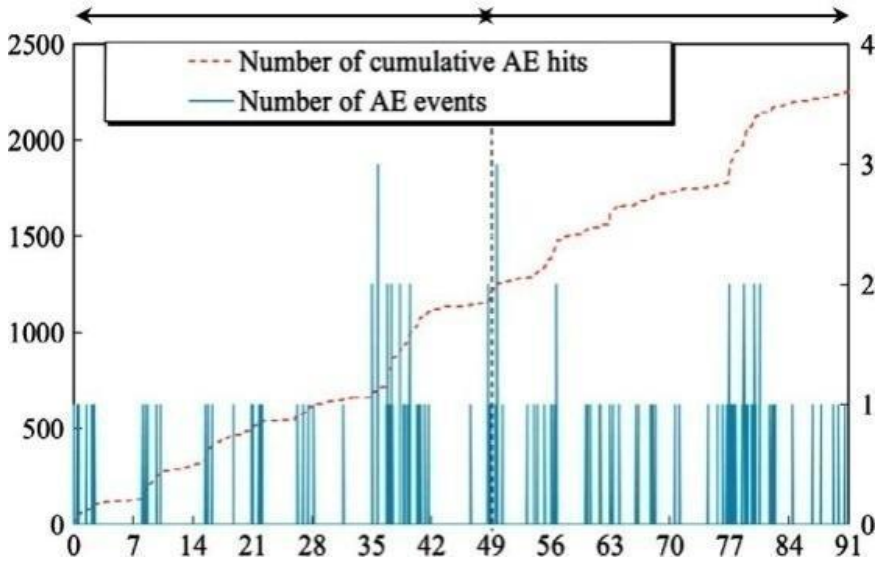

Fig 3.28 Number of cumulative AE hits and AE events (Kawasaki et al., 2013)

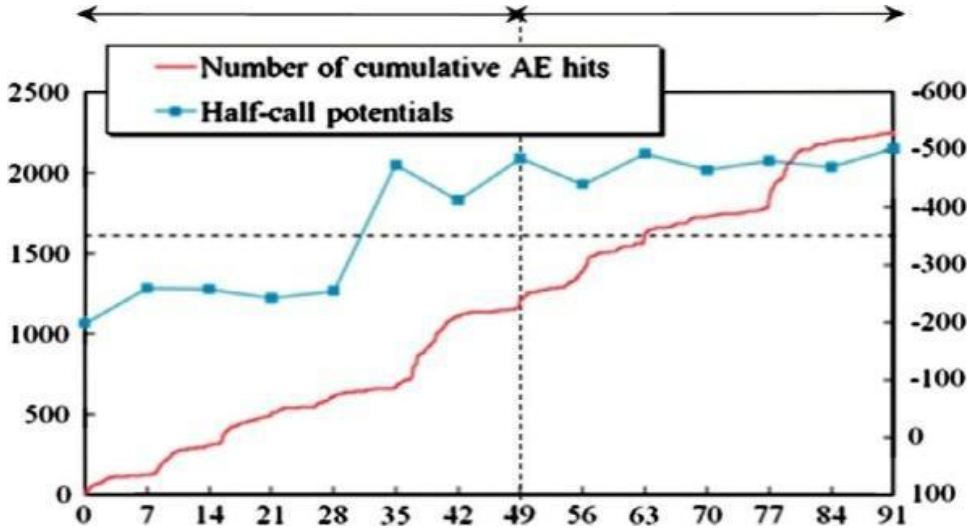

Fig 3.29 Number of cumulative AE hits and half cell potentials (Kawasaki et al., 2013)

Cumulative AE hits and AE events for every 1 hour of all 6 channels are shown in **Fig 3.28**. One AE event consists of 6 signals which were detected and analyzed by all 6 AE sensors. AE hits and AE events start to gradually increase during the first 42 days and the calm period of AE activity for a week is observed. The calm period is found after increase of the AE hits and AE events from 35 days to 42 days. In addition, the second increase of AE events was observed at 49 days. Therefore, the calm stage that was observed from 42 days to 49 days corresponds to Phase 2 in **Fig 3.30**.

Following the calm phase, AE hits and AE events increase continually. The curve of cumulative AE hits is in good agreement with the curve of corrosion loss. Thus, it leads to the fact that the onset of corrosion occurred during the first 42 days and the corrosion-induced cracks due to expansion of corrosion products could occur from 49 days to 91 days. Based on these findings, the corrosion process is divided into Stage 1 and Stage 2 as shown in **Fig 3.29**. Here, Stage 1 corresponds to Phase 1 and Phase 2, Stage 2 corresponds to Phase 3 and Phase 4. Cumulative AE hits are compared with half-cell potentials in **Fig 3.29**. The half-cell potentials start to decrease after 28 days. Then, the potentials keep negative and less than -350 mV in Stage 2. Thus, the increase in AE activity could be associated with the de-crease trend of the half-cell potentials. After Stage 1, corresponding to continuous increase in AE activity, corrosion-induced cracks in concrete is to be nucleated due to expansion of corrosion products in rebar. The corrosion could be started from the start. However, the half -cell potentials cannot detect the small corrosion. On the other hand, AE can detect very tiny corrosion phenomenon. That's why AE activities detected from the beginning in **Fig 3.31**.

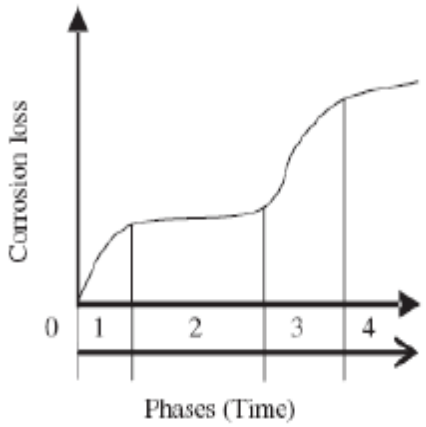

Fig 3.30: Evaluation of corrosion loss in steel under seawater immersion

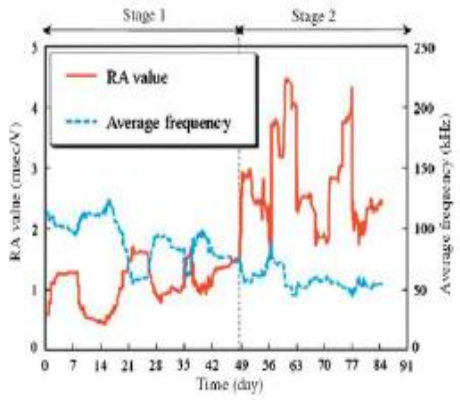

Fig 3.31 Variations of RA value and averaged frequency (Kawasaki et. al, 2013)

Variations of the RA values and the average frequency are given in **Fig 3.31**. Although the trend of variation is not clear at Stage 1, the RA values start to increase at Stage 2. From 14 days to 21 days elapsed at Stage 1, an abrupt increase in the RA value and the decrease in the average frequency are observed. This suggests that generation of other than tensile cracks due to the onset of corrosion in rebar. Interestingly the decrease of the half -cell potentials follows this generation. At Stage 2, the increase in the RA values and the decrease in the average frequency are further observed, suggesting nucleation of corrosion-induced cracks in concrete.

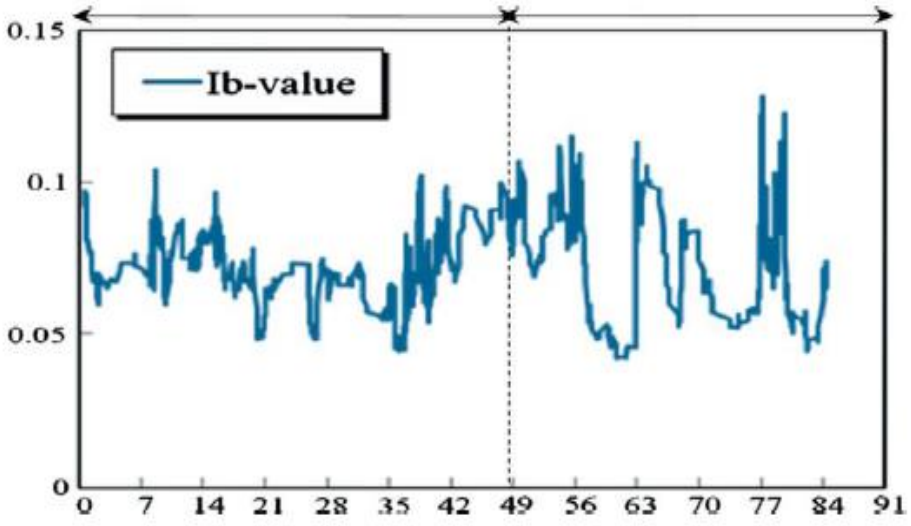

Fig 3.32 Variations of RA value and averaged Frequency (Kawasaki et. al, 2013)

Variation of the Ib-values is given in **Fig 3.32**. The large drops observed between 21 days and 35 days, before the first dramatically increase of AE activities. This might be implied that modest micro-cracks are generated as the onset of corrosion at the surface of the rebar. Due to high AE activity at Stage 2, the Ib-values decrease. Since results of Ib-values at 56 and 84 days elapsed are comparatively lower than those of the Stage 1, large-scale cracks are considered to be actively generated as corrosion-induced cracks in concrete. Furthermore, fluctuations of Ib-values in Stage 2 are even bigger than those of Stage 1. These results imply that cracks were repeatedly generated as the onset of corrosion and the corrosion-induce cracks in concrete.

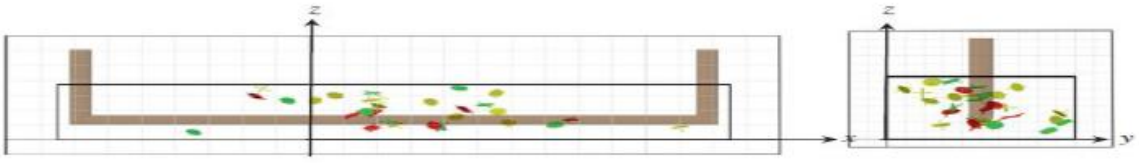

Fig 3.33 Results of SiGMA analysis during the first 49 days (Kawasaki et al., 2013)

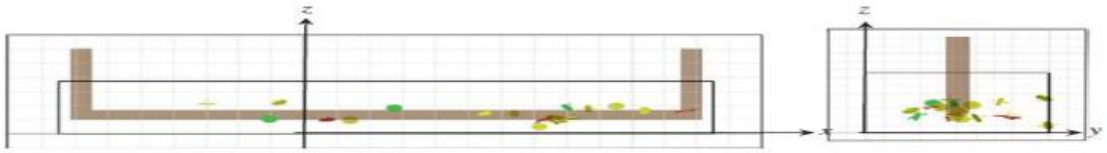

Fig 3.34 Results of SiGMA analysis from 49 days to 90 days (Kawasaki et al., 2013)

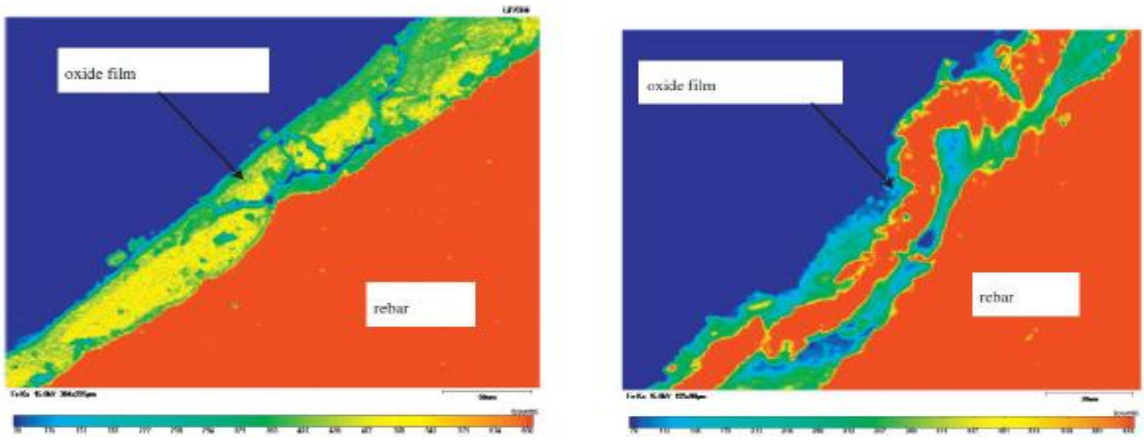

Fig 3.35 Mapping image of Fe of rebar on EPMA at 49 days (stage 1) and 90 days (stage 2)

Two Stages in the corrosion process are confirmed, in relation to the onset of corrosion in rebar and the nucleation of corrosion-induced cracks in concrete. At the onset of corrosion, the decrease of the RA value and the increase of the average frequency are observed. At the same time, the decrease of the Ib-value is confirmed. It implies that the onset of corrosion could be identified by AE parameter analysis. Particular AE activity is found at Stage 2, corresponding to Phase 3 and Phase 4 in the phenomenological model. Due to corrosion-induced cracks, many of AE hits are observed. At Stage 2, the in-crease of the RA value and the decrease of the aver-age frequency are observed. Then, the fluctuations of Ib-values in the Stage 2 are even bigger than those of Stage 1. This implies that Ib-value is effective to detect both the onset of corrosion and the corrosion-induced crack. At Stage 1, AE events were located in the specimen while no cracks were observed by the stereo-microscope. It implies that AE phenomena occurred due to corrosion initiation as the shear and the mixed-mode cracks. At Stage 2, micro-cracks were observed at the cross-section by the stereo-microscope. The locations of the AE sources by the SiGMA analysis (shown in **Fig 3.33** and **Fig 3.34**) are agreement with those of the corrosion-induced cracks in concrete, and AE sources are mostly of tensile cracks.

3.5 Review of Literature on Acoustic Emission for Monitoring the Setting of Cement Mortar and Concrete

Abeele et al. (2009) studied microstructural changes occurring in freshly poured concrete during curing have been monitored on a laboratory scale using a combination of the Acoustic Emission (AE) Technique with linear and nonlinear ultrasonic/elastic wave spectroscopy. The AE technique is a passive ultrasonic signal recording technique capable of online monitoring the internal microstructural activity of young concrete during the hydration process. Ultrasonic wave spectroscopy is traditionally used to evaluate the material's longitudinal and shear wavespeed and attenuation properties (providing properties such as Young's Modulus of Elasticity, Poisson's Ratio and Quality factor) by means of an active excitation of a medium with pulsed sound waves. In addition to these traditional techniques, we have implemented a nonlinear version of ultrasonic wave spectroscopy which probes the nonlinear elastic properties of the microstructure (offering information about the micromechanical behaviour) through the analyses of the harmonic generation from a continuous wave transmission through the concrete sample. The evolution in the AE events, and in the linear and nonlinear ultrasonic behaviour of young concrete is analyzed as a function of the degree of hydration for various initial compositions during the first three days of the curing process. The results show a good correlation between the linear and nonlinear acoustic properties and the phase changes in the concrete due to chemical reactions and mechanical setting seen in the temperature profile.

Haneef (2013) studied the crack growth behavior of plain and fly ash concretes with different curing periods during uniaxial compression testing using acoustic emission (AE) technique. Compressive strength of plain and fly ash concrete increase with curing periods and it becomes almost same order for 56 days curing. AE results have shown three distinct stages of AE activity in both concretes. The AE generated from the three stages has been attributed to crack closure/microcracking, steady crack propagation and unstable crack propagation. Fly ash concrete with proper curing produces evident filling effect for the pores and the occurrence of pozzolonic reaction leads to reduction of microcracking and corresponding decrease in amplitude of AE activity in the initial loading of fly ash concrete. The results showed that fly ash concrete specimen can withstand higher stress and strain without unstable crack propagation. An attempt has been made to compare types of cracking in both plain and fly ash concrete using AE parameters and it has been correlated with SEM images and final cracking pattern.

3.5 Summary

From the literature review, it is clear that very less work has been done in monitoring the freshly poured concrete using Acoustic emission technique. The aim of this research is to find out the behavior of freshly poured concrete and study the process of concrete setting and hydration by recording the signals from the changes that take place inside the concrete.

CHAPTER 4

EXPERIMENTAL INVESTIGATIONS

4.1 Introduction

Setting and hardening of fresh concrete are the most critical phases during the construction works, on which depend properties of concrete structure during its service life. During setting process, concrete mixture transforms from fluid state whose properties is important for placing into formworks into solid whose properties are important for the proper behavior of material in the service. Control of hardening phenomena can be used for determination of right moment for formwork removal, or load the structure. So, knowledge of fresh and young concrete is important from both, technical and economical aspects. It follows that accurate and useful testing methods for properties of young concrete properties determination are of great interest.

This chapter investigates the monitoring of early age setting of concrete during the first forty-eight hours of pouring concrete in accordance with IS 516 using Active(Ultrasonic guided wave and Ultrasonic pulse velocity technique) and Passive(Acoustic emission technique) monitoring techniques.

4.2 Experimental Program & Methodology

4.2.1 General

In this work, the setting and hardening of concrete will be monitored using Ultrasonic Guided Wave (UGW) technique, Acoustic Emission monitoring technique and Ultrasonic Pulse Velocity technique. To characterize the phenomenon of early age setting and hardening of concrete, destructive tests of compressive tests were also conducted at different stages of the setting and hardening phases. The idea was to correlate and investigate the efficiency of NDT techniques i.e. Ultrasonic & Acoustic Emission test results with other established strength development methods and also with in-situ strength of concrete.

4.2.2 Experimental Program

The proposed experimental work in this research has been detailed in the next page in flow chart in **Fig 4.1**.

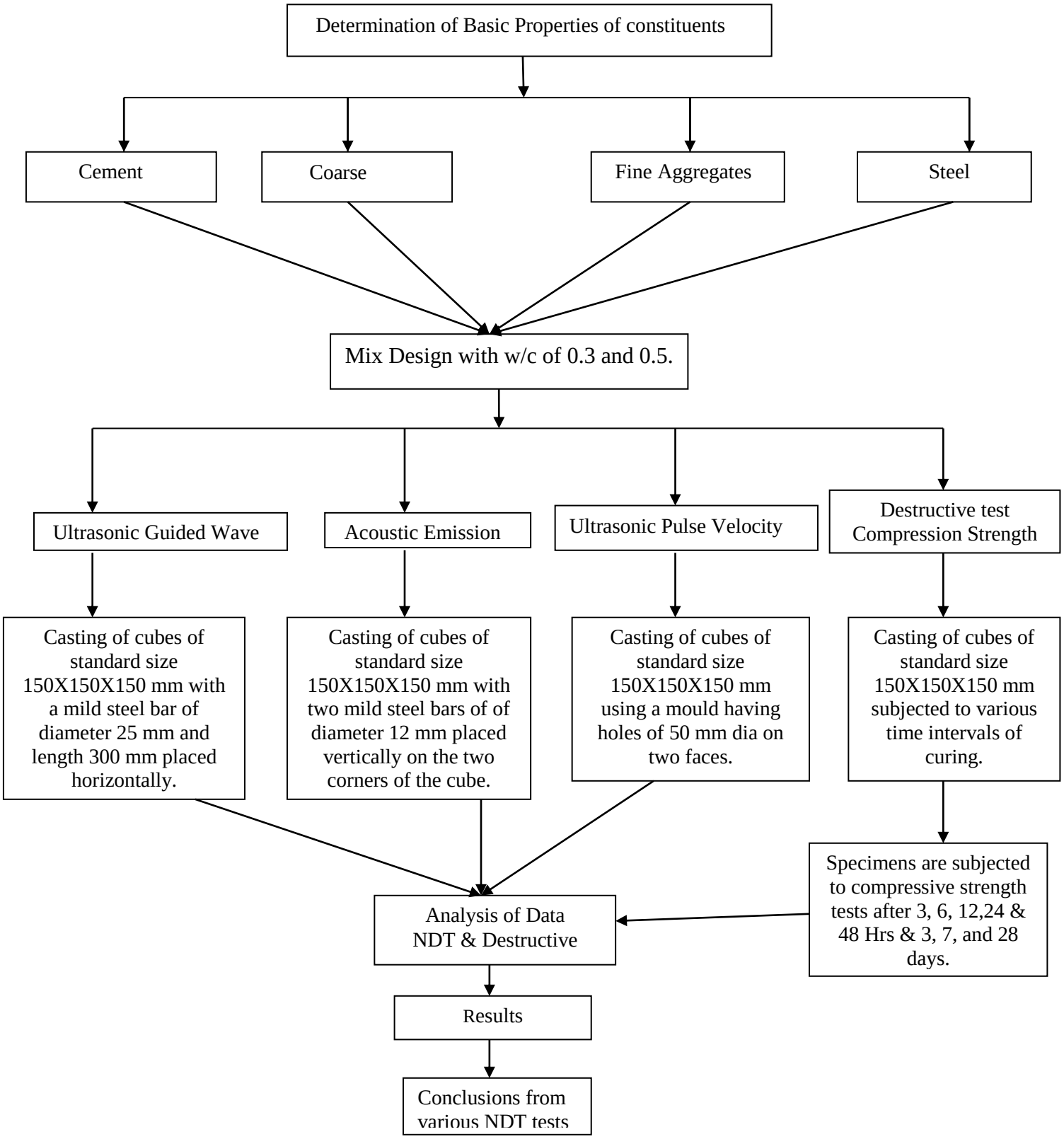

Fig 4.1 Experimental Program & Test Matrix

4.3 Materials used

Cement, fine aggregates, coarse aggregates, water and MS bars are used in casting of slabs. The specifications and properties of these materials are as under:

Cement: Ordinary Portland cement of 43 grades is used for the present investigation. The cement is of uniform colour i.e. grey with a light greenish shade and is free from any hard lumps. Summary of various tests conducted on cement are given in **Table 4.1**. All these tests are carried out in accordance with procedure laid down in IS: 8112 -1989.

Fine aggregates: The fine aggregates used for the experimental work is locally procured and conformed to grading zone III .Sieve analysis of the fine aggregate is carried out in the laboratory as per IS 383 -1870.The sand is first sieved through 4.75 mm sieve to remove any particle greater than 4.75 mm sieve and then washed to remove the dust. The physical properties and sieve analysis of fine aggregates are shown in **Table 4.2 and 4.3**.

Table 4.1 Physical properties of cement

S. No.	Characteristics	Values obtained	Standard Values
1	Normal consistency	33%	_
2	Initial setting Time	48 min	Not less than 30 min
3	Final setting Time	240 min	Not more than 600 min
4	Fineness	4.8 %	_
5	Specific gravity	3.09	_

Table 4.2 Physical properties of fine aggregates

S. No	Characteristics	Value
1	Specific gravity	2.59
2	Bulk density	1.33 g/cc
3	Fineness modulus	2.63
4	Water absorption	0.89
5	Grading zone (based on percentage passing 0.60 mm) Zone III	–

Table 4.3 Sieve analysis of fine aggregates

Sr.No.	IS-Sieve (mm)	Wt. Retained (gm)	%age Retained	%age Passing	Cumulative % retained
1	4.75	14.5	1.45	98.55	1.45
2	2.36	37	3.70	94.85	5.15
3	1.18	246.5	24.65	70.20	29.80
4	600 µ	205.5	20.55	49.65	50.35
5	300 µ	287.5	28.75	20.90	79.10
6	150 µ	177	17.70	3.20	96.80
7	Pan	32	3.20		
	Total	**1000.00**		**SUM**	**262.65**
				FM =	*2.62*

Total weight taken: 1000gm
Fineness modulus of fine aggregates = 2.68

Coarse aggregates: Crushed stone aggregates (locally available) of nominal size 10 mm are used throughout the experimental study. The aggregates are washed to remove the dust and dirt and are dried to surface dry conditions. The aggregates are tested as per IS: 383-1970.The results of various tests conducted on coarse aggregates are given in **Table 4.4** and **Table 4.5** shows the sieve analysis results.

Table 4.4 Physical properties of coarse aggregates

S. No.	Characteristics	Value
1	Type	Crushed
2	Specific gravity	2.69
3	Water absorption	0.5557 %
4	Fineness Modulus	6.91

Table 4.5 Sieve Analysis of Coarse aggregates

S. No.	Sieve size	Weight retained(gm)	Percentage retained	Percent Passing	Cumulative Percentage Retained
1	80	0.00	0.00	100.00	0.00
2	40	0.00	0.00	100.00	0.00
3	20	68.5	2.28	97.72	2.28
4	10	2776.5	92.55	5.17	94.83
5	4.75	113.5	3.78	1.38	98.62
6	Pan	0.00	0.00	0.00	
	Total	**3000.00**		**SUM**	**195.73 + 500 =**
				FM =	**6.95**

FM of 10 mm coarse aggregates= (195.73+500)/100 = 6.95

Water: Fresh and clean tap water is used for casting slabs in the present study. The water is relatively free organic matter, silt, oil, sugar, chloride and acidic material as per Indian standard.

Steel reinforcement: Mild steel bars of 25 mm diameter and 300 mm length were used as reinforcement for UGW monitoring and 12 mm diameter mild steel bars of 150 mm length were used for AET monitoring.

4.4 Preparation of specimen

4.4.1 AET and UGW monitoring

Cubes of standard size 150 x 150 x 150 mm size is cast with a mix proportion of 1:1.5:2.9 with two different water-cement ratios of 0.3 and 0.5. An average slump of 60-80 mm was observed and an ambient temperature of 30^0 C was kept throughout the experiment. A mild steel bar of diameter 25 mm is kept embedded in the cube horizontally in centre of crossection such that 75 mm length of the bar exposed to the environment from both sides **(Fig 4.2).** This scheme of set-up was used for guided wave monitoring. For AET monitoring, two mild steel bars of diameter 12 mm and 150 mm length were kept embedded in concrete vertically such that 75 mm of the bar is exposed to air. These bars were place diagonal to each other and have been shown in **Fig 4.2 & Fig 4.3** and Actual specimen are shown in **Fig 4.3**.

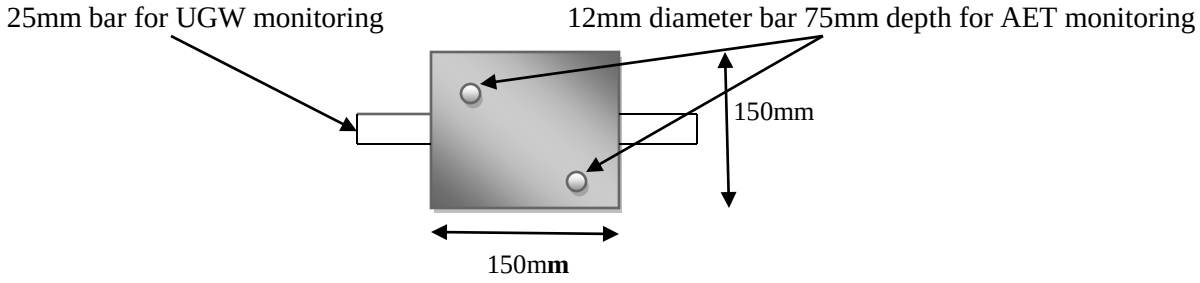

Fig 4.2 Schematic details of specimen (Plan)

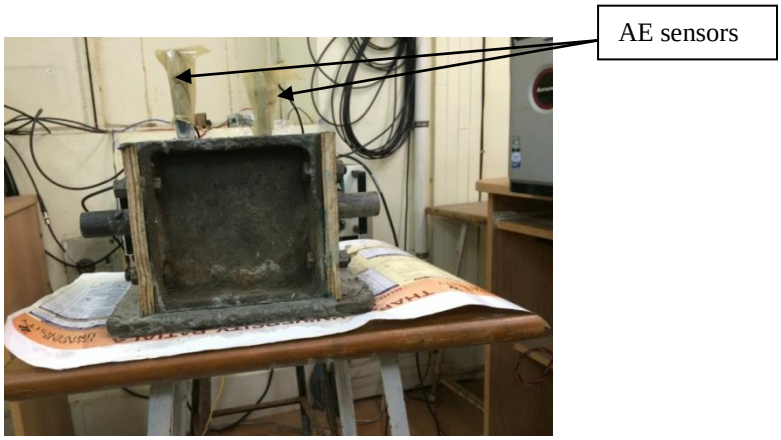

Fig 4.3 Actual Specimen for AET and UGW

4.4.2 UPV monitoring

Cubes of standard size 150x150x150 mm size are cast with the same mix proportion i.e. 1:1.5:2.9 using two different w/c of 0.30 and 0.45. Same mix as used in UGW and AET was used. The centerpoint of the cube was marked on two opposite faces and two perpendicular lines of length 25 mm were drawn passing through the center point. This was primarily done to ensure that the UPV transducers were kept exactly opposite to each other for better transmission and receiving of waves. The specimen is shown in the **Fig 4.4.** This arrangement of testing is called direct transmission. The basic purpose was to determine the variation in UPV with setting of concrete.

Fig 4.4 Actual UPV testing

The test matrix and scheme of NDT performed during the research are outlined in **Table 4.6** below.

Table 4.6 Test Matrix & scheme of experiments

Specimen nomenclature	w/c Ratio	Method of Testing	Duration of Test (hours)
C1	0.3	UGW & AET	48
C2	0.3	UGW & AET	48
C3	0.3	UGW & AET	48
C4	0.5	UGW & AET	48
C5	0.5	UGW & AET	48
C6	0.5	UGW & AET	48
C7	0.3	UPV	48
C8	0.3	UPV	48
C9	0.3	UPV	48
C10	0.5	UPV	48
C11	0.5	UPV	48
C12	0.5	UPV	48

4.5 Ultrasonic Guided Wave Investigations

4.5.1 Set-Up Detail

The Ultrasonic Guided Wave setup consists of a DPR 300 pulser receiver which generates an electronic pulse. It is used to excite a piezoelectric transducer which in this case was a cylindrical transducer. The mechanical vibration of the PZT patch emits ultrasonic waves. The transmitter was kept in contact with the solid mild steel bar of 25mm diameter and 300mm length which is embedded in a concrete cube of size 150 mm x 150 mm x 150 mm **(Fig 4.5)** The contact was ensured with the help of a couplant (ultrasonic gel) and a holder assembly. The receiver transducer is arranged on the opposite end of bar. These receiver is connected back to the pulser receiver, which sends the signals to the digitizer card and is displayed on LCD of computer screen **(Fig 4.6)**.

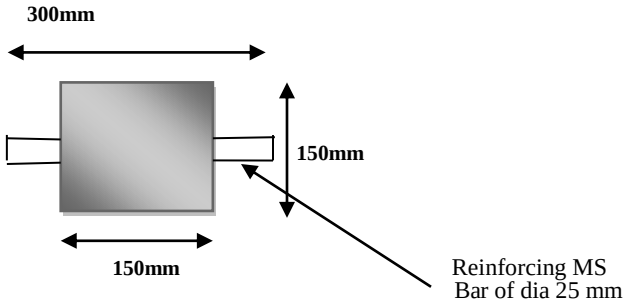

(a) Front view

Fig 4.5 Concrete cube specimen for ultrasonic investigation

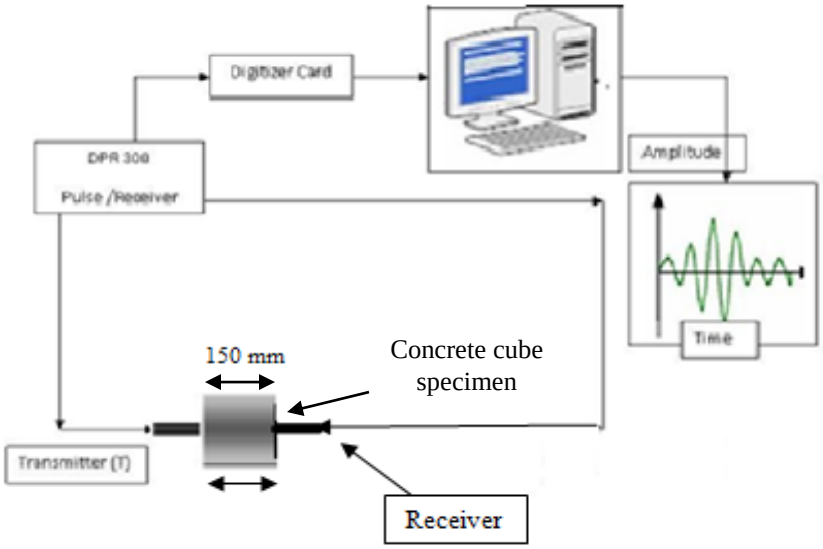

Fig 4.6 Experimental Set-Up for UGW investigation

Driven by the pulser/receiver, the compressional transducer generates ultrasonic pulse that propagates through the steel bar in the form of guided waves.

When concrete start setting the surrounding concrete begins making bond with the embedded steel rod which result in attenuation i.e. loss of wave energy occurs into the surrounding concrete. This attenuation is due to material absorption and energy leakage into the surrounding concrete. This attenuation energy is picked up by the receiver transducer and then converted into an electrical signal which has been processed in a computer and digitized for display.

Features of the UGW equipment used are as follows:

(a) Transducer

It is a single element longitudinal wave transducer. It can be used in straight beam flaw detection and thickness gauging, detection and sizing of delamination, material characterization and sound velocity measurements, inspection of plates, billets, bars, forgings castings, extrusions, and a wide variety of other metallic and non-metallic components. S 24 HB 0.1S (KARL DEUTSCH) & S 24 HB 0.1 E (KARL DEUTSCH) Standard transducers of 0.1 MHz frequency and 24 mm diameter has been used, as shown in **Fig. 4.7**.

Fig. 4.7 Contact used KARL DEUTSCH transducer

(b) JSR Ultrasonics DPR 300 Pulser/ Receiver System

JSR Ultrasonics DPR300 pulser shown in **Fig 4.7** produces a high voltage electrical excitation pulse (up to 475 Volt) and applies this pulse to the instruments T/R connector. An ultrasonic transducer connected to the T/R connector via a length of 50 Ω coaxial cable has been then

employed to convert the electrical energy of the excitation pulse into an ultrasonic pulse that has been propagated into a test material or medium.

(a)

(b)

Fig 4.8 JSR Ultrasonic's DPR300 Pulser/Receiver (a) Front View & (b) Back View.

DPR 300 can be configured to both pulse-echo and through transmission mode operations as discussed below;

- With the DPR300 configured for pulse-echo mode operation, acoustic echoes reflected from interfaces or defects within the test material are converted by the transducer into electrical signals that are presented to the T/R connector of the DPR300. The low-noise DPR300 receiver amplifies these electrical signals, and the signals then pass through adjustable high pass and low pass filters. The DPR300 receiver gain has been adjustable between -13 dB and 66 dB, and there are six high pass and six low pass filter settings for band-limiting the receiver frequency response. The amplified and filtered signals are available on the instruments Receiver Output connector.

- The DPR300 may also be used in transmission mode operation wherein a separate receiving transducer has been used to detect acoustic pulses that have propagated through a test material or medium.

4.5.2 Methodology for UGW monitoring

4.5.2.1 General

Pulse-transmission method is used for characterizing the young concrete strength and hardening process. To produce guided waves in the bar of concrete cube two transducers are attached at the two ends of the bar in projected cube. One transducer acting as a transmitter and the other acting as a receiver are attached parallel to the axis at the two ends of bar.

4.5.2.2 Selection of Excitation Mode and Frequency

The selection of frequencies for testing is done using the software Disperse (Pavalakovic & Cawley,2000). The selection of a suitable test mode and frequency can be made by close examination of the dispersion curves. The modes that are easily distinguishable and have lowest signal attenuation are selected. It is desirable to use a mode at a point of low attenuation, to maximize the inspection range, and to use a mode at a point of maximum energy velocity, to limit the effects of dispersion, and to reduce the risk of other modes complicating the received signal (Beard et al. 2003).

Dispersion curves for a 25mm bar embedded in concrete are plotted as shown in **Fig 4.9.** Only longitudinal modes have been considered in the study as the flexural and torsional modes experience high theoretical attenuation. Guided longitudinal waves are produced in the embedded bars by keeping compressional transducers parallel to the guiding configuration at the two ends of the bars embedded in concrete. The different longitudinal modes are excited by varying the excitation frequencies.

The selection of frequencies for testing is done based on the phase velocity dispersion curves **Fig 4.9(a).** They are validated by experimentally confirming the signal fidelity. In this work where bars are embedded in concrete, which is a layered waveguide system and leakage plays an important role. High frequency low attenuating modes with displacement profiles centered in the middle of bar to minimize leakage are found to be the best for layered systems. Phase velocity dispersion curves show the fundamental L (0,1) mode starting at zero frequency with each

higher order mode starting from a higher cut off frequency. Each of the higher modes shows a plateau region around the steel longitudinal bulk velocity line. This mode is selected for ultrasonic investigation being the lowest attenuation **(Fig 4.9(c))** and having lower frequency. Another contributing factor to the selection of mode is the relative sensitivity of ultrasonic waves to setting of concrete. **Fig 4.9(b)** shows the displacement mode shape and radial strain energy density distribution for L(0,7) mode not selected in the present investigation. The energy is concentrated in the central core portion of the bar and has relatively less surface component. Hence, it should be more sensitive to local bar topography or loss of material changes and not the surface profile changes.

Another contribution factor to the selection of L(0,1) mode is the mode shape of this mode. This mode has significant surface component would be sensitive to bonding effect of concrete on the bar. This mode shows significant axial displacement at the interface and is a ***surface sensitive mode*** (**Fig 4.10(a))** and hence, is chosen to monitor the bond development at 100 kHz.

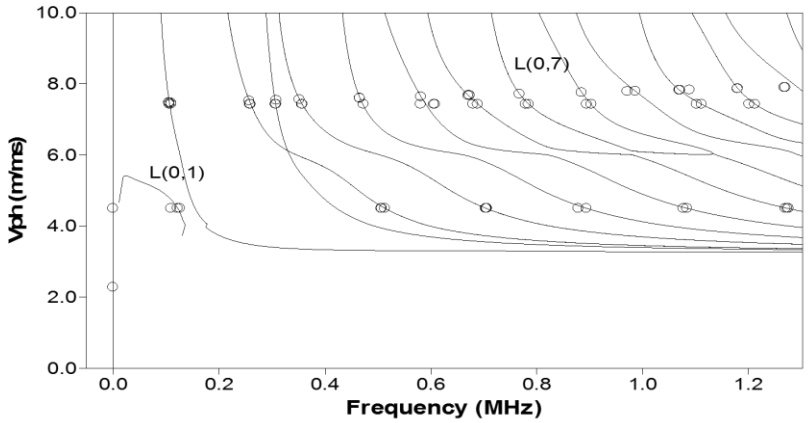

Fig.4.9 (a): Phase velocity Vs Frequency

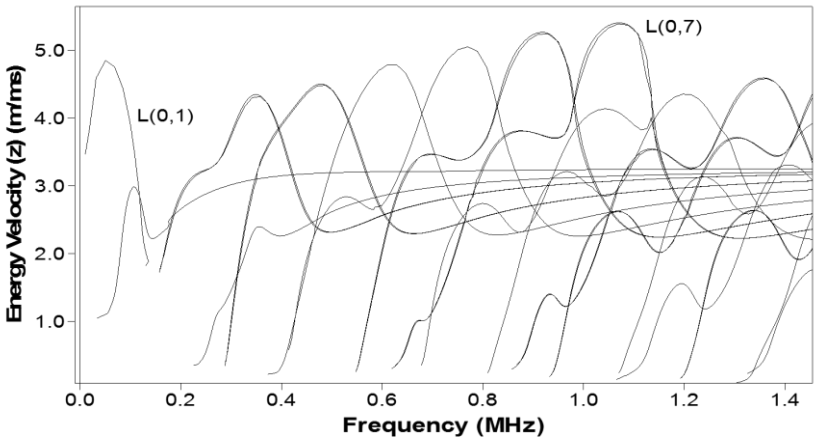

(b): Energy Velocity Vs Frequency

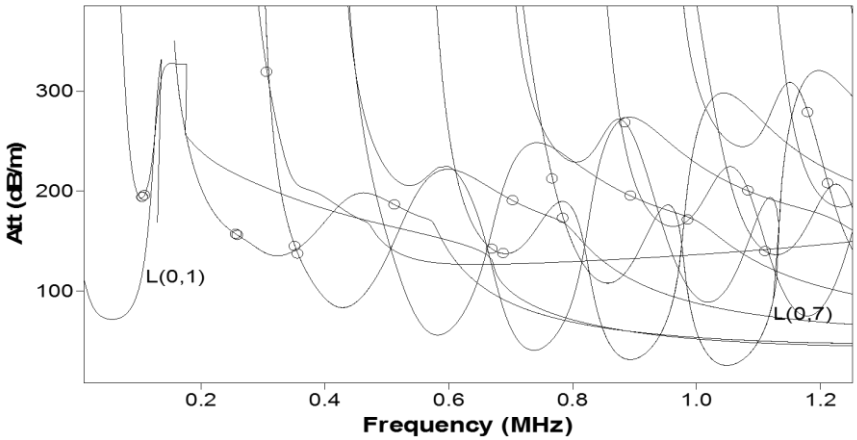

Fig.4.9 (c): Attenuation Vs Frequency

(Sharma & Mukherjee, 2014)

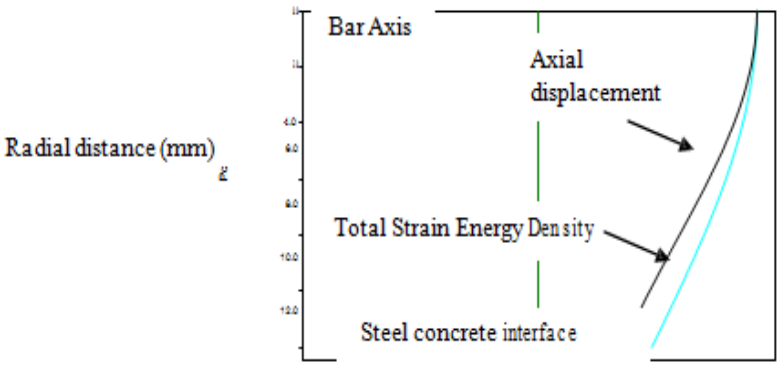

(a) Surface Sensitive Mode L(0,1) at 0.1 MHz

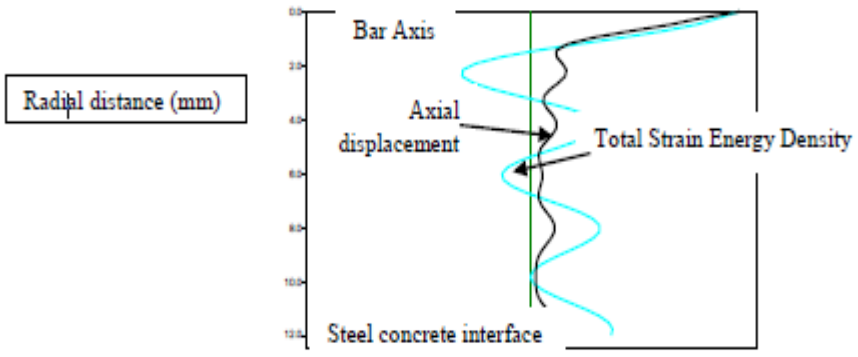

(b) Surface Seeking Mode L(0,7) at 1 MHz

Fig 4.10 Mode Shapes (Sharma & Mukherjee, 2010)

Transducers having longer wave form duration and a relatively narrow frequency bandwidth with centre frequency of 0.1 MHz (surface seeking mode) has been used because the main aim of the experiment was to monitor the bonding between the 25mm mild steel rod & the surrounding concrete in the cube.

4.6 Acoustic Emission Setup Details

The phenomenon of acoustic emission is defined as the propagation of elastic waves due to release of localized internal energy, such as micro-fracture in elastic material. Structural deformation processes such as plastic deformation, crack expansion and other kinds of material degradation are the sources of the AE activity. Detection, amplification, filtering and analysing the signal are some of the important issues in AE technology. AE monitoring system typically consists of sensors, preamplifiers and AE acquisition and analysis system. The schematic representation of AE set up is as shown in the **Fig 4.10.**

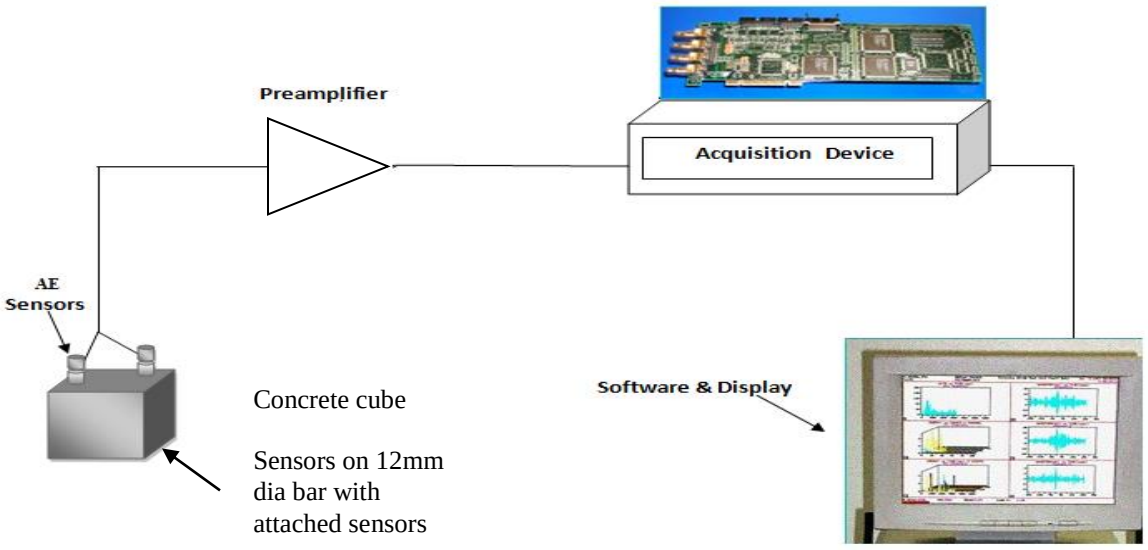

Fig.4.11 Schematic representation of the AE monitoring set-up

AE data acquisition system used for experimentation consists of Micro II digital AE system provided by PAC (Physical Acoustics Corporation) **Mistras Group** which is shown in the **Fig.4.12**.

Fig.4.12 Data acquisition set up used for the study

Sensors are placed on the surface of the structure to record acoustic emission signals. AE sensors are available in wide range of shapes and sizes as shown in the **Fig.4.13**.

Fig.4.13 Acoustic Emission Sensors

Acoustic Emission sensors which were used for monitoring the corrosion in the present study are shown in the **Fig.4.14** with detailed specification outlined in **Table 4.7**

Fig.4.14 R3α Sensors for AE acquisition used in the study.

Table 4.7 Specifications of AE sensors used in study

LABEL	**R3α**
Operating frequency range	35-100 KHz.
Resonant frequency	150 KHz
Physical Dimensions	19mm dia.× 22.4mm height
Weight	31 grams
Case Materials	Stainless Steel

The preamplifiers used in the study are shown in the **Fig.4.15.**

Fig 4.15 Pre-amplifier used

4.6.1 AE Monitoring Methodology

Good coupling of the sensors to the test specimen is necessary for the effective transmission of AE signals. Sensors are attached on the surfaces using magnetic holders, glues, even rubber bands and tapes. A layer of couplant such as vacuum grease, ultrasonic gel, and oil is applied between the two surfaces. Operating frequency range is important during sensor selection. The common frequency range for AE testing in civil infrastructure is 100-300 kHz.

In this experimental study, two AE sensors R3α sensors (resonant at 150 KHz) were mounted on the 12 mm dia steel bars and held tightly with brown tape. The sensors were attached to the steel bars using grease as a coupling agent. Two amplifiers were used with a gain set at 40 db and frequency range of 20-1200 KHz(**Fig 4.3)**. A band pass filter of 20-400 KHz was set in the software control of the data acquisition system. A threshold value was set at 45 db for experimental purpose.

Any acoustic activity occurring in the specimen is detected by the AE sensors mounted on 12mm dia reinforcing bar. These signals are amplified by the pre-amplifiers before entering the data acquisition system. The data acquisition set (Micro II Digital AE system) which processes the data and finally displays the data on the monitor screen.

AE signals were confirmed by breaking 0.5mm pencil leads at selected locations on the plate and in each position pencil lead break tests were done thrice. (**Fig. 4.16**)

Fig.4.16 Pencil lead break apparatus

4.6.2 Pencil Break Test study

The AE signals were generated by breaking 0.5mm pencil leads on the selected locations on the surface of the RC cube specimen and in each position pencil lead break test were done twice. This was done to make sure that sensors are mounted properly on the bars of Cube specimen and they are able to detect the reflections though their amplitude would be smaller than the crack related signal. AE process involves the use of sensors to detect released strain energy from the growing cracks. Hence, this technique has been widely used in the field of civil engineering for health monitoring and will be used in this research to investigate the setting and hardening of concrete.

4.7 Ultrasonic Pulse Velocity Methodology

4.7.1 Set-Up & Specimen Detail

TICO Ultrasonic Instrument: ZI 10006 as shown in **Fig 4.17** was used to measure the pulse velocity (m/sec) of the ultrasonic wave as it passes from concrete specimen as it gain its strength during setting & hardening.

Fig 4.17 TICO Ultrasonic Instrument: ZI 10006

150 mm sized cubes are used for UPV investigations, UPV readings are taken during the entire setting process of concrete at the interval of every 2 Hrs for 48 Hrs. The UPV readings are taken in direct transmission method keeping the 54 kHz probes on opposite faces of cube mould having two cut outs to attach the probes.

The various components of TICO UPV Instrument have been shown in **Fig 4.18**

Fig 4.18 Components of TICO Ultrasonic Instrument

A pulse of longitudinal vibrations is produced by an electro-acoustical transducer, which is held in contact with one surface of the concrete specimen under test. When the pulse generated is transmitted into the concrete from the transducer using a liquid coupling material like grease, it undergoes multiple reflections at the boundaries of the different material phases within the concrete. A complex system of stress waves develops, which include both longitudinal and shear waves, and propagates through the concrete. The first waves to reach the receiving transducer are the longitudinal waves, which are converted into an electrical signal by a second transducer and displayed in the digital display unit as shown in **Fig 4.19**. Electronic timing circuits enable the transit time T of the pulse to be measured.

Longitudinal pulse velocity (in km/s or m/s) is given by:

$$v = L/T \qquad \textbf{(4.1)}$$

Where; V is the longitudinal pulse velocity, L is the path length, T is the time taken by the pulse to traverse that length.

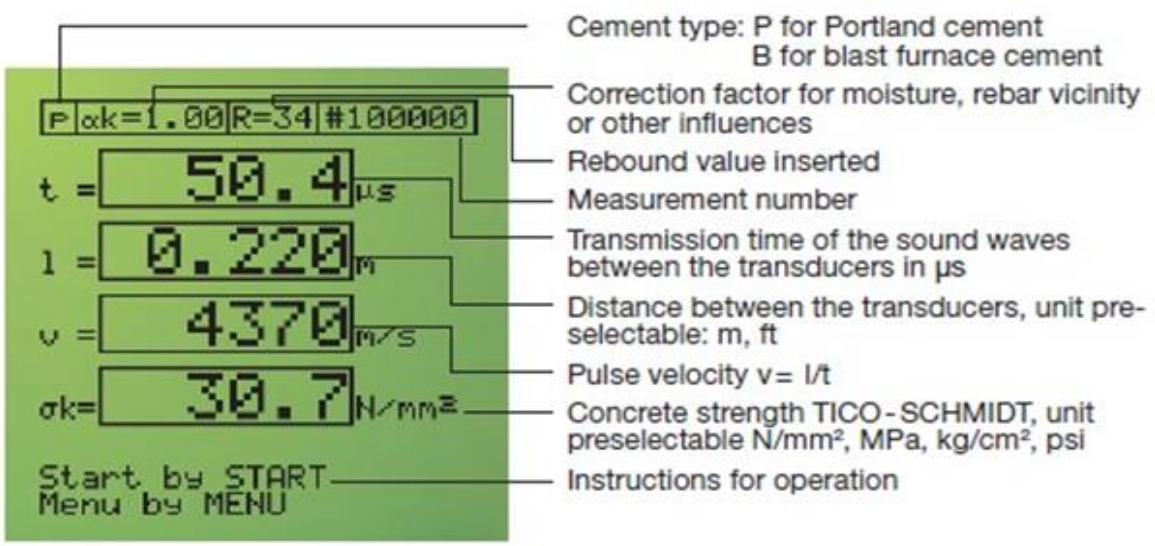

Fig 4.19 Display Unit of TICO Ultrasonic Instrument

The technical specifications of the display unit are given in **Table 4.8** as follows;

Table 4.8: Specifications of TICO Ultrasonic Instrument Display Unit

Display	128 x 128 graphic LCD
Interface	RS 232 or with adapter* to USB
Integrated software	for transmission of the measured values
Measuring range	~15 to 6550 µs
Resolution	0.1 µs
Voltage pulse	1 KV
Pulse rate	3/s
Impedance at input	1MΩ
Temperature range	-10° to + 60°C for instrument
Recommended range for measurements	0°C to 50°C only
Battery	6 LR 6, 1.5 V (30 hours operation)

4.7.2 Transducer arrangement in UPV Testing

The receiving transducer detects the arrival of that component of the pulse, which arrives earliest. This is generally the leading edge of the longitudinal vibration. Although the direction in which the maximum energy is propagated is at right angles to the face of the transmitting transducer, it is possible to detect pulses, which have travelled through the concrete in some other direction. It is possible, therefore, to make measurements of pulse velocity by placing the two transducers on either:

- opposite faces (direct transmission)
- adjacent faces (semi-direct transmission): or
- the same face (indirect or surface transmission).

These three arrangements are shown in Fig 4.20

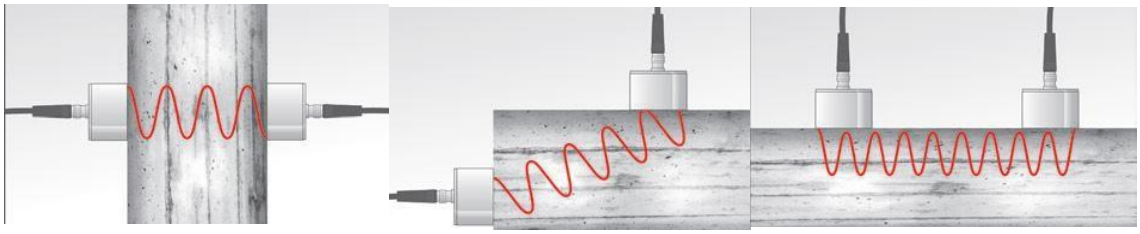

(a) Direct Transmission (b) Semi-Direct Transmission (c) Indirect Transmission

Fig 4.20 Different Transducer arrangements in UPV Testing

In our thesis we used direct transmission arrangement of transducer.

4.7.3 Methodology for UPV Testing

In this research work, UPV measurements are taken by direct transmission arrangement of transducers in first 48 hours at the interval of every 2 hours. Direct transmission arrangement of transducers was used, since the transfer of energy between transducers is at its maximum and the accuracy of velocity determination is therefore governed principally by the accuracy of the path length measurement.

Fig 4.21 Early age setting or strength monitoring (during first 48 Hrs)

The above figures clearly show that during the first phase the concrete specimen need to be kept inside a special steel assembly (mould) in order to measure the velocity (m/sec). This is because the specimen is wet & can easily loosen its shape during its removal from the frame.

4.8 Compressive Strength Testing

Compression test was carried out in order to determine the strength developed by the concrete during the initial setting phase. Cubes were cast for testing after 3,6,12,24 & 48 hrs of pouring concrete in the mould. This was done to ensure the relation between NDT of UGW & AET and destructive tests compression strength results. Further to check for strength of concrete, cubes were also tested for Compressive Strength after 3,7 & 28 days of curing to confirm the characteristic compressive strength of concrete mix.

(a) Complete setup **(b) Before Testing** **(c) After Testing**

Fig 4.22 Compression Testing of Cube using UTM

4.9 Closing Remarks

This chapter discusses in detail the working, technical information & various components of different testing equipment used in this experimental study. Emphasis is also given on the different concrete mix, Types & number of concrete specimens casted. The next chapter discusses the results obtained under various test conducted in the two different phases.

CHAPTER 5
RESULTS AND DISCUSSIONS

This chapter discusses about the results obtained by non destructive tests of Ultrasonic Guided Wave, Acoustic Emission Technique and Ultrasonic Pulse Velocity tests on the setting & with varying w/c ratios. Experiments as per the methodology discussed in last chapter have been carried out. However, it is to be noted that the integrated monitoring using NDT of Ultrasonic pulse transmission and Acoustic Emission monitoring was performed. The setting characteristics have been investigated during Non destructive and Destructive techniques.

5.1 Ultrasonic Pulse Transmission Investigations and Results

This test was conducted on a cube specimen of size 150 mm x 150 mm x 150 mm with an embedded mild steel bar of 25 mm diameter and 300 mm length **(Fig 4.3)**. The guided wave readings are taken with L (0,1) mode at 0.1 MHz and L (0,7) mode at 1MHz. First a healthy signature i.e. Voltage Vs Time graph is captured **(Fig 5.1a and b)** and then compared with signals taken at different times. Finally peak to peak voltage is measured and results are plotted as V-t (Voltage Vs Time) graphs.

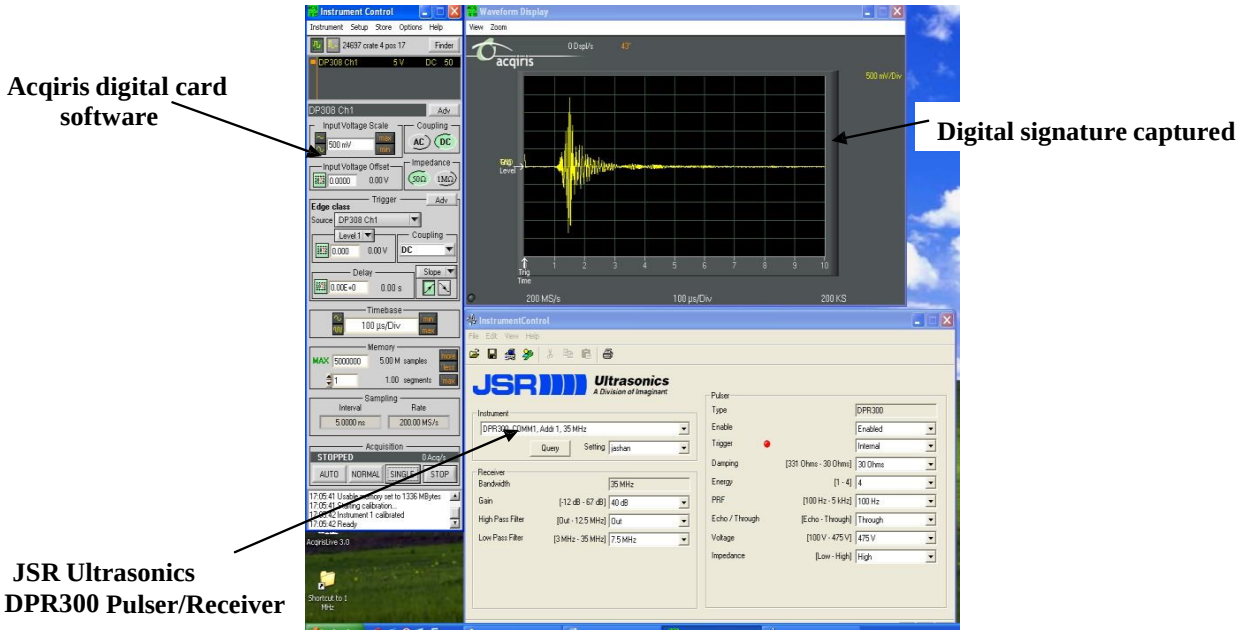

Fig 5.1(a) Image of waveform captured

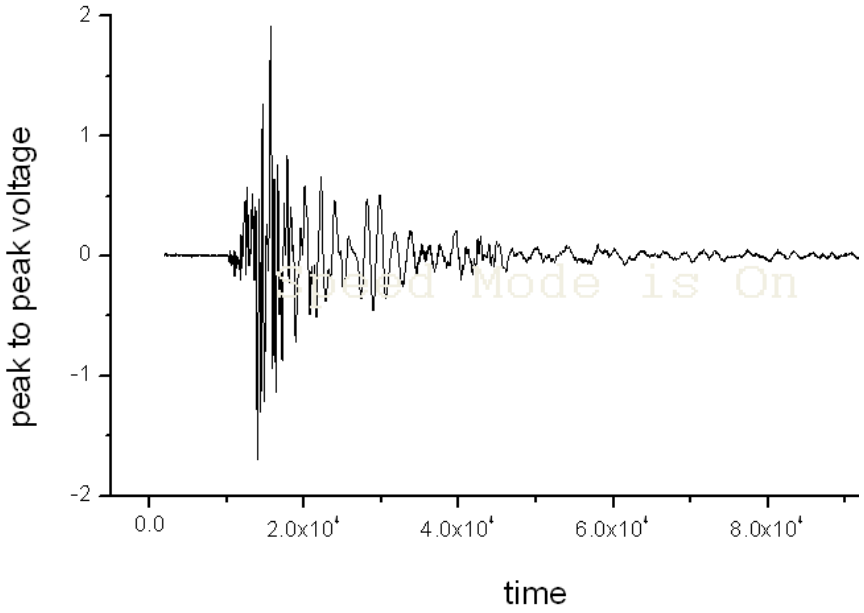

Fig 5.1 (b) Pk-Pk Voltage Vs Time Signature (Plotted in Origin 8)

As concrete sets and hardens, peak to peak voltage of signal of L(0,1) mode. This is because of the surface seeking nature of the mode selected. This mode picks up the bond development between the reinforcing embedded mild steel and surrounding concrete. As the concrete sets, bond develops between steel and surrounding concrete indicating more energy leakage into the surrounding concrete thus causing drop in signal strength. Hence the fall in signal strength is a measure of development of bond and hence setting of concrete with L(0,1) mode.

As outlined in chapter 4, the Ultrasonic Guided wave (UGW) readings are taken throughout 48 hrs of setting of concrete at regular time intervals (i.e. after every 2 hrs). The ultrasonic measurements are taken for concretes with two different water cement ratios 0.3 & 0.5 The UGW results were also taken with L(0,7) mode at 1 MHz to show that signal does not change with this mode as setting of concrete progresses with time.

To correlate the ultrasonic guided wave investigations with in-situ strength of concrete, the test matrix was developed. Along with the Ultrasonic guided wave investigations, destructive test after various intervals of setting and curing were performed. This was done for developing a better relationship between the ultrasonic monitoring and the in-situ strength of concrete.

5.1.1 Ultrasonic Guided Wave Investigation with w/c = 0.3

Ultrasonic pulse transmission signals were recorded using the selected modes for test no. 1, three specimens (i.e., C1, C2, and C3) were prepared with w/c ratio of 0.3 and Ultrasonic pulse transmission signals were recorded using selected modes immediately after pouring the concrete in cube at regular intervals of two hours for 48 hrs continuously. Both surface-seeking modes and the core seeking modes were used for monitoring the concrete samples.

Fig. 5.2 and Fig.5.3 show the pulse transmission signatures recorded at different times after pouring concrete in the mould using L(0,7) at 1 MHz and L(0,1) at 0.1 MHz respectively. From the signatures obtained at different intervals, peak to peak voltage amplitudes of the signals are calculated. This peak–peak voltage amplitude values are normalized with respect to input pulse amplitude obtained from an oscilloscope. This is reported as peak–peak voltage ratio (R). A plot of 'R' vs. age of concrete is plotted for both selected modes of L (0,1) at 0.1 MHz **(Fig 5.5)** and L(0,7) at 1 MHz respectively **(Fig 5.4**) at different instants.

From the signatures (**Fig 5.2**) and the peak to peak voltage ratio plot with increasing age of setting concrete (**Fig 5.4**), it is seen that with 1 MHz frequency and L(0, 7) mode, no drastic change in voltage amplitude of the first transmitted and received signal (Travel length = 300 mm) is observed throughout the 48 hour of pouring concrete though minor change is observed in second transmitted signal (Travel length = 600 mm) which is not measurable and of practical interest.

But when setting concrete is monitored using surface seeking L(0,1) mode at 0.1 MHz (**Figs. 5.3 and 5.5**), the peak–peak voltage amplitude of the received signals drops continuously with increasing age of concrete and the signal attenuates. This mode is sensitive to the interfacial changes. As the concrete sets, the bond between the embedded rebar and the surrounding concrete improves. It leads to increase in leakage of energy into the surrounding concrete; thus, causing a drop in signal strength. Hence, fall in transmitted signal strength with this low frequency mode is a good measure of development of bond between the embedded bar and the surrounding concrete and can characterize the setting phenomenon of concrete. These observations are made with concrete prepared with w/c = 0.3.

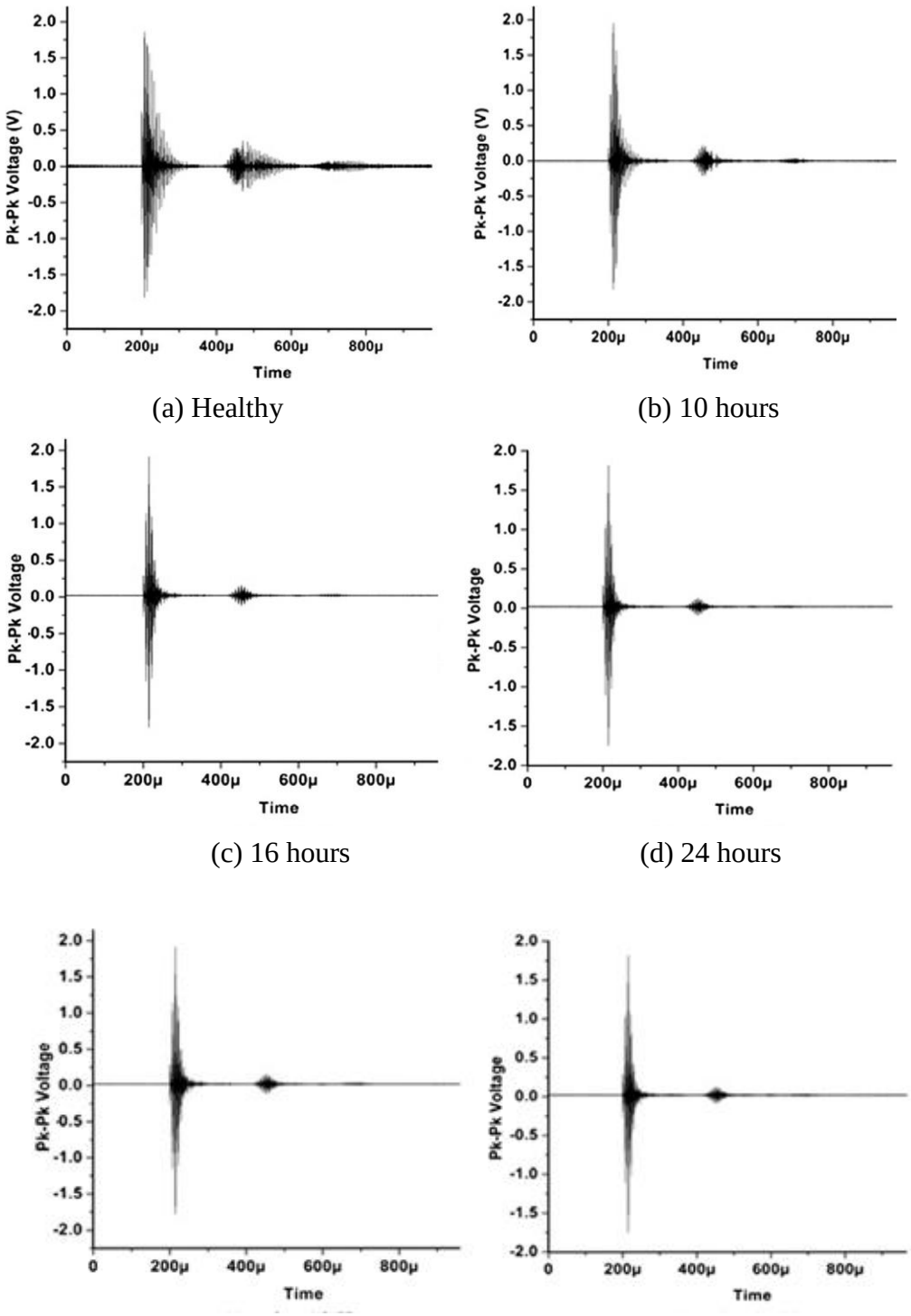

(a) Healthy (b) 10 hours

(c) 16 hours (d) 24 hours

(d) 36 hours (e) 48 hours

Fig.5.2: Pulse transmission signatures at different instants of pouring concrete using L(0,7) at 1 MHz

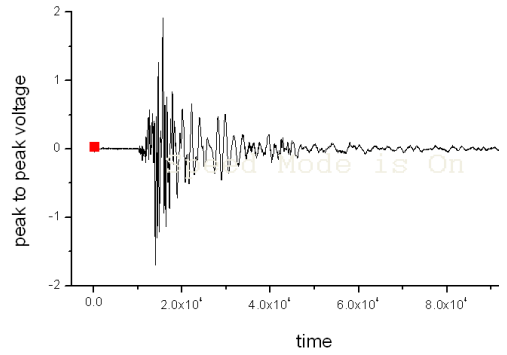

(a) Healthy

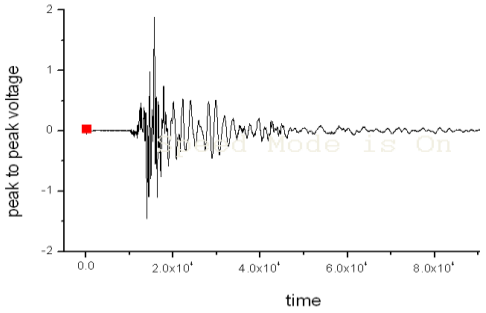

(b) 10 hours

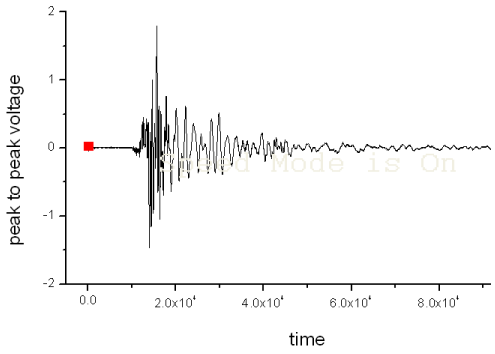

(c) 16 hours

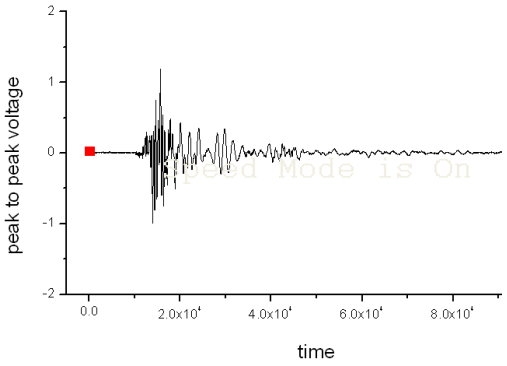

(d) 24 hours

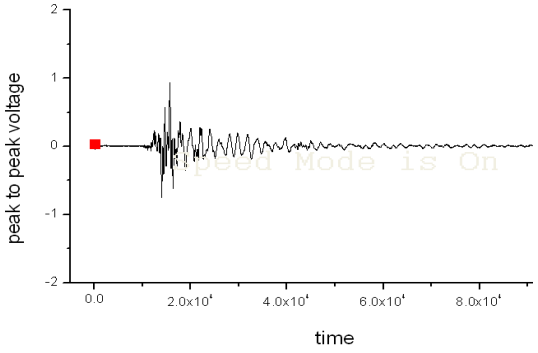

(e) 36 hours

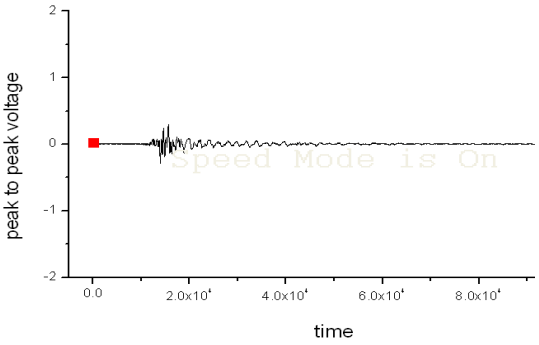

(f) 48 hours

Fig 5.3 Pulse transmission signatures at different instants of pouring concrete using L(0,1) at 0.1 MHz

The sensitivity of L(0,1) at 0.1 MHz can be explained by comparing its energy distribution profile vis-a-vis that of L(0,7) mode at 1 MHz The radial distribution of displacement and strain energy density of L(0,7) is concentrated mainly in the core area of the bar and has negligible surface component (**Fig. 4.9a**). Hence, signal in this mode is more sensitive to irregularities and deteriorations inside the bar rather than its surface. So it is not able to record bond development of bar with surrounding concrete.

On the other hand, L(0,1) at 0.1 MHz has significant surface component and is sensitive to changes

in interface characteristics like bond development due to setting of concrete. Such a mode is referred to as surface seeking mode and would be used for determining the setting pattern of freshly poured concrete using ultrasonic pulse transmission (**Fig. 4.9b**). This experiment illustrates the importance of selecting the right mode for ultrasonic monitoring of the setting process of concrete.

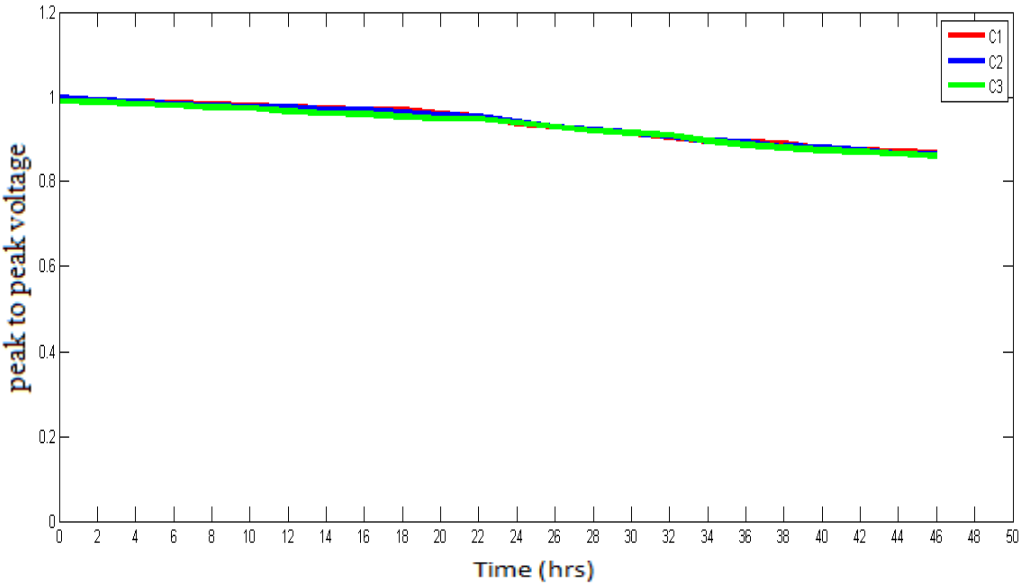

Fig 5.4 UGW monitoring with L(0,7) mode at 1 MHz

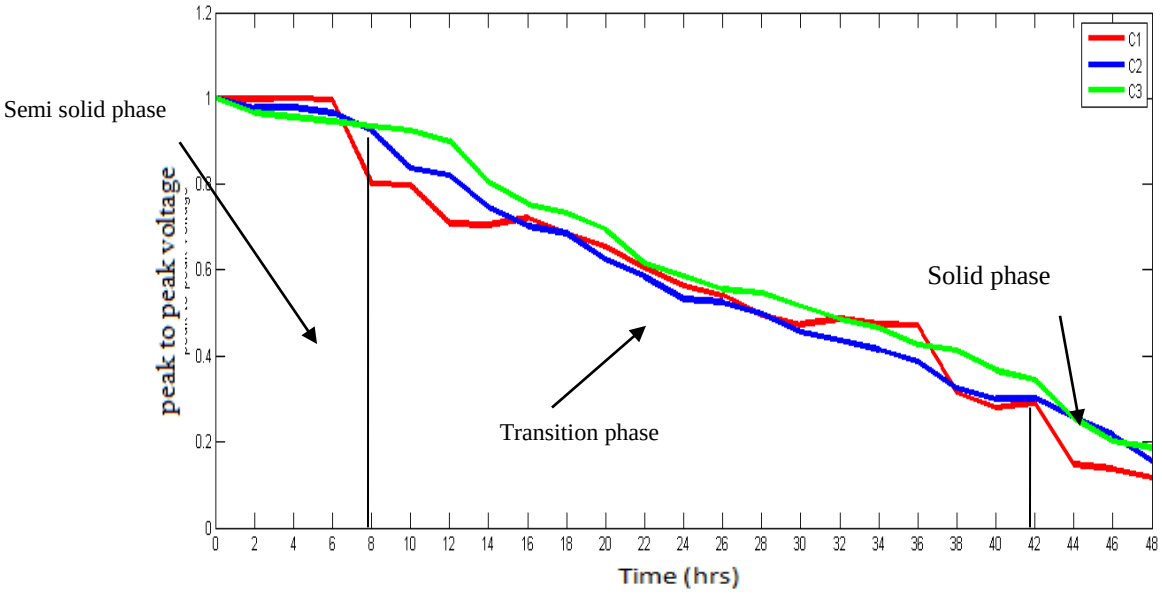

Fig.5.5 UGW monitoring with L(0,1) mode at 0.1 MHz

It is clear after seeing the UGW result graph that concrete setting involves three phases as

discussed below:

(1) Semi-solid Phase: In the **first 8 hrs**, the concrete is still in **semi-solid phase**. It is marked by very small peak-peak voltage of transmitted signal. Thus indicating there is not significant setting or bonding between the mild steel bar and the surrounding concrete.

(2) Transition Phase: From **9 - 42hrs**, The maximum fall in peak-peak voltage is observed in this phase indicating maximum bond development between steel bar and surrounding concrete. Concrete undergoes a change of phase from semi- solid to solid state or in other words concrete is starting to set or making bond with the embedded mild steel bar.

(3) Solid Phase: From **42hrs - 48 hrs**, there is again marginal fall in peak-peak voltage of the signal, indicating the concrete has become almost solid and no leakage takes place in surrounding concrete. There is hardly any setting or bonding occurring in this phase which shows that the maximum setting or bonding occur upto 42 hrs after casting.

5.1.2 Guided Wave Investigation with w/c = 0.5

For w/c ratio of 0.5, three specimens (i.e., C4, C5, and C6) were prepared ultrasonic pulse transmission signals were recorded using selected modes immediately after pouring the concrete in cube at regular intervals of two hours.

Fig 5.6 shows the UGW results with L(0,7) and **Fig 5.7** with L(0,1) at w/c = 0.5.

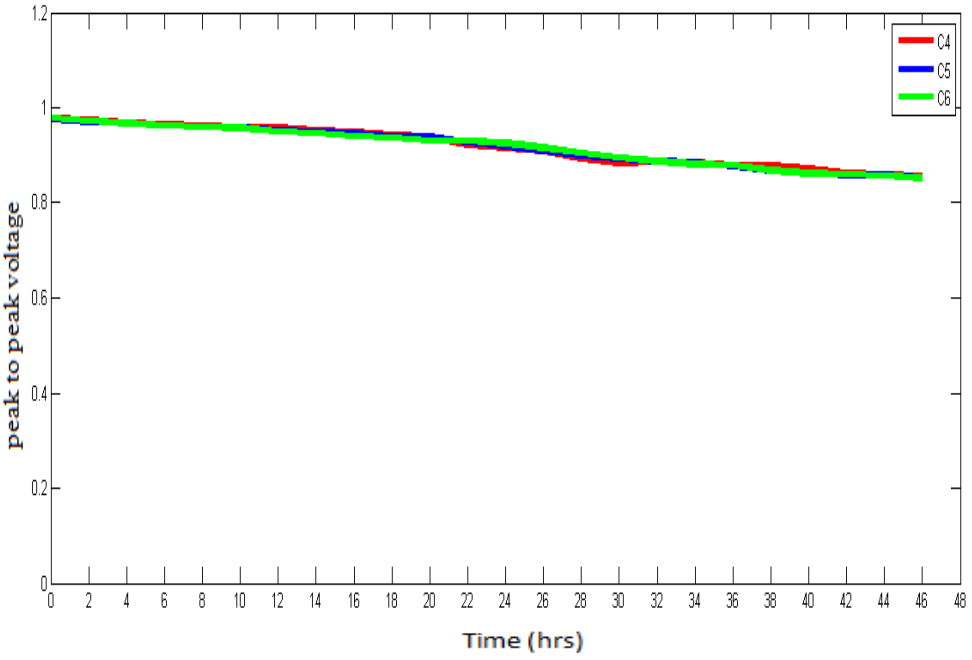

Fig 5.6 UGW monitoring with L (0, 7) mode at 1 MHz

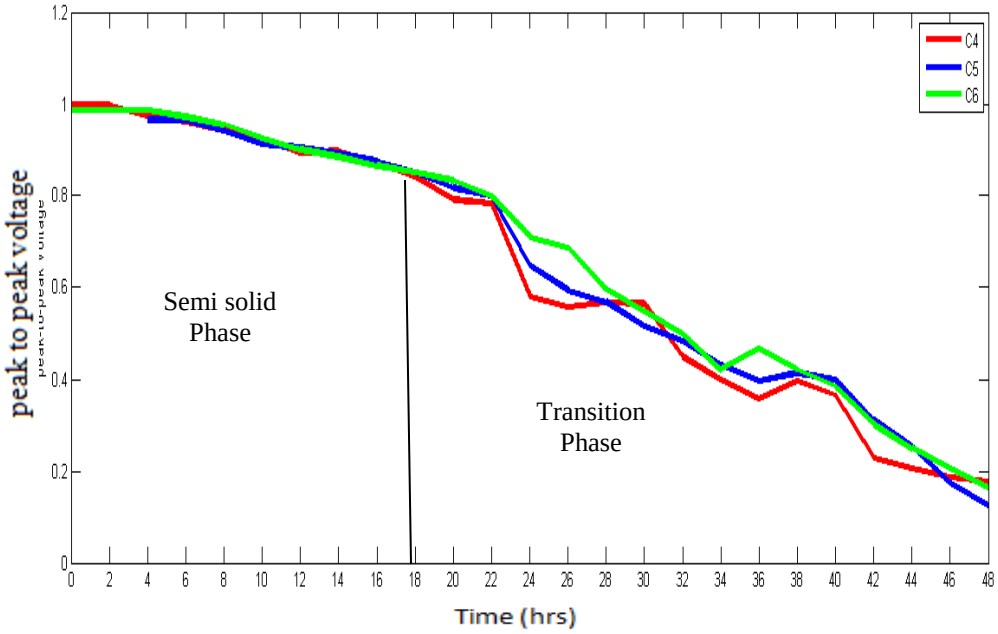

Fig.5.7 UGW monitoring with L(0,1) mode at 0.1Mhz

- With w/c = 0.5 the bond development process is slow and the semi solid and transition phases in setting of concrete is extended.
- In the first 18 hrs, voltage amplitudes remain steady in UGW (R falls from 1 to 0.97) indicating slow development of bond between the mild steel bar and the surrounding concrete (**Fig. 5.7**). It indicates that when concrete is in fluid phase and the bond between rebar and concrete is still not appreciable. This corresponds to 'Initial Setting of concrete' and the zone is referred to as **'Semi Solid phase'**. As against w/c of 0.3, where semi-solid phase is for 8 hrs it continues for 18 hrs with a w/c =0.5 this points towards slow setting with higher w/c ratio.
- From 18 to 48 hours, with a water cement ratio of 0.5, R drops from 0.9 to 0.1 in longer duration. It indicates development of bond between steel bars and embedding concrete and is an indicator of setting of the freshly poured concrete.
- There is no **solid phase** with increasing w/c ratio for same duration of testing.

From the results obtained with w/c = 0.5 signal attenuation and the corresponding drop in amplitude is not as sharp as with w/c of 0.3. This could be primarily because of the more water content thereby leading to slow rate of hydration due to which setting of concrete is delayed. The phases are extended due to delayed bond formation between steel bar and concrete. Also solid phase is missing or extended as the testing has been done for 48 hours only.

From the results it can be concluded that:

Various changes in concrete hardening process can very well be monitored using the ultrasonic guided wave technique using L(0,1) surface sensitive mode at 0.1 MHz

5.2 Acoustic Emission Investigation

5.2.1 Acoustic Emission Investigation with w/c=0.3

AE signals are picked up using the AE sensors are recorded using AE win software and are displayed in form of various parameters like Amplitude, Absolute Energy, Signal Strength, Duration and Hits etc. Out of the various parameters recorded during the 48 hours of monitoring, only few parameters i.e. Amplitude, cumulative signal strength and cumulative counts have been used to analyze the whole process of setting and hardening of concrete with AE events.

(1) Cumulative Counts Vs Time

Counts are defined as the number of times the signal crosses the pre-set threshold. **Fig. 5.8** shows the plot of Cumulative Counts Versus time for the whole setting process of concrete with a w/c ratio of 0.3 carried out on three samples (C1, C2, and C3). From the graph it can be clearly seen that there is a sharp increase in the number of Cumulative AE counts in the early hours of setting of concrete.

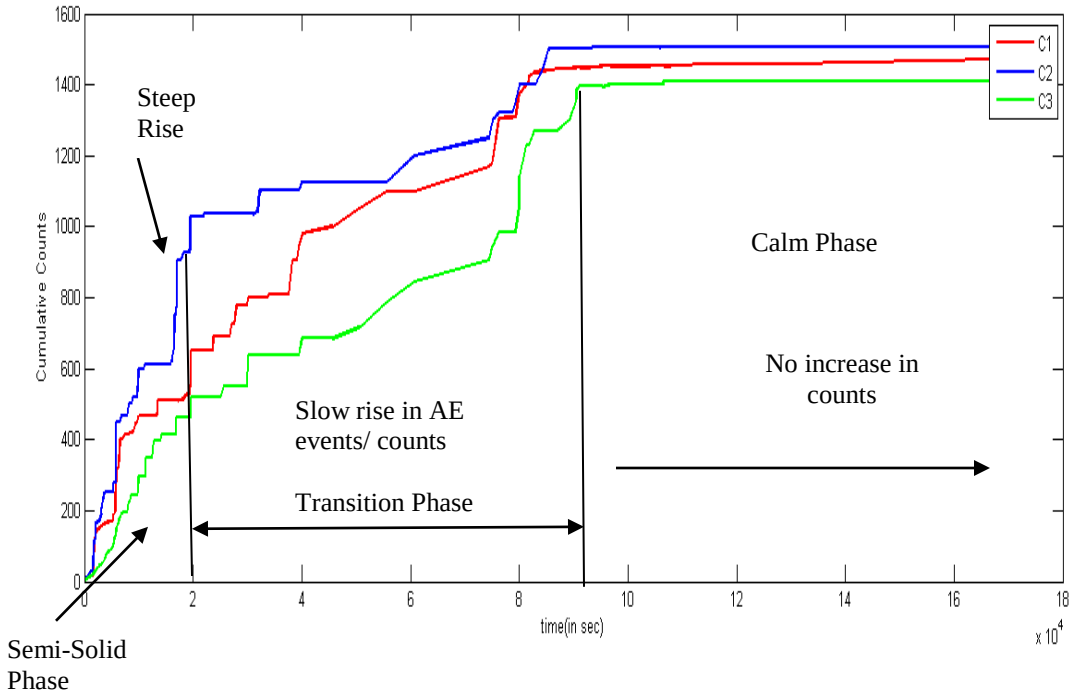

Fig 5.8 Cumulative Counts Vs Time

From the Cumulative Counts graph with setting of concrete with a w/c ratio of 0.3, following observations made:

- In **Semi-Solid Phase** i.e. from 0 to 8 hours, the rate of rise of Cumulative Counts is very steep. This points towards high rate of hydration in this duration and is equivalent to semi-solid phase. Ultrasonic guided waves indicate slow development of bond between steel and concrete by slow fall in voltages but steep rise in AE cumulative counts indicate fast rate of hydration in this phase. Bond development is not visible much but rate of hydration being very high initially causes release of heat of hydration and hence, initial rise in AE activity.
- In **Transition phase** i.e. 8 to 24 hours, the rate of change of cumulative counts is not as steep as it was during the semi-solid phase. Since the change in slope is gradual and not very steep i.e, less no. of counts are recorded during this period. This corresponds to the fact that the rate of hydration process is reduced during this period and is equivalent to transition phase.
- In **Calm phase** i.e. 24 to 48 Hrs there is hardly any increase in the number of counts suggesting that the very less signal or no signal has been recorded by the instrument. This suggests that hydration process has slowed down to a great extent and is equivalent to calm phase.

The slope of the cumulative number of counts during various time intervals can very well be related with the process of hardening of concrete with time. The initial steep slope i.e. the time interval immediately after pouring when the concrete is in fluid phase may be attributed to the fact that there is a lot of heat of hydration which is released with the setting of concrete. The greater the loss of heat of hydration, greater will be the molecular changes amongst the stress planes inside the concrete and hence greater amount of Acoustic Emissions shall be recorded.

With the progression of time, loss of heat of hydration reduces therefore explaining the gradual slope of cumulative counts during the transition phase. And after 24 hours of pouring of concrete, most of the heat of hydration has been lost and concrete is set and also the bond between the concrete and the steel has been well developed.

(c) Amplitude of Hits

Amplitude of the signals is expressed in volts or in AE decibel scale where 1 uV at the sensor is defined as 0 dB. **Fig.5.9** (C1,C2,C3) gives Amplitude of AE hits Vs time plot for all the three samples with w/c ratio of 0.3. From typical Amplitude Vs time graph it is seen that during the initial phase (0-8 Hrs) the amplitude of AE hits is in the range of 40-80 dB and is high. This points towards loss of heat of hydration due to hydration in concrete initially. The same continues in the

transition phase (8- 42 Hrs). Amplitude of AE hits is 40-60 dB and is predominant. But after 24 hrs in Calm phase the concrete has solidified enough and the energy of AE events is very less and hardly detectable by sensors with threshold.

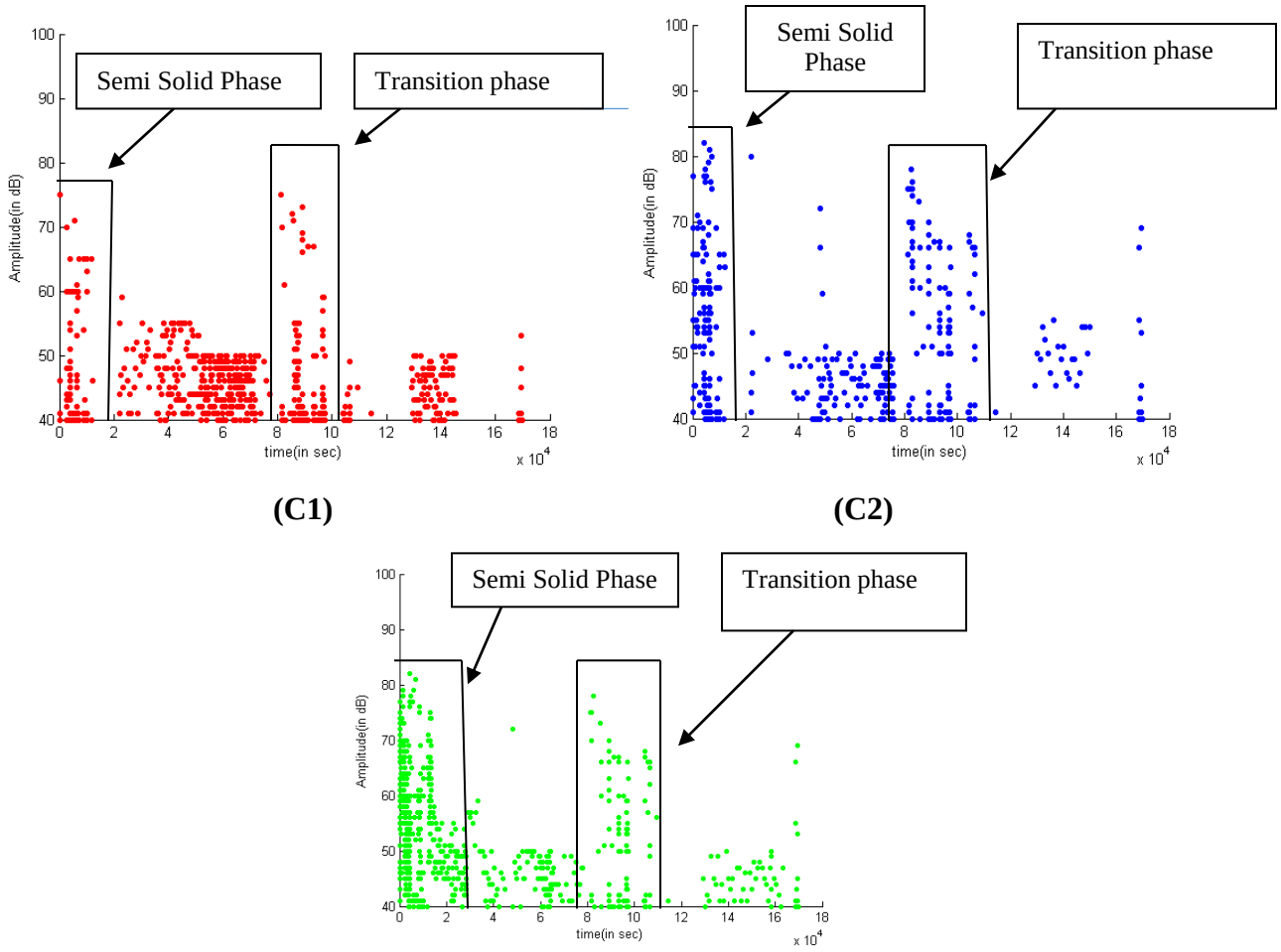

Fig 5.9 Amplitude of AE Hits Vs Time

From the graphs it can be very clearly seen that the signals recorded in the early period after the pouring of fresh concrete have high amplitudes ranging from 40-80 dB and this can be termed as the "**Semi-Solid phase**". This very much corresponds to the initial chemical action between cement, water and aggregates in concrete which is an exothermic reaction and points towards release of heat energy marked by high amplitude AE hits. This phase starts from beginning till 8 Hrs.

- After this period, during the bond between the steel and the concrete strengthens at a faster rate. The Amplitude of AE hits is still significant during this phase. Heat of hydration also

takes place during 8-24 hrs and is indicator of concrete hardening and bond strengthening. This leads to Acoustic Emission Signals with high amplitudes marked by high dB AE records. This corresponds to transition phase of concrete from semi-solid to solid.

- After 24 hours, the AE signals recorded have low amplitude. This point towards completion of hydration reaction in 24 hrs. The release of heat energy after 24 Hrs in concrete marked by low amplitude AE signals. Almost complete hydration takes place in 24 Hrs in concrete as indicated by AE signals. But development of bond strength between steel and concrete continues upto 48 Hrs after pouring concrete as indicated by significant signal drop in Guided Wave pulse amplitudes.

(3) Cumulative Signal Strength

AE Cumulative Signal strength which can be used for studying setting of concrete after pouring in mould. It is a reliable parameter as it is dependent on amplitude and duration and is independent of gain and referred to as the measure of the total energy released by the specimen. **Signal Strength** is the measured area of the rectified AE signal with units equal to pico-volt-sec.

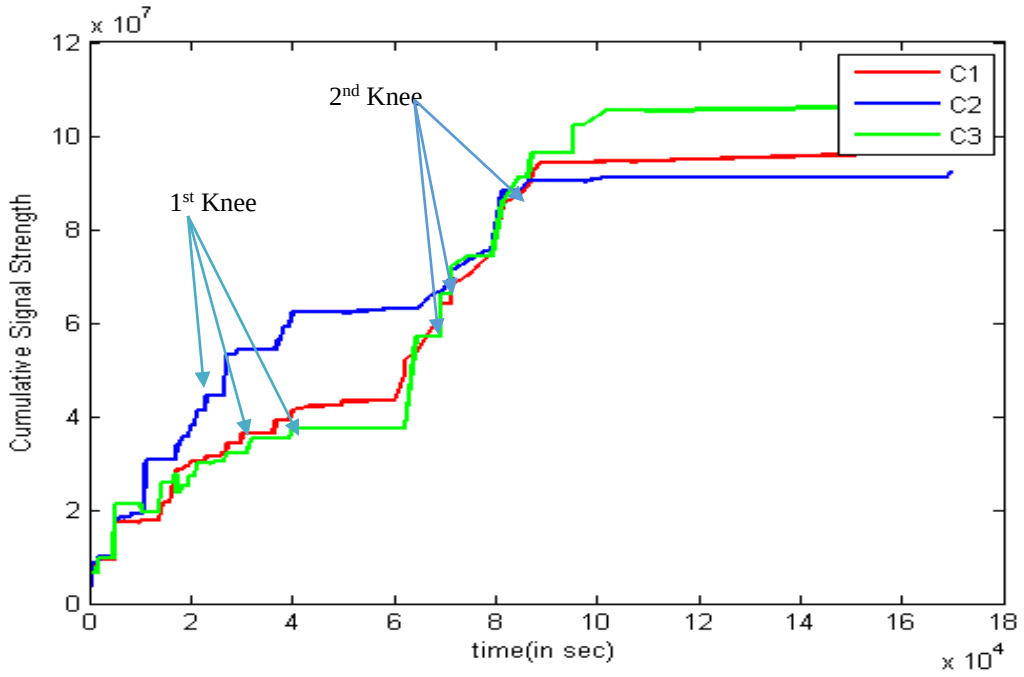

Fig 5.10 Cumulative Signal Strength Vs Time

Fig. 5.10 shows the plot of cumulative signal strength versus time for all three samples (C1, C2 & C3) with w/c ratio of 0.3.The AE signal strength data was determined using ASCII UTILITY option of AE Win software and later on cumulated for plotting graphs.

In the graph, it can be clearly seen that there are sharp changes in the slopes of the CSS curves

occurring after a duration of 8 hours and 24 hours of pouring of concrete. These sharp changes are sometimes called as "Knee on the CSS curve" and are considered as the positive manifestation of the major changes in concrete.

- The **1st knee** signifies the greater loss of heat of hydration and faster rate chemical reaction between the constituents of concrete, leading to concrete setting. But from the graph (amplitude), it can also be seen that the values of amplitude are not very high. This implies that the initial recorded signals is entirely because of large amount of disturbances occurring in the concrete and the lower amplitudes may be because of the semi-liquid phase of concrete where the attenuation of the signal would be very high. The 1st knee is followed by a gradual change in slope suggesting smaller changes still occurring in the concrete.
- The **2nd knee** around 20 to 24 Hrs suggests greater amount of concrete hardening. This is even evident from the **Fig 5.10** that the values of signal amplitudes are very high during this period. This also suggests that the greatest amount of chemical reaction and setting occur during this time period. There is less attenuation in the signal amplitude.

5.2.2 Acoustic Emission Investigation with w/c=0.5

For w/c ratio 0.5, three samples C4, C5 & C6 were cast with the same mix proportion.

(1) Cumulative Counts Vs Time

Fig. 5.11 shows the plot of cumulative counts plotted against time for all the three samples with w/c ratio of 0.5. From the graph, following observations can be made:

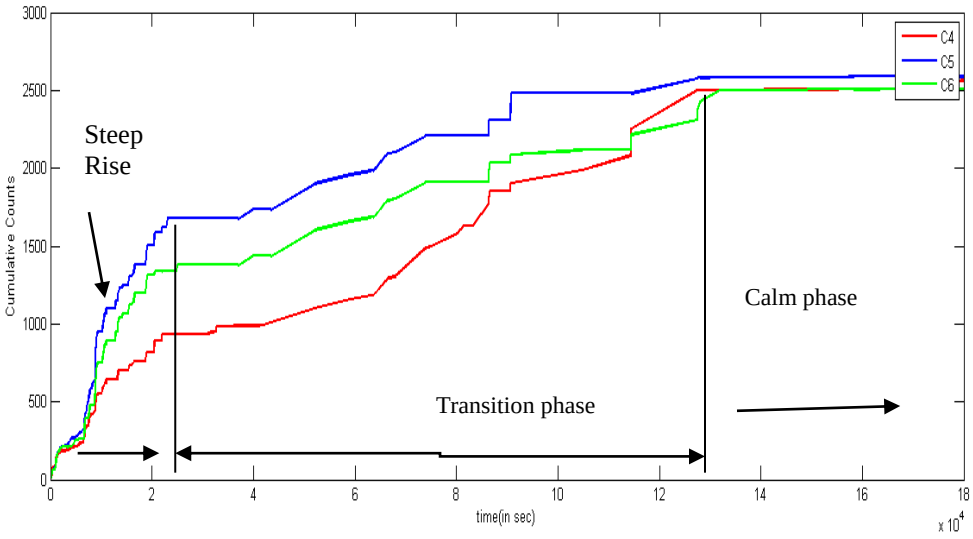

Fig 5.11 Cumulative Counts Vs Time

- In **Semi-solid phase** i.e. 0 to 10 hrs the rate of rise of Cumulative counts is very steep suggesting that the hydration process immediately started at a higher rate and at a faster rate. The semi-solid phase is of relatively longer period than it was in the case of 0.3 w/c ratio.
- In **Transition phase** i.e. 10 to 40 Hrs the change in slope is gradual but the increase in counts is almost upto 40 hours after the pouring of concrete. This may be attributed to the fact that in concrete with w/c ratio of 0.5, the hardening takes a little longer than those with lesser w/c ratios. The primary reason is that the loss of heat of hydration is delayed with greater w/c ratio which is a proven fact. Also, from ultrasonic readings it is clear that the bond strengthening would depend upon the setting and hardening of concrete which would ultimately be delayed. This is very much evident from the graph that the length of the **Transition phase** in this case is much greater than that in the case of samples with lower w/c ratio. This implies that the rate of setting and also the concrete hardening is much slower than with lower w/c ratio and depends on w/c.
- In **Calm phase** i.e. 40 to 48 Hrs there is hardly any increase in the number of counts suggesting that the very less signal or no signal has been recorded by the instrument. This further suggests that most of hydration has occurred and the rate of hydration has been slowed down to a great extent.

(2) Amplitude of Hits

It is also evident from the Amplitude versus time plot for all the three samples with w/c ratio 0.5. In all the three graphs, three peaks of high signal amplitudes can be observed. These can be regarded as **semi-solid phase** in this case shows less Hits due to slow hydration process.

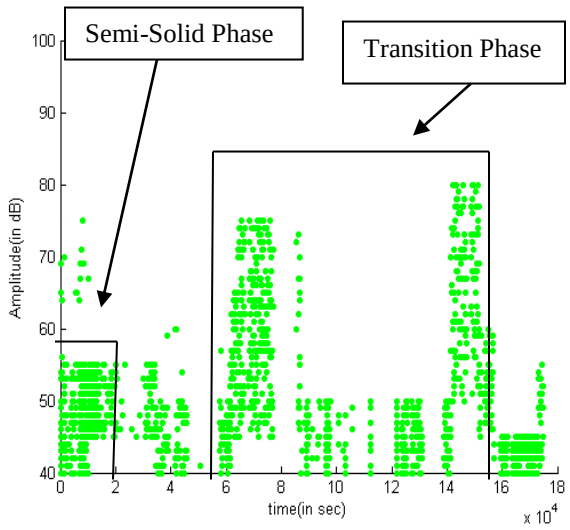

(C4)

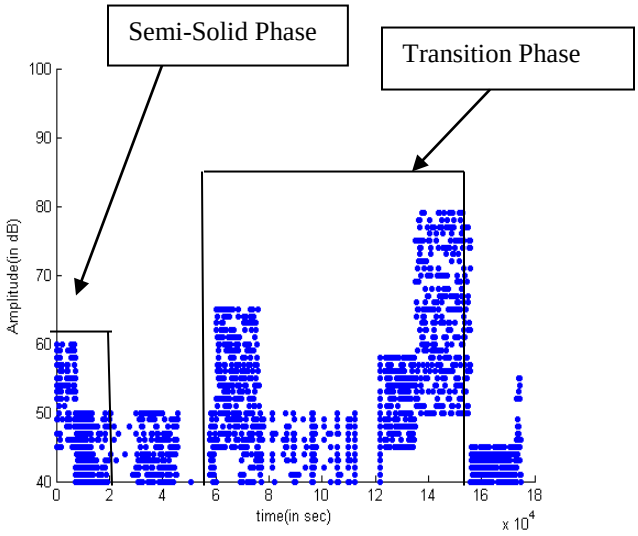

(C5)

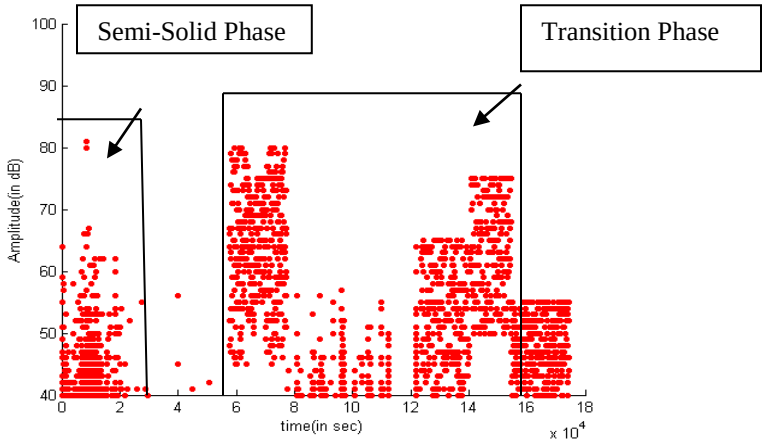

(C6)

Fig 5.12 Amplitude of AE Hits

The **Transition phase** in this has been longer duration which we can clearly see in the graphs which implies that the initial concrete setting and hardening took longer time as compared to 0.3 w/c ratio. The **Calm phase** in this test is also delayed in all the samples signifying the delayed concrete setting.

(3) Cumulative Signal Strength

From the graph, it can be clear seen that three sharp rise in the slope of the CSS curve "Knee's" have been observed. This can be very much related to the slow process of setting and hardening occurring in the three stages.

- The **1st knee** when compared with the signal amplitudes (**Fig 5.12 C4** amplitude) tells us that the signal attenuation is more which is majorly due to the **semi-solid phase** of the concrete and large disturbances in the concrete due to beginning of loss of heat of hydration.
- The **2nd knee** corresponds to the **Transition phase** of the **Fig 5.12**(**C5** amplitude) with relatively higher values of signal amplitudes corresponding to the lesser attenuation and thus concrete hardening.
- The **3rdknee** very well relates the longer **Transition phase** in this case shown in the **Fig 5.12** (**C6** amplitude) as the values of the signal amplitude are highest depicting the least signal attenuation, greater concrete hardening.

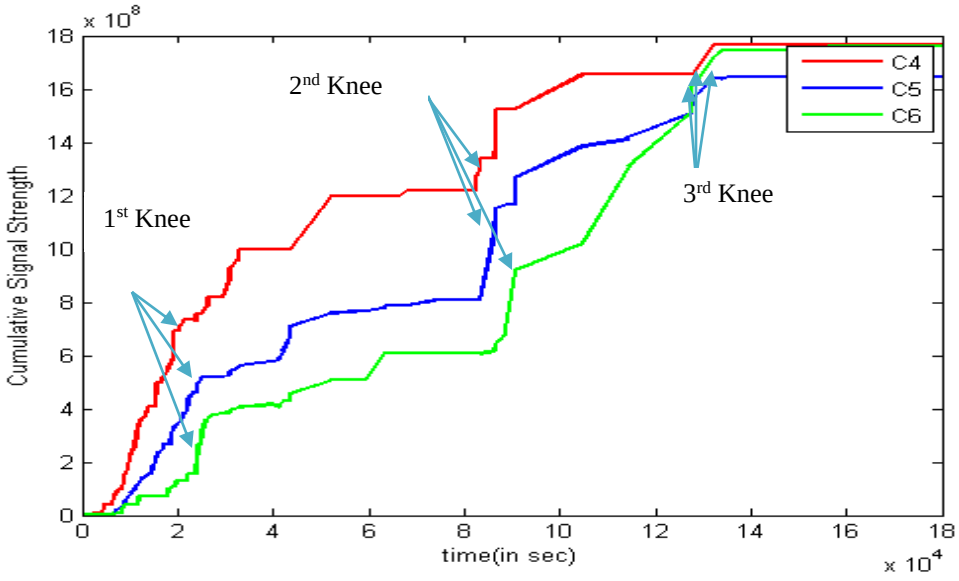

Fig 5.13 Cumulative signal Strength Vs Time

5.3 Ultrasonic Pulse Velocity Investigation

UPV tests were also conducted on cubes of size 150 mm x 150 mm x 150 mm alongside UGW tests with a w/c ratio of 0.3 in order to check the microstructure development of concrete during its early or setting phase**.**

5.3.1 Ultrasonic Pulse Velocity Investigation with w/c = 0.3

For this purpose three samples (C7, C8&C9) were cast with the same w/c ratio 0.3 and mix design proportion of 1:1.5:2.9. The results obtained are plotted as velocity Vs time graphs for 48 Hrs.

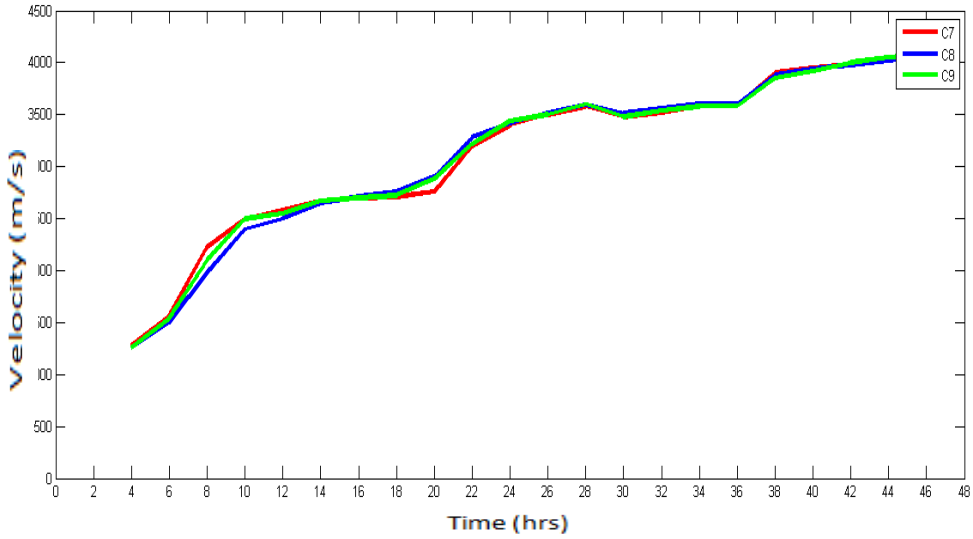

Fig 5.14 Velocity Vs Time Graph for 48hrs cube specimen (w/c = 0.3)

Above **Fig 5.14** clearly shows the velocity increases with time. This is because as the concrete starts to set the amount of ultrasonic wave attenuation i.e. loss of energy decreases and thus wave velocity increases.

5.3.2 Ultrasonic Pulse Velocity Investigation with w/c = 0.5

For this purpose three samples (C10, C11&C12) were cast with the mix design proportion of 1:1.5:2.9.

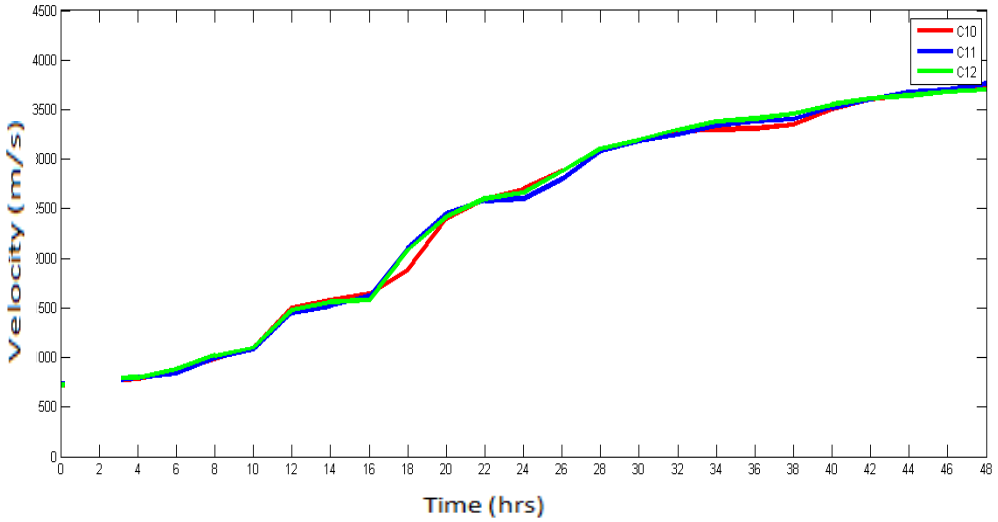

Fig 5.15 Velocity Vs Time Graph for 48hrs cube specimen (w/c = 0.5)

Discussion

- As **Fig (5.14 & 5.15)** shows that the velocity increases with time. This is because as the concrete starts to set and the phenomenon of amount of ultrasonic waves attenuation (i.e. loss of energy) decreases and thus wave velocity increases.
- The earliest setting of concrete is seen in case of w/c ratio of 0.3, i.e. 6 hours and 18 hours. When w/c ratio is 0.5, the setting occurs at 10 and 20 hours while the late setting is seen in case 0.5 w/c.
- The cause of this early and prolonged increase of UPV with low w/c of 0.3 is that the cement hydration in concrete constituents takes place faster and concrete hardens at a faster pace as compared to w/c of 0.5.

5.4 Destructive Test results

5.4.1 Initial Phase

Along with non-destructive tests like Ultrasonic Pulse Velocity and Ultrasonic Guided Wave and Acoustic Emission technique, compressive tests are also conducted on specimens with w/c ratios of 0.3 & 0.5 and results have been listed in **Table 5.1.**

Compressive tests are conducted to serve as parameters of in-situ strength development of concrete in this phase.

Table 5.1 Compressive strength test results for initial phase (i.e. 48 Hrs)

Durations(Hrs)	Compressive Strength (N/mm^2)					
	w/c = 0.3			w/c = 0.5		
3	0.59	0.68	0.58	0.55	0.64	0.41
6	1.64	1.98	1.54	1.48	1.22	1.68
12	3.20	3.80	3.42	2.80	2.28	3.21
24	10.84	11.20	9.84	8.49	8.39	9.14
48	14.8	13.4	14.2	11.14	10.20	11.30

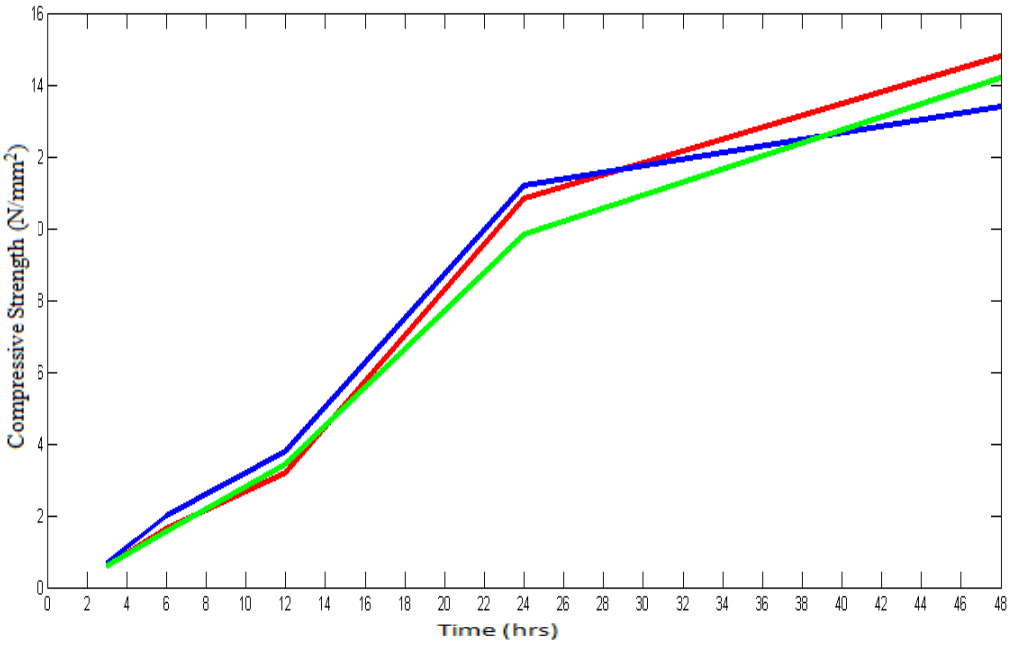

Fig 5.16 (a) Compressive Strength Results (w/c = 0.3)

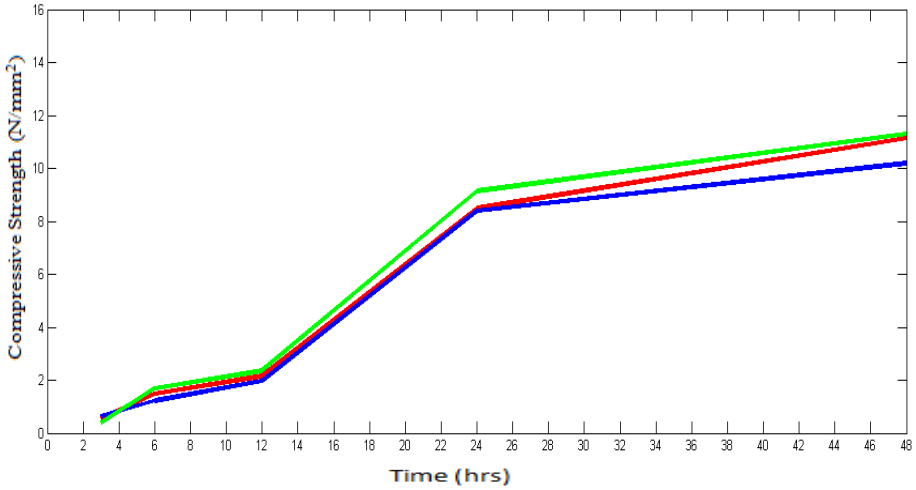

Fig 5.16 (b) Compressive Strength Results (w/c = 0.5)

- From the destructive compressive strength results, the max strength gaining zone occur between 24hrs to 48hrs. This max strength gaining zone occurs in the same period as the **Solid phase (**when concrete has almost set or become solid) and concides with Solid phase of Ultrasonic Guided Wave and Acoustic Emission results.

5.4.2 Final Hardening Phase (After Curing)

Compressive strength Tests were also conducted on specimens at different ages of curing of 3,7 & 28 days in two different types of concretes with w/c = 0.3 and w/c = 0.5. Results are tabulated in **Table 5.2**

Table 5.2 Compressive strength test results for second phase (i.e. 3, 7&28 Days)

Durations(Days)	**Compressive Strength (N/mm²)**					
	w/c = 0.3			**w/c = 0.5**		
3	**20.08**	**20.71**	**19.96**	**11.40**	**13.46**	**12.94**
7	**24.44**	**22.04**	**21.86**	**14.44**	**17.55**	**15.46**
28	**31.28**	**33.48**	**30.86**	**28.62**	**24.56**	**25.11**

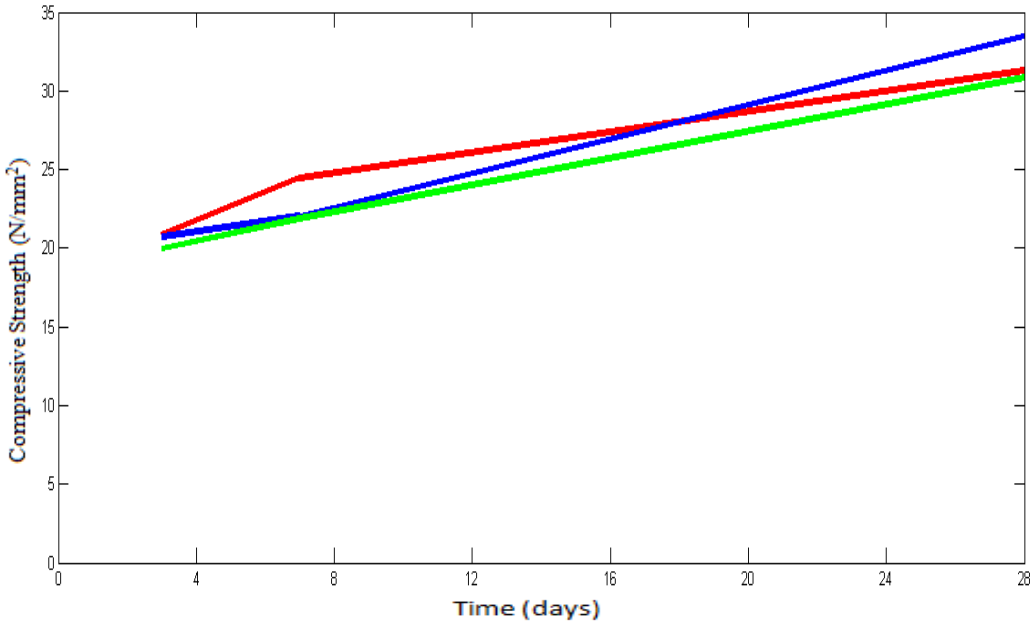

Fig 5.17 (a) Compressive Strength Results (w/c = 0.3)

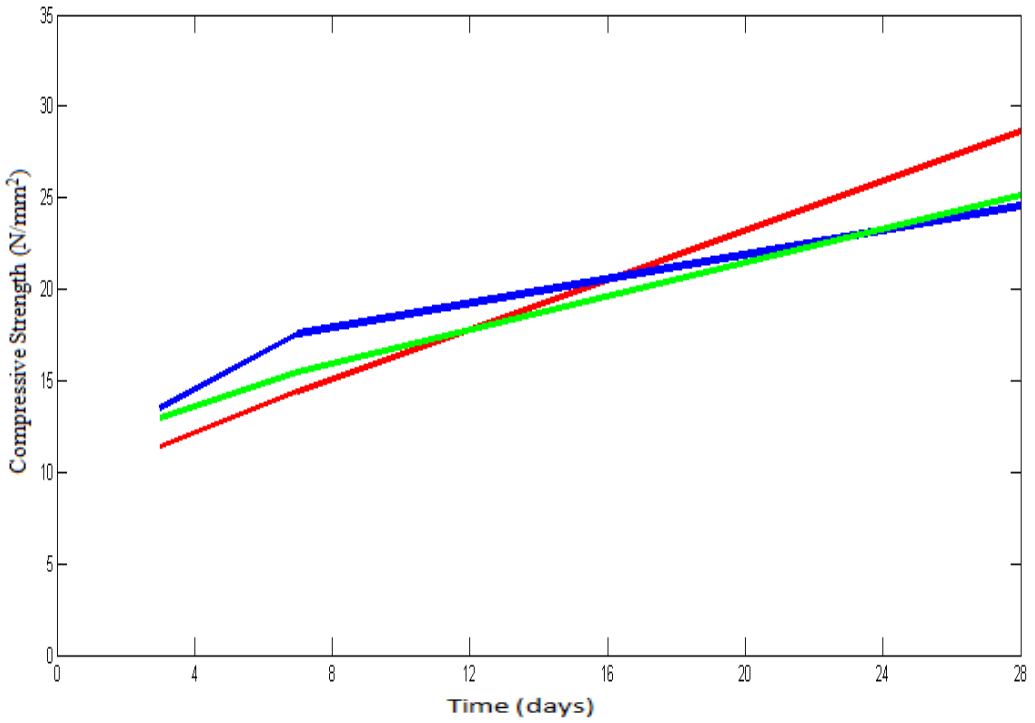

Fig 5.17 (b) Compressive Strength Results (w/c = 0.5)

Discussion

- Compressive test shows a very gradual increase in strength from 3 to 7 days but there is a rapid increase strength from 7 to 28 days. This is because concrete requires minimum 28 days to achieve its full strength. In order to check the repeatability and accuracy minimum three readings has been taken during the test.
- As w/c ratio increases from 0.3 to 0.5, the ratio of strength development slows with increase w/c ratio. This is because concrete with low w/c ratio is less porous as compared to high w/c ratio. Therefore, lower the porosity higher is the strength, Also more water content delay the hydration process means lower strength. This will justifies the use of optimum w/c ratio in concrete.

5.5 Closing Remarks

This chapter discusses investigates the setting process of concrete with different w/c ratios using non- destructive techniques of ultrasonic guided waves, ultrasonic pulse velocity and acoustic emission techniques. A vis-o-vis comparison of the efficiency of three techniques in relating to the setting process of concrete in done and investigated. It would help a lot in developing in-situ techniques for monitoring the setting process in concrete.

CHAPTER 6

CONCLUSIONS AND SCOPE OF FUTURE WORK

6.1 Conclusions

The Destructive and Non-Destructive investigations carried out in this research involving the setting behavior of two different concretes having w/c ratio of 0.3 and 0.5 is done. Two Non Destructive Techniques of Acoustic Emission and Ultrasonic Guided Wave were used to study the same. Both the techniques are capable of detecting the early age setting and hardening (within first 48 hrs) of concrete. The results were well collaborated by destructive compressive strength results.

The main conclusions drawn from the study are as follows:

6.1.1 Ultrasonic Pulse Velocity Investigation

- Ultrasonic Pulse Velocity increases with increase in setting time of concrete. The increase in ultrasonic pulse velocity of concrete is proportional to the improvement in setting and hardening of concrete with time.
- With increase in w/c ratio, the Ultrasonic Pulse Velocity decrease with setting is prolonged. Concrete with a larger w/c ratio sets in longer time since the hydration is delayed.
- In Comparison to Ultrasonic Guided Wave and Acoustic Emission Techniques, Ultrasonic Pulse Velocity method is unable to record the velocity during the semi-solid phase, as concrete is wet and starts sticking to the transducers. To overcome this problem, special frame arrangement has to be made, thus making it unpractical during the in-situ monitoring of concrete.
- In transition phase, the UPV results show a maximum velocity gain. During transition phase, when the bond between steel and concrete is developing the gain in velocity is maximum, but no significant increase in velocity is observed during the solid phase. Hence, Ultrasonic Pulse Velocity works best in transition phase.
- It is not suitable during semi-solid or solid phase. Ultrasonic Pulse Velocity values are not a very reliable indication of setting of concrete as there is no homogeneity in the values of UPV. This is due to variable properties of concrete.

6.1.2 Ultrasonic Guided Wave Investigations

- Ultrasonic guided wave technique and Acoustic emission technique using low frequency L(0,1) mode at 0.1 MHz has proven to be very effective in monitoring the hydration and setting of concrete with varying w/c ratios.
- In initial hours (0-8hrs), the fall of peak to peak voltage is nominal indicating there is not significant setting or bonding between the mild steel bar and the surrounding concrete.
- During transition phase from (8-42hrs) comes the fall in transmitted pulse voltage is observed as concrete undergoes a change of phase from semi-solid to solid phase i.e. transition phase.
- As the concrete solidifies after 42 hrs there is marginal fall in peak to peak voltage which means that has already set or hardened and bond development is almost done in 42 hrs.
- It is also seen that at another L(0,7) mode at 1 MHz , no drastic change in voltage amplitude of the first transmitted and received signal is observed throughout the 48 hours of pouring concrete. A minor change is observed in second transmitted signal which is not measurable and of practical interest.

6.1.3 Acoustic Emission Technique Investigations

- Acoustic Emission monitoring has been successfully been able to identify various stages of stetting of concrete which occur after pouring of concrete. It very well relates with the hydration process and setting phases as identified by guided wave monitoring.
- It is divided into three phases i.e. Semi-Solid phase, Transition phase and Calm phase. Semi-Solid phase i.e. (0- 8 hrs) is categorised by the large number of acoustic emission recorded during a short interval of time immediately after the pouring of concrete. During the transition phase (8- 24 hrs), acoustic emissions are continuously recorded for a longer period and they keep on increasing with time but the rise in AE emission is slower in comparison to Semi-Solid phase. Further the last phase (24 - 48 hrs) called Calm phase is identified by very little AE.
- An AE parameter called Cumulative AE counts are very much able to differentiate between the concrete setting and hardening phases of samples. As the w/c ratio increases the concrete setting and hardening is delayed and prolonged. The Semi-Solid phase is prolonged to (0-10 hrs) as against 8 hrs for concrete with w/c of 0.3. Transition and Solid phase also prolonged

by (10-40hrs) and (40-48hrs) indicating slow bond development and setting with layer w/c ratios.

- Another AE parameter, i.e. Amplitude of AE hits was also studied and it has been observed that it clearly distinguishes the setting phases of concrete. During the Semi-Solid phase, the amplitude of AE hits recorded are high (40-80) dB suggesting high activity inside the concrete during this phase, due to high release of heat of hydration. During Transition phase the values of amplitude of AE hits falls relatively to (40-60) dB indicating slower activity. In Calm phase very small values of amplitude of AE hits are recorded suggesting very low AE activity and pointing towards almost negligible setting and hence complete hydration of concrete by 24 hours.
- One more AE parameter considered i.e., Cumulative Signal Strength, was studied. The various phases of concrete setting are indicated by sharp knees (Semi-Solid phase) in the graph in the various phases. Here, the three distinct phases are observed by sharp rise called knees at different intervals of time during the monitoring distinguishing the different phase.
- With increase in w/c ratio from 0.3 to 0.5 the sharp rise i.e. knees increases from two to three which indicates delayed hydration and setting process.
- Acoustic emission technique has been able to bring out a clear distinction between the setting processes of freshly poured concrete with two varying water cement ratios. For samples with low w/c ratios, it has been observed that transition phase recorded by various parameters like Cumulative counts and Amplitude of AE hits is of shorter length that in the case of samples with higher w/c ratios. However, the parameter Cumulative Signal strength clearly distinguishes the process wherein two peaks i.e. knees are formed for the samples with low water cement ratios and three peaks are formed with samples with higher w/c ratios pointing towards delayed or prolonged or slow setting.

6.2 Scope of Future Work

The present study emphasized on the two non-destructive techniques (ultrasonic guided waves technique and Acoustic Emission Technique) for the monitoring early strength development and hardening of concrete constitutes important and challenging area of study, where wave propagation provides an efficient means of characterizing various microstructure developments in various ages of concrete. Combination of Acoustic Emission Technique and Ultrasonic Guided Wave can be used to understand the complete setting and hardening of concrete. The combined experimental

methodology using Ultrasonic Guided Wave and Acoustic Emission Technique discussed in this work can be further extended for:

- Setting properties of various types concrete with different mineral admixtures can be investigated further.
- Correlations of ultrasonic guided wave & voltages & acoustic events with destructive tests can be established.

REFERENCES

Aveline,D.; Staquet,S.; Espion,B.; Germain,O.; Pierre,C. (2009), "*Comparison between different techniques for monitoring setting and hardening of concrete"*. NDTCE"09, Non-Destructive Testing in Civil Engineering Nantes, France, June 30th– July 3rd, 2009.

Abeele, K. V. D.; Desadeleer, W.; Schutter, G. D.; Wevers, M. (2009) "*Active and passive monitoring of the early hydration process in concrete using linear and nonlinear acoustics".* (39) pg 426- 432.

Aleshin, V.A.; Abeele, K. V. D. (2007*),"Microcontact based theory for acoustics in microdamaged materials",* J. Mech. Phys. Solids 55 (2) 366–390.

Acciani, G., Fornarelli, G., Giaquinto, A., Maiullari, D. and Brunetti, G.,2008, "*Non-Destructive Technique for Defect Localization in ConcreteStructures Based on Ultrasonic Wave Propagation"*, ICCSA, Part II, LNCS5073, pp 541-554.

Aggelis, D., Soulioti ,D., Sapouridis, N., Barkoula, N., Paipetis, A. and Matikas, T., 2011," *Acoustic emission characterization of the fracture process in fibre reinforced concrete"*. Construction and Building Materials, 25, pp 4126–4131.

Ahmad, S., 2003, "*Reinforcement corrosion in concrete structures, it's monitoring and service life prediction"* - A review, Cement & Concrete Composites, Vol. 25, pp. 459-471.

Baron, J. A. and Ying, S.P., 1987, *Acoustic Emission Source Location, Nondestructive Testing Handbook, American Society for Non-destructive Testing*, Columbus, OH,5,6, pp 136-154.

Baxter, M., 2007, Ph.D. Thesis, *Damage assessment by Acoustic Emission(AE) during landing gear fatigue testing*, Cardiff School of Engineering,Cardiff University

Benin, A. V., 2006, *Analysis of the Acoustic Emission Technique Used inLaboratory Tests of Reinforced-Concrete Structures*, ISSN 1061-8309,

Benson, S.D.P., 2003, PhD Thesis, CARDIFRC®: *development and constitutive behaviour*, Cardiff School of Engineering, University ofWales, Cardiff.

Beard, M. D., Lowe, M. J. S. and Cawley, P. (2003), *Ultrasonic Guided Waves for inspection of grouted tendons and bolts*. Journal of Materials in Civil Engineering.

Behnia,A., Chai, H.K. and Shiotam, T.O,(2014*). Advanced structural health monitoring of concrete structures with the aid of acoustic emission*. Construction and Building Materials (65),282-302.

Bindal, V.N. (1999), *Transducers for Ultrasonic Flaw Detection*. Narosa Publishing house.

Biot, M. A. (1956), *Theory of propagation of elastic waves in a fluid saturated porous solid*. Low-frequency range. J. Acoust. Soc. Am. 28 (1956), S. 168-178, Higher-frequency range, S. 179-191.

Broomfield, J. P., Davies, K., Hladky K., (2002), "*The use of permanent corrosion monitoring in new and existing reinforced concrete structures",*Cement & Concrete Composites, 24, pp 27–34.

Buck, O.; Morris, W.L.; Richardson, J.N. (1978), *"Acoustic harmonic generation at unbonded interfaces and fatigue cracks"*, Appl. Phys. Lett. 33 (5) (1978) 371–373.

Bunnori, N., Pullin, R., Holford ,K. M. and Lark, R. J., (2008), *A practical investigation into Acoustic Wave propagation in concrete structures,*Advanced Material Research, Vols. 13-14, pp 205-211.

Bunnori, N., Holford, K. M. and Lark, R. J., (2006b), *The Application of Acoustic Emission Monitoring to the Assessment of concrete structures suffering from reinforcement corrosion*. Concrete Communication Conference, University College London, 5-6 September 2006.

Carpinteri, A., Lacidogna, G. and Pugno, N., (2007), *Structural damage diagnosis and life-time assessment by acoustic emission monitoring*, Engineering Fracture Mechanics 74, pp 273–289.

Carpinteri, A., G. Lacidogna, and Puzzi S., (2009), *From criticality to final collapse: Evolution of the "b-value" from 1.5 to 1.0*." Chaos, Solitons& Fractals 41(2): 843-853.

Cawley, P., (2002). *Practical Long Range Guided Wave Inspection – Applications to Pipes and Rail*. Department of Mechanical Engineering, Imperial College, London SW7 2BX, UK.

Chang, C.W. ; Lien, H.S. (2008), *Nondestructive Measurement of Concrete Strength at Early Ages*. Department of Civil Engineering and Engineering Informatics, Chung- Hua University. No.707, Sec. 2, Wufu Rd., Hsinchu City 300, Taiwan (R.O.C.)

Colombo ,I. S., Main, I., Forde, M., (2003), *Assessing damage of reinforced concrete beam using b-value" analysis of acoustic emission signals, Journal of Materials in Civil Engineering*, ASCE, pp. 280–286.

Dhonde, H.; Song,G.;, YLMo and Yan, S. (2006), *Concrete early-age strength monitoring using embedded piezoelectric transducers* Institute Of Physics Publishing Smart Materials and Structures. 15 (2006) 1837–1845.

Eaton, M. 2007, Ph.D. Thesis, *Acoustic Emission (AE) monitoring ofbuckling and failure in carbon fibre composite structures*, Cardiff School ofEngineering, Cardiff University.

Elfergani, H., Pullin, R. and Holford, K., (2011), *Acoustic emission analysis of prestressed Concrete structures*, Journal of Physics: Conference Series,305 (1), 012076.

Ervin, L. B., Kuchma ,A.D., Bernhard, T.J, Reis,H., , (2009 *)"Monitoring Corrosion of Rebar Embedded in Mortar Using High-Frequency Guided Ultrasonic Waves***",** *JOURNAL OF ENGINEERING MECHANICS © ASCE*

Haneef, T.K., Kumari, K. , Mukhopadhyay, C.K. , Venkatachalapathy , Purnachandra B. R. , Jayakumar, T. , "*Influence of fly ash and curing on cracking behavior of concrete by acoustic emission technique"* Construction and Building Materials 44 (2013) 342–350.

Hellier, C. J., (2001), *Handbook of Non-destructive Evaluation*, McGraw- Hill, USA.

Holford, K.M., (2000), *Acoustic Emission-Basic Principles and FutureDirections*, *Strain*, Vol.36 No.2.

Hsu, N.N. and Breckenbridge F.R, (1979), *Characterization and Calibration of Acoustic Emission sensors, Materials Evaluation* 39, pp 60-68.

http://www.googleimages.com

http://www.ndted.org

Irfan, M.; Khokhar, A.; Staque, S.; Roziere, E. and Loukili, A. (2009), "*Ultrasonic monitoring of setting of green concrete containing high cement substitution by mineral additions*" NDTCE"09, Non-Destructive Testing in Civil Engineering Nantes, France.

Joseph, R. L. (2004), "*Ultrasonic Guided Waves in Structural Health Monitoring*", Department of Engineering Science and Mechanics, Penn State University, 212 Earth- Engineering Science Bldg., University Park, PA 16802, USA.

Kawasaki ,Y., Tomoda,Y. and Ohtsu, M., (2010), *AE monitoring of corrosion process in cyclic wet–dry test*, Construction and Building Materials, 24,pp.2353–2357.

Kawasaki, Y., Wakuda, T., Kobarai, T., and Ohtsu, M. (2013). "*Corrosion mechanisms in reinforced concrete by acoustic emission*." Constr. Build. Mater., 48, 1240–1247.

Kim, S. Y.; Kwun, H. & Light, G.L. (2001), "*Long-Range Guided Wave Inspection of Structures Using the Magnetostrictive Sensor*" Applied Physics Division, Department of NDE Science and Technology, Southwest Research Institute, San Antonio, Texas, U.S.A.

Kundu, T., Ehsani, M. R., Na, W. B.(2001), "*Ultrasonic Guided Waves for steel bar concrete interface testing*". *Material Evaluation*, pp. 436-444.

Kundu, T. (2007), *Advanced Ultrasonic Methods for Material and Structure Inspection.*

Landis, E., (1999), *Micro-macro fracture relationships and acoustic emissionin concrete*, Construction and Building Materials, 13, pp.65-72.

Lee, H.K.; Lee, K.M.;Kim, Y.H.; Yim, H.B & Bae, D.B. (2004), "*Ultrasonic in-situ monitoring of setting process of high-performance concrete*" Cement and Concrete Research 34 631–640.

Lee, H.K. & Tawie, R. (2010), "*Piezoelectric-based non-destructive monitoring of hydration of reinforced concrete as an indicator of bond development at the steel–concrete interface*" Department of Civil and Environmental Engineering, KAIST 373-1 Guseong-dong, Yuseong-gu, Daejeon 305-701, South Korea.

Liu, Y. (1996), Ph.D. Thesis, *Modelling the Time-to-Corrosion Cracking of the Cover Concrete in Chloride Contaminated Reinforced Concrete Structures*, Faculty of the Virginia Polytechnic Institute and State University.

Lubos, P.; Topolar, L.; Bilek, V.; , Smutny, J.; Kusak, I.; Lunak, M.; Korenska, M.; Matysik, M. and Mazal, P. (2010), "*Application Nondestructive Testing during Concrete hardening and setting*" Czech Society for Nondestructive Testing NDE for Safety / DEFEKTOSKOPIE 2010 November 10 - 12, 2010 - Hotel Angelo, Pilsen - CzechRepublic.

Miller, R. K., Hill, E. K., Moore P. O. (2005) *Non Destructive Testing Handbook, Vol 6, Acoustic emission techniques*. Americal society for non destructive testing, Columbus, pg 428.

Miller, R. K. and Mclntire, P. (1987) *Text Book on Non destructive testing*, vol (5), American society of Non Destructive Testing 2 Edition, p 603.

Nicolas, R. & Nele, D. B. (2009), "*Monitoring the setting of concrete by measuring the change in ultrasonic p-wave energy*" NDTCE‟09, Non-Destructive Testing in Civil Engineering Nantes, France, June 30th – July 3rd, 2009.

Ohno, K. (2010). "*Application of acoustic emission for structure diagnosis*". Konfrencia, Naukowa, 317-334.

Ohtsu M. and Ohno, K., (2010), *Crack classification in concrete based on acoustic emission*, Construction and Building Materials, 24, pp. 2339-2346.

Ohtsu M. and Tomoda Y., (2007a), *Damage evaluation and corrosion detection in concrete by acoustic emission*. Proc of the 6th international conference on fracture mechanics of concrete and concrete structures, Vol 2, pp. 981-989.

Ohtsu, M. and Tomoda Y., (2007b), *Corrosion process in reinforced concrete identified by acoustic emission*, Materials Transactions, Vol 48, pp.1184 -1189.

Ohtsu, M., Uchida M., Okamoto T. and Yuyama S., (2002), *Damage assessment of reinforced concrete beams qualified by Acoustic Emission*, ACI Structural Journal (Technical paper) July-August, pp. 411-417.

Pavalakovic, B.N., and Cawley, P.(2000), Disperse User‟s Manual Version 20.11.2000. Imperial college, University of London.

Pavalakovic, Lowe,M.J.S., and Cawley, P.(2001), "*High-Frequency Low- Loss Ultrasonic modes in imbedded bars*", *ASME Journal*, Vol. 68/67, pp. 67-75.

Pollock, A. A., (1986), "*Classical Wave Theory in Practical AE Testing,Progress in Acoustic Emission III, the Japanese of NDI"*.A, pg 235-240.

Pullin, R, Baxter ,M.G., Holford, k. M. and Evans, S. L. (2007), *Novel Acoustic emission source location.* 6th International Conference on Acoustic Emission. Lake Tahoe-Nevada, USA, pp.235-240.

Redwood, M.; Mechanical Waveguides, (1960), "*The Propagation of Acoustic and Ultrasonic Waves in Fluids and Solids with Boundaries*" Pergamon, New York.

Reinhardt ,H.W & Grosse,C.U. (2003), "*Continuous monitoring of setting and hardening of mortar and concrete*" Construction and Building Materials 18 (2004) 145–154.

Reis, H., Ervin, B.L., Kuchma, D.A., and Bernhard, J.T. (2005), "*Estimation of Corrosion Damage in Steel Reinforced Mortar Using Guided Waves*" Journal of Pressure Vessel Technology;August 2005, Vol. 127 / 255-261.

Reis, H., Ervin, B.L, (2008)"*Longitudinal guided waves for monitoring corrosion in reinforced mortar*," Journal of Measurement Science and Technology, vol. 19, no. 5, Article ID 055702.

Rindorf, H. J., (1981), "*Acoustic emission source location in theory and inpractice, Bruel and Kjaer Technical Review"*, 2, pp. 3-44.

Rindorf, H. J., (1981), Acoustic *emission source location in theory and inpractice*, Bruel and Kjaer Technical Review, 2, pp. 3-44.

Rippengill, S., Worden, K., Pullin, R., and Holford, K., (2003), *Automatic classification of acoustic emission patterns*, Strain, 39, pp. 31-41.

Robeyst, N., Gruyaert, E. & De Belie N. (2007), "*Ultrasonic monitoring of setting and hardening behaviour of concrete and mortar with blast-furnace slag cement"* Proceedings 12th International Congress on the Chemistry of Cement, Montréal, 2007, T2-03.2 on CDROM.

Rokhlin, S.I., Kim, J.Y. , B. Xie, Zoofan B.," *Nondestructive sizing and localization of internal*

microcracks in fatigue samples" NDT&E International 40 (2007) 462–470.

Rose, J. L. and Jhang, L., (2004) " *Guide Wave Particle Motion in a Hollow Cylindrical, Procedings of QNDE, 24:1952-7.*

Sekulić, D., Bjegović, D. & Mikulić, D (2004), "*Determination of Early Age Concrete Properties With Ultrasonic Methods*", Proceedings of the International Conference MATEST 2004, Zagreb, Croatian Society of Non-Destructive Testing, Zagreb, 33-44.

Sharma, S., Mukherjee, A., (2010) "*Longitudinal guided waves for monitoring chloride corrosion in reinforcing bars in concrete*", *SAGEPUB Journals,* Vol 9(6) , 555-13.

Sharma, S., Mukherjee, A., (2010 (c))"*Monitoring Corrosion in Oxide and Chloride environments using ultrasonic guided waves* " Journal of Materials in Civil , Vol 23, No. 2.

Sharma, S., Mukherjee, A., (2011 *)" Damage detection in reinforcing bars in concrete using ultrasonic waves*" *J. Pure Appl. Ultrasonic*,31 pp.85-93.

Sharma, S., Mukherjee, A., (2011) *"Monitoring Corrosion in Oxide and Chloride Environments Using Ultrasonic Guided Waves*"**,** *Journal of Materials In Civil Engineering © ASCE.*

Sharma, S., Mukherjee,(2012) A "*Non-Destructive Evaluation Of Corrosion In Varying Environments Using Guided Waves*", Research in non-destructive evaluation, 1-40.

Sharma, S., Mukherjee, A. (2014) "*Ultrasonic guided waves for monitoring the setting process of concretes with varying workabilities"* Construction and Building Materials 72 (2014) 358–366.

Sharma, S., Mukherjee, A. (2015) "*Monitoring freshly poured concrete using ultrasonic waves guided through reinforcing bars"* Cement & Concrete Composites 55 (2015) 337–347.

Shiotani,T., (2006), "*Evaluation of Repair Effect for Deteriorated Concrete Piers of Intake Dam Using AE Activity, Advanced Materials Research"*, 13- 14, pp 175-180.

Shiotani, T., (2006), *Evaluation of Repair Effect for Deteriorated Concrete Piers of Intake Dam Using AE Activity*, Advanced Materials Research, 13- 14, pp 175-180.

Song, H. and Saraswathy, V., (2007), *Corrosion Monitoring of Reinforced Concrete Structures – A Review*, International Journal of Electrochemical. Science 2, pp.1- 28.

Soulioti, D., Barkoula, N. M., Paipetis, A., Matikas ,T.E, Shiotani, T. and Aggelis D.G., (2009), *Acoustic emission behaviour of steel fibre reinforced concrete under bending*, Construction and Building Materials, 23, pp.3532-3536.

Travers, F., 1997, *Acoustic Monitoring of Prestressed Concrete pipe*,Construction and Building Materials, Vol. 11, No. 3, pp. 175-187.

Tomoda, Y., Isodo, T., Ohtsu, M.,(2003) " *Acoustic Emission Techniques Standardized for Concrete Structures. Vol. 5, pp 234- 255*.

Uddin, A., Numata, K., Shimasakia, J., Shigeishi, M. and Ohtsu, M., (2004), *Mechanisms of crack propagation due to corrosion of reinforcement in concrete by AE-SiGMA and BEM*, Construction and Building Materials, 18, pp. 181–188.

Watanabe, T., Nishibata, S., Hashimot,o C. and Ohtsu, M., (2007), *Compressive failure in concrete of recycled aggregate by acoustic emission*, Construction and Building Materials, 21, pp. 470-476

Wheat, H. G., (2007), *Monitoring Corrosion Behavior Using Acoustic Emission Techniques, NACE International*, Corrosion, Conference &Expo, paper No 07291.

Xiong, H., Li, P. and Li, Q., 2010, *FE model for simulating wire-wrapping during prestressing of an embedded prestressed concrete cylinder pipe*, Simulation Modelling Practice and Theory, 18, pp. 624–636.

Ye, G.; Breugel, K.V.; Fraaij, A.L.A. (2001), *Experimental study on ultrasonic pulse velocity evaluation of the microstructure of cementitious material at early age* HERON, 46(3) ISSN 0046-7316.

Yoon, D.J., Weiss,J.W. and Shad, P.S., (2000). "*Assessing damage in corroded reinforced concrete using acoustic emission*.

Yun, H., Choi W. and Seo S., 2010, *Acoustic emission activities and damage evaluation of reinforced concrete beams strengthened with CFRP sheets*, NDT & E International, 43, pp. 615–628.

Yu, J., Ziehl, P., Zárate, B. and Caicedo, J., (2011), *Prediction of fatigue crackgrowth in steel bridge components using acoustic emission, Journal ofConstructional Steel Research*, 67, pp. 1254–1260.

Yuyama, S., Yokoyama K., Niitani, K., Ohtsu M. and Uomoto T., (2007), "*Detection and evaluation of failures in high-strength tendon of prestressed concrete bridges by acoustic emission, Construction and Building Materials"*, 21, No.3, pp. 491-500.

Zhu, J. & Kee, S. H. (2010), "*Monitoring early age microstructure development of cement paste using bender elements*" Department of Civil, Architectural and Environmental Engineering, University of Texas at Austin, TX USA 79712.